MSc thesis in Geomatics

Scenario-based energy simulation: Modelling tree planting strategy to reduce heating and cooling demand under 2050 climate conditions

Adhisye Rahmawati

October 2025



MSc thesis in Geomatics

Scenario-based energy simulation: Modelling tree planting strategy to reduce heating and cooling demand under 2050 climate conditions

Adhisye Rahmawati

October 2025

A thesis submitted to the Delft University of Technology in partial fulfilment of the requirements for the degree of Master of Science in Geomatics

Adhisye Rahmawati: *Scenario-based energy simulation: Modelling tree planting strategy to reduce heating and cooling demand under 2050 climate conditions* (2025)
This work is licensed under a Creative Commons Attribution 4.0 International License.
To view a copy of this license, visit http://creativecommons.org/licenses/by/4.0/.

The work in this thesis was carried out in the:



3D geoinformation group
Delft University of Technology

Supervisors:	Dr. Weixiao Gao
	Dr. Camilo León Sánchez
	Dr. Giorgio Agugiaro
Co-reader:	Dr.ir. B.M. Meijers

Abstract

In recent years, rising energy demand and intensifying climate change impacts have placed urban energy systems under growing pressure. Higher average temperatures and more frequent heatwaves are projected to substantially increase cooling demand. UBEM offers a means to analyse such dynamics at the district scale; however, vegetation effects on building energy use remain under-represented. Existing approaches often rely on multiple coupled models, apply to small spatial extents, or omit future climate scenarios, thereby limiting their usefulness for urban planning and climate adaptation strategies.

In this thesis, we introduce a neighbourhood-scale workflow that integrates a tree planting scenario into a single simulation-based UBEM platform. The main characteristic of the method lies in its use of standardised CityGML building models, simplified yet seasonally dynamic vegetation representations, and a unified modelling environment that allows consistent comparison of a planting strategy under both current and projected 2050 climate conditions. Six scenarios were applied to two contrasting Rotterdam neighbourhoods to quantify heating and cooling demand at building and neighbourhood levels while separating climate-driven changes from vegetation impacts.

Results indicate that, between 2023 and 2050, cooling demand increases by 32–39%, while heating demand decreases by approximately 12%. Adding deciduous trees reduces neighbourhood cooling demand by 3–10%, depending on location and climate scenario, but winter shading introduces heating penalties of up to 2%, leading to small net annual changes at the neighbourhood scale (0.9% to 0.4%). Building-level effects are more heterogeneous: in compact districts, additional trees sometimes block limited winter solar gains, while in open areas with high cooling exposure, they consistently reduce peak summer loads. Orientation and façade exposure emerge as key factors shaping the balance between summer benefits and winter penalties.

The workflow produces spatially explicit maps and scenario comparisons to support an energy-aware, location-specific planting strategy. However, simplified tree geometry, static building stock assumptions, monthly climate inputs, and computational limits constrain the accuracy and scalability of the results. Future research should integrate hourly climate data, species-specific vegetation models, dynamic retrofitting scenarios, and larger spatial domains to better capture seasonal variability, urban morphological diversity, and the interactions between greening and energy system decarbonisation pathways.

Acknowledgements

Within this section, I would like to take the opportunity to thank a few people who had an impact during the execution of this research.

First, I would like to thank my supervisors, Dr. Weixiao Gao, Dr. Camilo León Sánchez, and Dr. Giorgio Agugiaro, for their guidance, advice, and support throughout this work. The road to completing this thesis was not always smooth, but their encouragement along the way made it possible for me to finish. I am also grateful to Dr.ir. B.M. Meijers for reviewing this thesis and for the constructive comments that improved it.

The work described in this thesis was carried out in the framework of the European project DigiTwins4PEDs[1], which examines the application of Urban Digital Twins as digital representations of real-world environments to investigate the energy aspects of cities. I am grateful to the DigiTwins4PEDs consortium for providing the setting for this research and for the opportunity to learn from the collaboration it enabled. I would also like to thank the municipality of Rotterdam for its support during the project. Marie-Emilie Ingen Housz, Roland van Rooyen, and F. M. Freyre Hechavarria gave their time and shared their knowledge, which was valuable for this work.

Finally, I would like to thank my mommy, dad, brother, sister, my extended family and Jimmy Ong for their constant love, patience, and support throughout this journey. Their encouragement has given me strength, especially during the more difficult moments. I am also grateful to all my closest friends, especially those in Rotterdam, The Hague, and Delft, whose understanding and encouragement created a supportive environment that made the challenges of this study more manageable.

[1] https://digitwins4peds.eu/

Contents

1. Introduction **1**
- 1.1. Motivation . . . 1
  - 1.1.1. Urban energy challenges . . . 1
  - 1.1.2. Urban building energy modelling (UBEM) . . . 2
  - 1.1.3. Vegetation in UBEM . . . 2
  - 1.1.4. Research gaps . . . 3
- 1.2. Research questions . . . 3
- 1.3. Scope . . . 4
- 1.4. Thesis outline . . . 4

2. Theoretical background and related work **5**
- 2.1. Building energy modelling . . . 5
- 2.2. Physics-based UBEM tools for heating and cooling demand . . . 8
- 2.3. Representation of trees in physics-based UBEM tools . . . 8
- 2.4. GIS-based UBEM: SimStadt . . . 14
  - 2.4.1. DIN V 18599: Monthly energy balance standard . . . 14
  - 2.4.2. CityGML . . . 15

3. Method **17**
- 3.1. Research design and workflow overview . . . 17
- 3.2. Scenario development . . . 17
- 3.3. Simulation tool and data requirements identification . . . 18
- 3.4. Modelling simplifications and assumptions . . . 20
- 3.5. Model configuration . . . 21
  - 3.5.1. Building model preparation . . . 21
  - 3.5.2. Vegetation model preparation . . . 22
  - 3.5.3. Model integration . . . 22
- 3.6. Simulation, post-processing, analysis, and visualisation . . . 23

4. Experiments **25**
- 4.1. Study area . . . 25
- 4.2. Data required . . . 26
  - 4.2.1. Building model in CityGML LoD2 . . . 26
  - 4.2.2. Current and 2050 projection climate inputs . . . 26
  - 4.2.3. Vegetation data . . . 28
  - 4.2.4. Land use layers . . . 29
  - 4.2.5. Data summary . . . 29
- 4.3. Tools and software . . . 30
- 4.4. Implementation details . . . 30
  - 4.4.1. Preparing building data . . . 30
  - 4.4.2. Preparing existing tree data . . . 31
  - 4.4.3. Preparing proposed tree data . . . 32

4.4.4. Configuring the Tree Model . . . 37
4.4.5. Configuring the simulation model . . . 41
4.4.6. Processing climate data . . . 42
4.4.7. Scope adjustment due to computational constraints . . . 43
4.5. Simulation setup in SimStadt . . . 45
4.5.1. Post-processing, analysis, and visualisation . . . 47

5. Results and analysis **49**
5.1. Energy demand results . . . 49
5.2. Comparative analysis . . . 51
5.2.1. Current vs. future climate scenarios . . . 51
5.2.2. Identification of potential planting areas . . . 60
5.2.3. Effectiveness of proposed tree planting strategies . . . 62
5.3. Urban vegetation and greening benchmark assessment . . . 70

6. Conclusion **73**
6.1. Research overview . . . 73
6.2. Synthesis of findings . . . 74
6.3. Contributions . . . 75
6.4. Limitations and challenges . . . 75
6.5. Recommendations for future work . . . 76
6.6. Conclusion . . . 77

A. Tables **79**

B. Energy Demand Results **83**
B.1. Energy Demand under Current Climate . . . 83
B.1.1. Without Trees . . . 83
B.1.2. With Existing Trees . . . 84
B.1.3. With Existing and Proposed Trees . . . 84

C. Energy Demand Results Comparison (Proposed Trees Effect) **85**
C.1. Under Current Climate . . . 85
C.1.1. Cooling Demand Change . . . 85
C.1.2. Heating Demand Change . . . 86
C.2. Under Future Climate . . . 87
C.2.1. Cooling Demand Change . . . 87
C.2.2. Heating Demand Change . . . 88

List of Figures

2.1. Physics-based UBEM workflow in general (adapted from [Ferrando et al., 2020]) 8

3.1. Methodological workflow for neighbourhood-scale energy demand assessment. 17
3.2. Overview of the six designed scenarios combining three vegetation settings with two climate conditions. Scenarios S0 and S3 are reference cases without vegetation, S1 and S4 include existing trees, and S2 and S5 include both existing and proposed trees under present and future climate conditions. . . . 18
3.3. Overview of the modules executed in the *SimStadt Heat Demand Analysis* workflow, including data import, preprocessing, climatic processing, and energy balance calculation. . . . 19
3.4. Flowchart for post-processing workflow. . . . 23
3.5. Flowchart for analysis and visualisation. . . . 24

4.1. Feijenoord District . . . 25
4.2. Building dataset viewed on the 3D Rotterdam web viewer (left) and in FME Data Inspector (right). The dataset represents the CityGML LoD2 building model of the Rotterdam area. . . . 26
4.3. Trees in the Feijenoord District of Rotterdam . . . 28
4.4. Tree Implicit Geometry . . . 28
4.5. Flowchart illustrating the complete processing workflow for deriving both summer and winter tree boundaries from CityGML data. . . . 31
4.6. Workflow for tree planting point generation . . . 33
4.7. BGT land-use layers defining areas suitable for planting . . . 34
4.8. BGT land-use layers defining areas unsuitable for planting . . . 36
4.9. General workflow for generating LoD1 tree models in FME Workbench. . . . 37
4.10. Simplification of tree geometries. The original models (left) and their simplified cylindrical representations (right). The middle image shows the overlap, showing that only the crown region was represented as cylinders. . . . 40
4.11. Examples of simulation-ready 3D models for Afrikaanderwijk. Source: Google Street View imagery (captured July 2024; approximate camera location: X = 93746.1464, Y = 435553.1237; CRS: EPSG:28992). . . . 42
4.12. Example of a memory allocation error (std::bad_alloc) encountered during the simulation. . . . 44
4.13. Workflow for post-processing . . . 48

5.1. Buildings with the highest simulated cooling (top) and heating (bottom) demand in Kop van Zuid. . . . 50
5.2. Change in cooling demand resulting from climate change in Afrikaanderwijk and Kop van Zuid under no tree condition. . . . 52
5.3. Cooling Demand Comparison Graph (2023 vs. 2050) – Afrikaanderwijk . . . 53
5.4. Cooling Demand Comparison Graph (2023 vs. 2050) – Kop van Zuid . . . 54

5.5. Change in heating demand resulting from climate change in Afrikaanderwijk under no tree condition. . . . 54
5.6. Change in heating demand resulting from climate change in Kop van Zuid under no tree condition . . . 55
5.7. Heating Demand Comparison Graph (2023 vs. 2050) – Afrikaanderwijk . . . 56
5.8. Heating Demand Comparison Graph (2023 vs. 2050) – Kop van Zuid . . . 56
5.9. Change in Energy demand resulting from climate change in Afrikaanderwijk and Kop Van Zuid under no tree condition. . . . 57
5.10. Distribution of changes in building energy demand under climate change scenarios for Afrikaanderwijk and Kop Van Zuid . . . 58
5.11. Plantable areas identified in Afrikaanderwijk . . . 60
5.12. Plantable areas identified in Kop van Zuid . . . 61
5.13. Proposed tree points generated for Afrikaanderwijk (1405 points) . . . 61
5.14. Proposed tree points generated for Kop van Zuid (374 points) . . . 62
5.15. Change in total energy demand resulting from proposed tree planting under the current climate in Afrikaanderwijk and Kop van Zuid. . . . 63
5.16. Highest net benefits building in Afrikaanderwijk . . . 64
5.17. Highest net benefits building in Afrikaanderwijk . . . 65
5.18. Building with high cooling benefits but substantial heating penalties in Afrikaanderwijk . . . 65
5.19. Building with high cooling benefits but substantial heating penalties in Kop van Zuid. . . . 66
5.20. Building heating penalties outweigh cooling benefits in Afrikaanderwijk. . . . 66
5.21. Building heating penalties outweigh cooling benefits in Kop van Zuid. . . . 67
5.22. Change in total energy demand resulting from proposed tree planting under the 2050 climate in Afrikaanderwijk and Kop van Zuid. . . . 68
5.23. Existing tree canopy coverage in Kop Van Zuid. Background Map Source: Luchtfoto 2025 Quick Ortho 8cm RGB . . . 70
5.24. Existing tree canopy coverage in Afrikaanderwijk. Background Map Source: Luchtfoto 2025 Quick Ortho 8cm RGB . . . 71
5.25. Aerial view of Christiaan de Wetstraat and De la Reystraat in Afrikaanderwijk. Background Map Source: PDOK Luchtfoto 2023 Ortho 25cm RGB. . . . 72

B.1. Cooling demand under current climate for the Afrikaanderwijk neighbourhood without trees. . . . 83
B.2. Cooling demand under current climate for the Afrikaanderwijk neighbourhood with existing trees. . . . 84
B.3. Cooling demand under current climate for the Afrikaanderwijk neighbourhood with existing and proposed trees. . . . 84

C.1. Change in cooling demand resulting from proposed tree planting under the current climate in Afrikaanderwijk. . . . 85
C.2. Change in cooling demand resulting from proposed tree planting under the current climate in Kop van Zuid. . . . 86
C.3. Change in heating demand resulting from proposed tree planting under the current climate in Afrikaanderwijk. . . . 86
C.4. Change in heating demand resulting from proposed tree planting under the current climate in Kop van Zuid. . . . 87
C.5. Change in cooling demand resulting from proposed tree planting under the 2050 climate in Afrikaanderwijk. . . . 87

C.6. Change in cooling demand resulting from proposed tree planting under the 2050 climate in Kop van Zuid. 88
C.7. Change in heating demand resulting from proposed tree planting under the 2050 climate in Afrikaanderwijk. 88
C.8. Change in heating demand resulting from proposed tree planting under the 2050 climate in Kop van Zuid. 89

List of Tables

2.1. Comparison of Urban Energy Use Modelling Approaches (adapted from [Abbasabadi and Ashayeri, 2019]) . . . 7
2.2. Summary of approaches that integrate trees into physics-based UBEM workflows. . . . 10
2.3. Comparison of selected physics-based UBEM tools based on key criteria for vegetation modelling (adapted from Ferrando et al. [2020]). . . . 12
2.4. Strengths and weaknesses of selected physics-based UBEM tools for vegetation modelling. . . . 13

3.1. Datasets required for the simulation workflow, including their purpose, format, and preprocessing considerations to ensure compatibility with *SimStadt*. . 20
3.2. Scenario datasets prepared for summer and winter simulations. Summer runs use full tree canopy dimensions, while winter runs use reduced dimensions. . 22

4.1. Monthly global (G_{Gh}), beam (G_{Bn}), diffuse (G_{Dh}) radiation in kWh/m^2 and average air temperature (°C) for current climate (1991–2019). . . . 27
4.2. Monthly mean air pressure (p), wind speed (FF), and cloud cover (N) for the projected 2050 climate scenario. . . . 27
4.3. Extracted layers and their geometry types . . . 29
4.4. Summary of datasets used in this study. . . . 30
4.5. Possible and impossible planting areas with buffer constraints. . . . 35
4.6. Attributes assigned to tree polygons prior to geometry generation . . . 38
4.7. Simulation-ready CityGML files prepared for the Afrikaanderwijk neighbourhood. Each scenario was simulated separately for summer and winter, resulting in twelve independent datasets. . . . 41
4.8. Monthly global (G_{gh}), beam (G_{bn}), and diffuse (G_{dh}) radiation in kWh/m^2 and average air temperature (°C) for the projected 2050 climate scenario. . . . 43
4.9. File size and simulation time per neighbourhood including tree data (preliminary tests). . . . 43
4.10. Simulation success for each neighbourhoods across scenarios. A tick (V) indicates successful completion; cells marked 'X' indicate failed runs. . . . 44
4.11. Simulation setup in SimStadt . . . 46

5.1. Statistical for the Kop van Zuid simulation without trees under the current climate scenario . . . 49
5.2. Comparison of total monthly cooling demand for the entire Afrikaanderwijk neighbourhood in 2023 and 2050, with percentage change . . . 53
5.3. Comparison of total monthly cooling demand for the entire Kop van Zuid neighbourhood in 2023 and 2050, with percentage change . . . 53
5.4. Comparison of total monthly heating demand for the entire Afrikaanderwijk neighbourhood in 2023 and 2050, with percentage change . . . 55

5.5. Comparison of total monthly heating demand for the entire Kop van Zuid neighbourhood in 2023 and 2050, with percentage change 56
5.6. Annual energy demand for cooling, heating, and total energy in 2023 and 2050 for Kop van Zuid and Afrikaanderwijk (no tree cover scenario). Change denotes the absolute difference (2050–2023), while % Change denotes the relative change. 59
5.7. Annual energy demand for cooling, heating, and total energy under the current climate for Afrikaanderwijk and Kop van Zuid, comparing existing trees and existing + proposed trees scenarios. 69
5.8. Annual energy demand for cooling, heating, and total energy under the future climate for Afrikaanderwijk and Kop van Zuid, comparing existing trees and existing + proposed trees scenarios. 69

A.1. Summary of attributes in the CityGML *SolitaryVegetationObject* dataset, grouped by CityGML schema components, with descriptions. 80
A.2. Tree genus classification into deciduous and evergreen categories. 81

Acronyms

Acronym	Full Term
ADE	Application Domain Extension (CityGML)
ASHRAE	American Society of Heating, Refrigerating and Air-Conditioning Engineers
BAG	Basisregistratie Adressen en Gebouwen (NL Building and Address Registry)
BEM	Building Energy Modelling
BGT	Basisregistratie Grootschalige Topografie (NL large-scale topography)
BIM	Building Information Modelling
CEA	City Energy Analyst
CFD	Computational Fluid Dynamics
CityGML	City Geography Markup Language
CRS	Coordinate Reference System
CSV	Comma-Separated Values
DIN	Deutsches Institut für Normung (German Standards Institute)
EPSG	European Petroleum Survey Group (coordinate reference codes)
GHI	Global Horizontal Irradiance
GML	Geography Markup Language
HPC	High-Performance Computing
ISO	International Organization for Standardization
IWU	Institut Wohnen und Umwelt (usage/behaviour profile in SimStadt)
KNMI	Koninklijk Nederlands Meteorologisch Instituut (Royal Netherlands Meteorological Institute)
LAI	Leaf Area Index
LAD	Leaf Area Density
LoD	Level of Detail
NTA	Nederlandse Technische Afspraak (Dutch Technical Agreement)
PDOK	Publieke Dienstverlening Op de Kaart (NL open data portal)
QGIS	Quantum GIS
RC	Resistance–Capacitance (thermal model)
SRA	Simplified Radiosity Algorithm
TMY3	Typical Meteorological Year (version 3)
UBEM	Urban Building Energy Modelling
UCM	Urban Canopy Model
UMI	Urban Modelling Interface
UUID	Universally Unique Identifier
XML	eXtensible Markup Language

1. Introduction

This chapter outlines the motivation for representing tree planting within Urban building energy modelling (UBEM) to address urban energy demand and climate change challenges. It then identifies research gaps in modelling tree effects on building energy use, formulates the main and sub-research questions focusing on the spatial representation of tree planting at the neighbourhood scale under future climate conditions, defines the scope of the study, and presents the overall thesis structure.

1.1. Motivation

1.1.1. Urban energy challenges

Urban areas face challenges in energy management and environmental sustainability. Population growth and expanding economic activities drive higher energy demand, increasing reliance on non-renewable energy sources and contributing to greenhouse gas emissions [International Energy Agency, 2021]. These emissions lead to climate change effects such as extreme weather, rising global temperatures, and intensified urban heat island impacts, which elevate energy needs for heating and cooling [International Energy Agency, 2021]. Furthermore, ageing infrastructure and inefficient energy use result in energy losses and resource waste, making urban areas vulnerable to climate-related risks [United Nations, 2019].

Urban energy systems must become more adaptive and resilient to address these challenges. They span multiple sectors, including transportation, industry, infrastructure, and the built environment. In 2010, the building sector accounted for approximately 32% of global final energy demand and 30% of energy-related CO_2 emissions, driven significantly by heating and cooling energy consumption in residential and commercial buildings [Ürge Vorsatz et al., 2015]. Moreover, urban areas are responsible for approximately 71% to 76% of global CO_2 emissions from final energy use, and between 67% and 76% of total global energy consumption [Seto et al., 2014]. Since energy use and associated greenhouse gas emissions primarily originate in urban rather than rural settlements, cities are essential to addressing global climate change [Seto et al., 2014].

One approach to improving energy efficiency in the built environment is the development of PED (Positive Energy District) [European Commission, 2020; JPI Urban Europe, 2019]. PEDs are energy-efficient and energy-flexible urban areas or groups of connected buildings that produce net-zero greenhouse gas emissions and actively manage a local or regional surplus of renewable energy annually [Smart Cities Marketplace, 2021]. Instead of addressing buildings in isolation, PEDs integrate high-performance building design, renovation strategies, and smart energy technologies across new and existing buildings. While new constructions are often more capable of reaching plus-energy status, retrofitted buildings may benefit from surplus energy generated within the district. This coordinated approach enables

energy-efficient buildings to support district-wide energy balancing, contributing to lower emissions and more resilient urban energy systems [Smart Cities Marketplace, 2021].

1.1.2. Urban building energy modelling (UBEM)

UBEM supports energy strategies by simulating the consumption and production of energy across multiple buildings, using inputs such as geometry, construction materials, usage patterns, and climate conditions [Reinhart and Davila, 2016]. UBEM approaches are commonly classified into *top-down* and *bottom-up* models [Swan and Ugursal, 2009]. Top-down models rely on aggregated historical energy data at urban or regional scales, incorporating socioeconomic, demographic, and technological factors to describe consumption patterns, though their resolution is often insufficient for detailed planning at the building or district scale [Reinhart and Davila, 2016]. Bottom-up models instead begin at the level of individual buildings or user characteristics and are typically divided into simulation-based and data-driven methods [Abbasabadi and Ashayeri, 2019; Ali et al., 2021]. Simulation-based approaches apply engineering principles, thermodynamic calculations, and standardised building archetypes, while data-driven methods employ statistical or machine learning techniques applied to empirical data [Nouvel et al., 2014; Biljecki et al., 2015; Ali et al., 2021].

Data-driven methods are gaining popularity with the increasing availability of energy and sensor datasets with fine temporal and spatial resolution (e.g., smart meter readings, building management system logs, energy performance certificates, and localized weather data). However, they depend heavily on the quality and representativeness of the data, which may be limited in many urban contexts [Ali et al., 2021; Abbasabadi and Ashayeri, 2019]. Meanwhile, simulation-based or physics-based methods rely on established physical models and building archetypes, enabling the systematic evaluation of building typologies, operational behaviours, and environmental conditions even when measured data are sparse. This approach has also demonstrated reliable performance at the district scale, with heating and cooling demand estimates falling within acceptable confidence bounds [García-López et al., 2024].

1.1.3. Vegetation in UBEM

Despite advances in UBEM, the representation of vegetation in physics-based UBEM workflows remains limited. Existing studies show that trees can reduce solar exposure, improve outdoor comfort, and lower cooling energy use at both building and neighbourhood scales [Shashua-Bar et al., 2011; Middel et al., 2015; Ziter et al., 2019]. Three main approaches have been developed to incorporate vegetation. The first integrates urban canopy, energy, and radiative models; for example, Burdet et al. [2014] used *CitySim* to simulate tree shading and radiative exchanges within a 100,m $\times$ 200,m neighbourhood containing 50–100 buildings. The second couples UBEM tools with microclimate models to capture local temperature, wind, and shading effects before energy simulation. This includes the *ENVI-met*–City Energy Analyst framework applied to 208 buildings over 503,956,m^2 in Zurich [Mosteiro-Romero et al., 2020] and the *ENVI-met*–*EnergyPlus* coupling used in a 40,000,m^2 residential district in Thessaloniki to assess tree species and planting configurations [Tsoka et al., 2021]. The third approach directly integrates tree inventory data into UBEM platforms; for instance, Hashemi et al. [2018] combined GIS and the *Urban Modelling Interface (UMI)* with

EnergyPlus to represent 1,142 trees and 933 buildings in the Capitol East neighbourhood of Des Moines.

1.1.4. Research gaps

The above examples demonstrate the potential for incorporating vegetation into UBEM but also highlight several limitations. While simulation-based UBEM methods can model energy demand across large building stocks, the representation of vegetation remains limited. When vegetation is included, applications are typically confined to the small neighbourhood scale, rely on multiple modelling tools, and often depend on microclimatic models that are difficult to scale. Moreover, few studies integrate climate projections or evaluate tree planting within broader PED frameworks.

Urban greening also offers well-documented benefits for climate adaptation, public health, and social equity. The recently proposed 3–30–300 rule provides a clear framework for integrating greenery into urban planning: each resident should see at least three trees from their home or workplace, neighbourhoods should achieve 30% tree canopy cover, and every home should be within 300 m of a public green space [Konijnendijk, 2023]. Achieving these targets is linked to reduced heat stress, lower cooling demand, and improved mental and physical health outcomes [Owen et al., 2024; Konijnendijk, 2023]. Yet, existing UBEM approaches rarely provide the spatial and energy insights needed to inform where trees should be planted to meet such guidelines effectively, limiting their usefulness for climate-resilient, energy-efficient urban design and the development of PEDs.

To address these gaps, this study develops a method for representing tree planting at the neighbourhood scale within a single simulation-based UBEM framework. A simplified tree planting scenario is modelled to examine how tree geometry and seasonal shading behaviour influence heating and cooling demand under current and projected climate conditions. The results show how this representation can generate insights that complement urban greening frameworks such as the 3–30–300 rule. In this way, the approach contributes to PED objectives by linking energy performance, spatial planning, and nature-based solutions. Based on these objectives, the following research questions are proposed.

1.2. Research questions

The study focuses on the spatial representation of tree planting within neighbourhood-scale UBEM. The main research question is:

> How can the spatial representation of tree planting be integrated into UBEM to assess its effectiveness in reducing heating and cooling demand under projected 2050 climate conditions?

To address this question, the study explores the following sub-questions:

- How can tree planting be spatially represented and incorporated into UBEM workflows to capture its impact on neighbourhood-scale building energy demand?
- What assumptions and simplifications are required when incorporating tree planting representations as shading effects on buildings under different climate conditions?

- How can the simulated impacts of tree planting representation be interpreted to support urban planning and climate adaptation strategies?

1.3. Scope

This study examines how the spatial representation of tree planting can be incorporated into UBEM to evaluate potential reductions in heating and cooling demand under projected 2050 climate conditions in the Feijenoord district of Rotterdam. The focus is on how spatial data describing trees can be prepared, represented, and applied within UBEM workflows to support simulation and interpretation of energy impacts at the neighbourhood scale.

The study employs Level of Detail (LoD) 2 city models for buildings, which capture building geometry and roof structures but lack façade, window, and interior detail. Tree data are represented using LoD 1 models, allowing their spatial configuration to be expressed in a simplified geometric form suitable for shading calculations within the energy model. The analysis focuses on how tree representations, as geometric shading elements, influence building energy demand. Other aspects of urban greening, such as biodiversity, social benefits, or microclimatic processes beyond shading, are not included. The intention is to improve the integration of spatial representations of vegetation within UBEM to support long-term simulations under future climate scenarios.

1.4. Thesis outline

This thesis is organised into five main chapters. Chapter 1 introduces the research by presenting the motivation, research gaps, research questions, and scope of the work. It sets the context for the study and explains why tree planting strategies are relevant for neighbourhood-scale energy modelling under future climate scenarios. Chapter 2 reviews the theoretical background and related work. It begins with an overview of building energy modelling before focusing on UBEM approaches. The chapter then examines how trees and vegetation are represented in urban energy systems, concluding with a discussion on CityGML. Chapter 3 describes the methodology used in the study. It outlines the overall research design and workflow, followed by data collection and preprocessing steps. The chapter also explains the development of scenarios, the configuration of models, and the execution of seasonal simulations. Methods for post-processing, analysis, and visualisation are described to show how results are derived and interpreted. Chapter 4 presents the experimental work. It introduces the study area and the datasets required, including building models, climate inputs, tree representations, and topographic information. The chapter then explains the tools and software used, as well as the implementation process. The chapter also outlines assumptions and simplifications, and describes the post-processing and visualisation of the results. Finally, Chapter 5 and 6 discusses and concludes the thesis. It provides a general discussion of the findings, identifies the main contributions, and reflects on the limitations of the work. The chapter concludes by suggesting directions for future research on integrating tree planting strategies into UBEM and their role in developing climate-resilient Positive Energy Districts.

2. Theoretical background and related work

This chapter reviews the theoretical foundations and existing literature relevant to UBEM. It introduces the principles of building energy modelling (BEM), discusses how these methods are adapted to the urban scale, and examines physics-based UBEM tools for estimating heating and cooling demand. Particular attention is given to approaches that integrate vegetation effects into UBEM workflows and evaluate their potential for climate adaptation. The chapter also assesses candidate UBEM platforms, with a focus on SimStadt.

2.1. Building energy modelling

Building Energy Modelling (BEM) is defined as the process of constructing physics-based computational representations of buildings to analyse energy flows, thermal behaviour, and system performance under diverse operational and design conditions [U.S. Department of Energy, 2017]. It has been described as a computational framework that integrates geometric data, envelope properties, mechanical systems, occupancy patterns, and environmental parameters into a unified simulation environment for evaluating building energy performance [U.S. Department of Energy, nd]. BEM has also been defined as a structured mathematical representation of building physics and operations aimed at estimating energy demand and indoor environmental quality [Brackney et al., 2018].

Across these definitions, estimating energy performance and energy demand consistently emerges as the primary goal of BEM. This emphasis is understandable, as buildings are responsible for over 30 % of global final energy consumption and a substantial share of greenhouse gas emissions [International Energy Agency, 2021; Programme, 2019]. Buildings require energy for a range of end uses, including space heating, space cooling, domestic hot water, lighting, appliances, and ventilation systems [Perez-Lombard et al., 2008]. Within this context, research frequently focuses on *heating and cooling loads*, as these account for the majority of building energy use. In Europe, for example, space heating accounts for about 62.5 % of household energy consumption, water heating contributes 15.1 %, and space cooling is 0.6 %, bringing the combined share to nearly 78 % [Eurostat, 2023]. However, cooling demand is projected to increase in many regions as climate change drives higher temperatures and more frequent heatwaves [Masson-Delmotte et al., 2022; Elnagar et al., 2023].

In building energy modelling, the estimation of heating and cooling loads relies on the *heat balance method*, a technique recommended by the American Society of Heating, Refrigerating and Air-Conditioning Engineers (ASHRAE) and the European Committee for Standardisation [Ghiaus, 2022]. This method dynamically balances all energy gains (such as solar and

internal heat) and losses (including conduction, ventilation, and radiation) across the building envelope [ASHRAE, 2014]. It serves as the foundation for various national and regional standards for building energy assessment.

In the European context, such methods are formalised in standards that specify how energy demand must be calculated for regulatory compliance. One widely used example is the German standard *DIN V 18599*, which provides a harmonised calculation framework for determining heating and cooling needs [DIN, 2018, 2016]. Similar frameworks exist elsewhere, such as ISO 52016 at the international level [International Organization for Standardization, 2017] or NTA 8800 in the Netherlands [NTA, 2020], both of which aim to ensure consistency and comparability in building energy assessments.

In DIN V 18599, heating and cooling demand is determined through monthly or hourly energy balances that integrate climatic conditions, envelope heat transfer, internal gains, and ventilation/infiltration within a standardised framework . The standard partitions the building into thermal zones and computes the net energy need in each zone from the balance of gains and losses against defined indoor criteria; heating demand occurs when losses exceed usable gains, while cooling demand is reported when gains surpass acceptable thresholds [DIN, 2016].

Underlying these standards are basic physical formulations of heat transfer. Heat flow through the building envelope is represented as a resistance-based process that accounts for conduction, convection, and radiation [Incropera et al., 2011]. The thermal resistance of a material layer is given by:

$$R_j = \frac{d_j}{\lambda_j} \tag{2.1}$$

The total resistance for a multi-layer assembly is calculated as:

$$R_{\text{tot}} = \frac{1}{h_i} + \sum_{j=1}^{n} R_j + \frac{1}{h_o} \tag{2.2}$$

The corresponding U-value, representing thermal transmittance, is the reciprocal of the total resistance:

$$U = \frac{1}{R_{\text{tot}}} \tag{2.3}$$

This U-value is used to estimate the specific heat flow across the envelope:

$$J = U \cdot (\theta_i - \theta_o) \tag{2.4}$$

where θ_i and θ_o represent indoor and outdoor temperatures, respectively. For transparent surfaces such as windows, DIN V 18599 incorporates additional parameters, including the

g-value (solar transmittance) and corrections for thermal bridges [International Organization for Standardization, 2008, 2017].

The methods discussed above provide detailed estimates of heating and cooling demand at the individual building level. However, applying these approaches directly to neighbourhoods or cities is often limited by data availability and computational complexity. To make large-scale studies feasible, many studies use simplified representations of buildings, such as archetypes based on construction period, typical U-values, or standard window-to-wall ratios [Ghiassi and Mahdavi, 2017]. These simplifications form the basis of UBEM, which adapts building energy modelling methods to the urban scale by combining reduced-order physical models with geographic, demographic, and climate data [Reinhart and Davila, 2016; Hong et al., 2020].

UBEM methods can be categorised into two main types: top-down and bottom-up [Ali et al., 2021; Abbasabadi and Ashayeri, 2019]. Top-down approaches analyse energy use at an aggregated level, incorporating socioeconomic trends, while bottom-up approaches model energy demand from individual buildings. Bottom-up methods include data-driven models, physics-based simulations, reduced-order models, and hybrid approaches that combine multiple strategies [Ferrando and Causone, 2019]. Table 2.1 summarises the strengths and limitations of the main approaches.

Table 2.1.: Comparison of Urban Energy Use Modelling Approaches (adapted from [Abbasabadi and Ashayeri, 2019])

Approach (Example Tools)	**Strengths**	**Limitations**
Top-down *(e.g., LEAP, EnergyPLAN, TIMES)*	- Captures long-term trends - Incorporates techno-socioeconomic effects	- Relies on aggregated data - Generalisation of the status quo - Lacks detail on individual end-uses
Data-driven (Bottom-up) *(e.g., ANN models, Regression, Random Forests)*	- Offers a precise depiction of urban energy consumption - Assesses energy demand across specific end-uses - Efficient in terms of time and computation - Accounts for occupancy patterns and socioeconomic variables	- Relies on historical data - Less cost-effective when data is unavailable - Limited flexibility for design modifications
Simulation-based (Bottom-up) *(e.g., SimStadt, CitySim, CEA)*	- Does not depend on historical datasets - Enables estimation by detailed end-uses - Integrates with BIM tools - Supports renewable energy modelling	- Requires detailed input - Time-consuming and computationally intensive - Simplifies complex urban factors

As shown in Table 2.1, among the approaches compared, only the simulation-based bottom-up method integrates with BIM tools, linking it most directly to detailed spatial representations. Because heating and cooling demand at the urban scale depends on building-level characteristics such as geometry, orientation, and envelope properties, which determine heat gains, losses, and overall energy needs [Ferrando and Causone, 2019; Nouvel et al., 2017], this physics-based approach is therefore selected as the basis for the UBEM tools introduced in the following chapter.

2.2. Physics-based UBEM tools for heating and cooling demand

A range of physics-based UBEM tools for estimating heating and cooling demand at the urban scale has been reviewed [Ferrando et al., 2020]. The study examined *CitySim*, *SimStadt*, *umi*, *CityBES*, *OpenIDEAS*, *CEA*, *URBANopt*, and *TEASER*. As shown in Figure 2.1, the common workflow for this approach typically involves input preparation, model setup, energy simulation, output generation, and post-processing for analysis and visualisation. The figure also shows that although supported by weather data, district system data, and utility rates, most of the model inputs focus on building-related information.

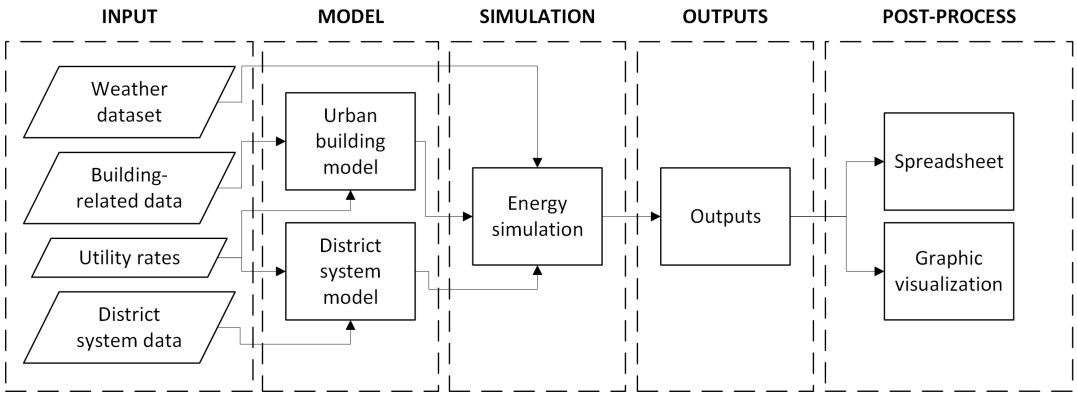


Figure 2.1.: Physics-based UBEM workflow in general (adapted from [Ferrando et al., 2020])

2.3. Representation of trees in physics-based UBEM tools

As shown in Figure 2.1, physics-based UBEM methods focus on building characteristics when estimating energy demand. One parameter that is missing in their typical workflow is vegetation. Yet the role of urban vegetation, such as trees, has gained increasing recognition in recent years. For instance, studies in hot-arid climates have shown that trees reduce solar exposure and improve outdoor thermal comfort [Shashua-Bar et al., 2011]. Modelling research further indicates that expanding tree canopy cover can lower cooling energy demand for individual buildings as well as entire neighbourhoods, with such benefits expected to persist under future climate scenarios [Middel et al., 2015; Ziter et al., 2019].

These energy savings arise from several physical mechanisms. Tree canopies intercept solar radiation, thereby limiting heat gains on building surfaces [Czekajlo et al., 2023]. Through evapotranspiration, leaves release moisture that cools the surrounding air, reducing ambient temperatures near buildings [Yin, 2024]. In colder seasons, trees can also act as windbreaks, slowing air movement and reducing heat loss through infiltration [Liu, 2008].

To capture these effects in physics-based UBEM workflows, three main approaches have been proposed in the literature. The first approach, for example, introduced by [Burdet et al., 2014], combines an urban canopy model, a simplified BEM, and a radiosity-based radiative transfer model into an integrated three-dimensional framework. The radiative exchanges, including the effects of trees, are solved using the *CitySim* software, which computes both short-wave and long-wave radiation fluxes for complex urban geometries. In this study, trees are incorporated as discrete canopy layers that interact with both the radiative and thermal components of the model. In the radiosity scheme, tree crowns reduce and filter incoming solar radiation before it reaches building façades or the ground, while in the BEM, their shading and cooling effects are translated into modified boundary conditions for surface heat gains and losses. The modelling framework is applied at the neighbourhood scale on four hypothetical morphologies, each covering a 100 m $\times$ 200 m plot with 40,000 m^2 of floor area.

The second approach couples UBEM tools with microclimate or urban canopy models that compute locally modified boundary conditions before feeding them into the energy simulation. Here, *ENVI-met* has been widely used. For example, [Mosteiro-Romero et al., 2020] applied a coupling between *ENVI-met* and the City Energy Analyst (CEA) in the Hochschulquartier district in Zurich (main area: 522 m $\times$ 498 m = 259,956 m^2; with a 100 m buffer zone: 503,956 m^2 total). *ENVI-met* simulated local air temperature, relative humidity, and wind speed using a 3D CFD approach with detailed inputs on building geometry, materials, vegetation, and surface properties, while trees were modelled with parameters such as height, leaf area density, albedo, and transmittance to capture shading, evapotranspiration, and wind-flow effects. Hourly microclimate outputs from *ENVI-met* were averaged per building and passed to CEA, which used a resistance–capacitance model to compute sensible and latent cooling loads, accounting for solar gains, ventilation, and infiltration. Comparing the Baseline case (off-site weather data) with the Microclimate case (local simulation data) showed that including microclimate conditions significantly altered predicted cooling energy demands at both the building and district scale.

Another example is presented in [Tsoka et al., 2021], where the influence of different tree species and planting patterns on building cooling energy needs was examined through a one-way coupling between the *ENVI-met* microclimate model and the *EnergyPlus* building energy simulation tool. The study was conducted in a 40,000 m^2 high-density residential neighbourhood in Thessaloniki, Greece, with mid-rise buildings 22–25 m tall. The objective was to assess how variations in Leaf Area Density (LAD) and planting configuration affect local air temperature, solar heat gains on building façades, and the cooling demand of residential units. Three tree species with LAD values of 1.5, 2.0, and 2.5 m^2/m^3 were simulated under two planting patterns. *ENVI-met* first modelled hourly microclimatic conditions for each scenario, and the results were then used to update the weather files in *EnergyPlus* to simulate cooling energy needs on the 1st and 3rd floors of representative residential units. Results showed that dense foliage with continuous canopy planting reduced cooling energy demand by up to 54% for lower floors, while spaced planting and upper floors provided smaller benefits due to reduced shading coverage.

Table 2.2.: Summary of approaches that integrate trees into physics-based UBEM workflows.

Author / Study	**Approach Description**	**Tools / Models Used**	**Scale (Area & Buildings)**	**Key Process Captured**
Burdet (2014)	Integrated 3D framework combining UCM, simplified BEM, and radiation model	• CitySim Urban Canopy Model (UCM) • CitySim Simplified BEM • CitySim Radiosity Model	Neighborhood (100 m × 200 m; 4 morphologies; ∼50–100 buildings)	Radiation + Building Energy + Tree Shading
Mosteiro Romero et al. (2020)	Coupled UBEM–Microclimate model (one-way coupling)	• ENVI-met (microclimate) • City Energy Analyst (CEA)	Neighborhood (Hochschulquartier, Zurich: 503,956 m^2; 208 buildings)	Microclimate (temp, wind) + Building Energy
Tsoka et al. (2021)	Coupled UBEM–Microclimate model (one-way coupling)	• ENVI-met (microclimate) • EnergyPlus (building energy)	Neighborhood (40,000 m^2; ∼20–30 mid-rise buildings)	Microclimate + Tree Species Effects + Energy Demand
Hashemi et al. (2018)	Direct tree inventory integration into UBEM	• GIS (tree/building data) • Grasshopper + Meerkat (3D modeling) • UMI + EnergyPlus (UBEM simulation)	City-near (Capitol East, Des Moines: 1,142 trees; 933 buildings)	Tree Shading Geometry + Energy Demand (no microclimate)

The third approach focuses on the direct integration of tree inventory data into UBEM workflows. In [Hashemi et al., 2018], detailed spatial data on buildings and 1,142 trees in the Capitol East neighbourhood of Des Moines, Iowa, were processed using GIS, Grasshopper, and the Meerkat plug-in to generate a 3D model incorporating both building footprints and tree canopy geometries. This model was then imported into the *Urban Modelling Interface (UMI)*, which relies on *EnergyPlus* for dynamic building energy simulations. Trees were represented as simplified shading devices. Results indicated potential cooling energy savings between 1.% and 20.% during summer months, with greater reductions observed for buildings receiving extensive tree shading, particularly on southern façades. Unlike the first two approaches, this workflow does not yet account for microclimatic processes such as evapotranspiration or wind effects.

Table 2.2 summarises the main approaches for integrating trees into physics-based UBEM workflows. The table shows that, when vegetation is included, most studies rely on multiple tools rather than a single modelling platform. Except for [Hashemi et al., 2018], these studies are also limited to the neighbourhood scale. Together, these findings indicate that no methods currently exist for incorporating vegetation at the city scale within a single modelling platform. Moreover, the widely used physics-based UBEM tools *CityBES*, *URBANopt*, *SimStadt*, and *TEASER/OpenIDEAS* have not yet been explored for vegetation modelling in any published studies. As these tools already support large-scale urban energy modelling, it is necessary to examine their capabilities to determine which platform offers the best potential for incorporating vegetation within a unified, neighbourhood-scale workflow.

To evaluate their potential, these four platforms were compared based on computational, modelling, and data-integration characteristics relevant to extending physics-based UBEM workflows. Following [Ferrando et al., 2020], the assessment considered five aspects that influence the ability of UBEM tools to incorporate vegetation and operate efficiently at larger scales:

- **Simulation engine:** Determines the physical processes that can be represented and the ease of integrating additional modules.
- **GIS and data integration:** Important for including spatially explicit information on vegetation, such as tree locations, and canopy geometry. Compatibility with standards such as CityGML supports the integration of these datasets into UBEM workflows.
- **Computing platform:** Affects scalability and accessibility. Web-based or HPC-dependent tools can handle large simulations, but they often require more complex workflows and external resources. In contrast, PC-based tools typically offer simpler development and deployment options.
- **Scale and applicability:** Determines whether a tool can be used for district-wide analyses. Platforms designed for neighbourhood- or district-scale studies may lack the computational efficiency or data-handling capacity required for larger areas.

Overall, the comparison shows that the tools differ in their ability to represent vegetation processes. *CityBES* and *URBANopt* inherit the physical fidelity of EnergyPlus but require additional modelling effort to incorporate trees beyond static shading. *TEASER/OpenIDEAS* offers flexibility for custom extensions but is less optimised for large-scale GIS workflows. *SimStadt* uses the ISO 13790 heat-balance model and native CityGML integration to achieve computationally tractable, city-scale simulations while maintaining spatial consistency across

Table 2.3.: Comparison of selected physics-based UBEM tools based on key criteria for vegetation modelling (adapted from Ferrando et al. [2020]).

Tool	Modelling Approach	Simulation Engine	GIS & Data Integration	Computing Platform	Scale & Applicability
CityBES	Heat-Balance	EnergyPlus + OpenStudio	CityGML, Energy ADE, GIS	Web-based	City-scale
URBANopt	Heat-Balance	OpenStudio + EnergyPlus	GIS data; HPC support	HPC	District to city-scale
SimStadt	Heat-Balance	ISO 13790 heat-balance model	Full CityGML integration	PC-based	City-scale
TEASER/OpenIDEAS	Reduced-order RC model	Modelica (FastBuildings)	CityGML, Energy ADE, archetypes	PC-based	District-scale

datasets. However, this comes at the cost of limited representation of microclimatic feedbacks such as evapotranspiration or wind sheltering, which would require external coupling.

Table 2.4.: Strengths and weaknesses of selected physics-based UBEM tools for vegetation modelling.

Tool	**Strengths**	**Weaknesses**
CityBES	- Mature web platform; EnergyPlus-based detail - Good documentation; supports Energy ADE	- No native vegetation module; vegetation typically via custom shading objects or external coupling - Heavier setup to represent microclimate effects
URBANopt	- Modular pipelines; HPC support for scale - EnergyPlus/OpenStudio ecosystem	- Vegetation requires external pre/post-processing or custom measures - Workflow complexity increases for city-wide runs with vegetation
SimStadt	- ISO 13790 heat-balance model scales to city - Native CityGML ingestion and Energy ADE interoperability - Workflow modularity for batch analyses	- Vegetation may be represented as building-like objects - Limited direct representation of evapotranspiration and wind effects without coupling
TEASER/ OpenIDEAS	- Python/Modelica openness; archetype flexibility - Useful for prototyping	- Weaker native GIS workflows at very large scale - Vegetation/microclimate needs external models or custom code

Table 2.3 and Table 2.4 indicate that *SimStadt* provides a suitable basis for extending UBEM workflows to include vegetation at the city scale. Its ISO 13790 heat-balance approach offers the computational efficiency required for large-scale simulations, while the native CityGML integration enables direct use of spatial datasets representing trees and canopy geometry. And as a PC-based platform developed for urban-scale applications, *SimStadt* combines scalability with moderate computational demands, aligning well with the requirements of this study.

A main limitation of this approach is that vegetation is represented as simplified building objects within the *SimStadt* workflow. This configuration enables the modelling of shading effects but not evapotranspiration, wind flow, or seasonal canopy dynamics. As a result, trees act as static obstructions to solar radiation rather than thermally dynamic vegetation elements. While this representation ensures consistent treatment of shading across the model domain, it may introduce minor artefacts in the radiative balance, as these objects are treated as opaque surfaces rather than porous or reflective canopies. Given the objectives of

this study, which focus on neighbourhood-scale assessment and scenario comparison, these simplifications are considered acceptable but should be acknowledged when interpreting results.

2.4. GIS-based UBEM: SimStadt

SimStadt is a workflow-driven simulation platform that supports the CityGML standard to facilitate energy analyses. It provides tools to assess energy demand, solar energy potential, CO_2 emissions, and refurbishment strategies using modular and extensible workflows [Nouvel et al., 2015]. Unlike high-resolution simulation tools such as EnergyPlus or CitySim, which rely on detailed building-level data and dynamic simulations, SimStadt employs a more scalable, archetype-based approach. It uses predefined building typologies and statistical assumptions to estimate annual energy performance, enabling large-scale urban analyses with lower computational demands. This trade-off makes SimStadt well-suited for district- or city-level planning [Nouvel et al., 2017].

SimStadt's modelling workflow is hierarchical and modular, consisting of sequential and parallel processing steps that handle tasks such as weather data integration, geometry preprocessing, building usage characterisation, radiation analysis, energy balance computation, and result visualisation. Each component is implemented in Java and can be edited or extended using a graphical user interface, which also allows for scenario customisation and inspection of intermediate results. The integration of physical and semantic building data, enriched through the Energy ADE extension [Nouvel et al., 2015]. The current version of SimStadt integrates historical or standard climate data from sources such as PVGIS and Meteonorm [Nouvel et al., 2015]. The modular structure permits the incorporation of alternative weather datasets. This feature enables users to simulate climate change scenarios by inputting projected temperature, humidity, and radiation profiles under various future conditions.

2.4.1. DIN V 18599: Monthly energy balance standard

An element of SimStadt's energy demand estimation is the calculation of monthly space heating demand based on the *DIN V 18599* standard, which is derived from the international norm *ISO 13790*. This standard forms the basis of the `MonthlyEnergyBalance` workflow step within the platform and provides a consistent methodology for evaluating building energy performance using parameters such as geometry, thermal properties, usage profiles, and local climatic conditions [Nouvel et al., 2015].

DIN V 18599 covers monthly energy balance calculations for heating, cooling, ventilation, domestic hot water, and lighting. Its application became mandatory in Germany in 2024 for both residential and non-residential buildings. The standard enables performance comparisons using a reference-building approach, where the evaluated building is compared against a baseline defined by standardised parameters. Compliance is achieved if the calculated primary energy demand remains within specified limits [GmbH, 2023]. Due to the level of detail involved, software tools such as SimStadt are typically used to apply the standard, particularly during early-stage design and scenario development [Reiser et al., 2008].

It should be noted that this study applies the *DIN V 18599* standard to a case study in the Netherlands. Since the standard was developed for the German context, including its building regulations and energy performance benchmarks, applying it to a different country introduces a limitation. Differences in building practices and regulatory frameworks may affect the accuracy and representativeness of the results, and these factors should be considered when interpreting the findings.

2.4.2. CityGML

CityGML is an open data model and XML-based standard for representing and exchanging virtual three-dimensional city models [Gröger et al., 2012]. Implemented as an application schema of the Geography Markup Language (GML), it combines geometric, semantic, and topological information within a unified framework. The standard is structured into a *core module* and several *thematic modules*, each addressing specific categories of urban features. Thematic modules include Building, Vegetation, Transportation, WaterBody, LandUse, Relief, Tunnel, Bridge, CityFurniture, CityObjectGroup, Generics, Appearance, and the now-deprecated TexturedSurface module [Gröger et al., 2012]. The core module defines common concepts such as object identifiers, metadata, and spatial references, while the thematic modules extend this foundation to represent domain-specific objects.

In practice, many three-dimensional city models focus on the *Building* module, which is considered the most developed and widely used within CityGML [Noardo et al., 2021]. Typical city models also incorporate the Vegetation, Transportation, and Relief modules, as these represent essential structural, environmental, infrastructural, and terrain-related features commonly required in urban planning and visualisation tasks [Ohori et al., 2018].

The **Building module** provides a framework for representing buildings across multiple levels of detail (LOD0–LOD4). At lower LODs, buildings are represented as simple footprints or roof outlines, while higher LODs include additional geometric and semantic details. LOD4, the highest level, supports interior representations such as rooms, doors, and furniture. The module is organised around the abstract class *_AbstractBuilding*, forming the basis for both the *Building* and *BuildingPart* classes. Attributes such as function, usage, roof form, year of construction, and number of storeys support a variety of analytical and planning applications [Gröger et al., 2012].

The **Vegetation module** extends the model to natural elements within urban environments. It differentiates between individual objects, represented by the *SolitaryVegetationObject* class, and continuous vegetation areas, described by the *PlantCover* class. Attributes such as species, height, canopy size, and coverage type support ecological analysis and visualisation. As with buildings, vegetation objects can be represented across multiple levels of detail, and repeated objects, such as identical trees, can be defined once and referenced in multiple locations to optimise data efficiency [Gröger et al., 2012].

CityGML provides the underlying data framework for UBEM by combining geometric and semantic information in a structured format. Its spatio-semantic model enables the representation of buildings at multiple levels of detail, linking geometric attributes with descriptive information such as function, construction year, and use. As noted by [Nouvel et al., 2014], this structure makes CityGML an effective database for analysing the heating demand of building stocks, since the same model can supply both geometric and semantic inputs to simulation tools such as SimStadt. This integration allows the automatic derivation of

energy-relevant parameters and supports consistent urban-scale analyses. A dedicated extension has also been developed, known as *Energy ADE (Application Domain Extension)*. The Energy ADE extends CityGML with concepts for building physics, occupant behaviour, construction materials, and energy systems, enabling both detailed simulations and city-wide assessments. By improving interoperability across tools and datasets, and through implementations such as its integration into the 3D City Database, the Energy ADE supports more consistent and scalable urban energy modelling [Agugiaro et al., 2018].

3. Method

Building on the theoretical background and tool assessment presented in Chapter 2, this chapter outlines the methodological framework developed to integrate the spatial representation of tree planting into neighbourhood-scale UBEM. The methods are designed to address the main research question. The chapter describes the overall research design and simulation workflow, including the development of climate and vegetation scenarios, data preparation, and model configuration within the *SimStadt* platform. It also details the simplifications and assumptions applied to represent vegetation, as well as the procedures for simulation, post-processing, and spatial analysis.

3.1. Research design and workflow overview

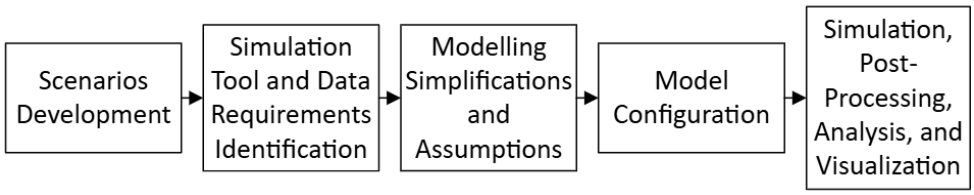


Figure 3.1.: Methodological workflow for neighbourhood-scale energy demand assessment.

This research uses a scenario-based simulation approach to address the main research question: How can tree planting scenarios, as nature-based strategies, be integrated into neighbourhood-scale simulation-based UBEM to evaluate their effectiveness in reducing heating and cooling demand under the projected 2050 climate conditions? Since existing district-wide UBEM tools provide only limited ways of representing vegetation, the study adopts a workflow that combines simplified vegetation modelling with climate scenario adjustments. As shown in Figure 3.1, the framework follows a five-stage process: (i) scenario development, (ii) simulation tool and data requirements identification, (iii) modelling simplifications and assumptions, (iv) model configuration, (v) simulation execution, post-processing, analysis, and visualisation.

3.2. Scenario development

To clearly separate the effects of vegetation and climate change on heating and cooling demand, six scenarios were designed with a stepwise approach. This structure avoids overlapping influences and provides a consistent basis for comparison across different conditions.

The control scenarios (S0 and S3) include only buildings and are simulated under present and 2050 climate conditions, serving as the reference cases. The baseline scenario (S1) adds existing trees under present conditions to represent the current district state, while the enhanced scenario (S2) includes both existing and proposed trees to assess the impact of additional planting. Under 2050 climate conditions, the baseline future scenario (S4) combines buildings with existing trees, and the enhanced future scenario (S5) adds proposed trees to evaluate whether increased planting can mitigate projected cooling demand. Figure 3.2 provides a visual illustration of all six scenarios.

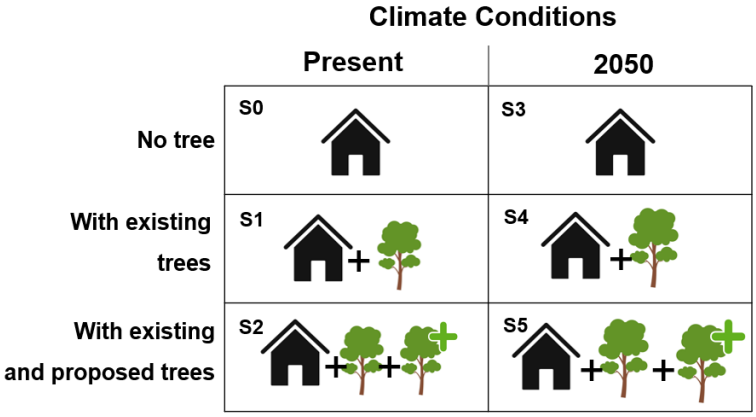


Figure 3.2.: Overview of the six designed scenarios combining three vegetation settings with two climate conditions. Scenarios S0 and S3 are reference cases without vegetation, S1 and S4 include existing trees, and S2 and S5 include both existing and proposed trees under present and future climate conditions.

3.3. Simulation tool and data requirements identification

After defining the simulation scenarios, a modelling framework was required to analyse district-scale heating and cooling demand. The framework needed to handle multiple scenarios, integrate spatial and climatic datasets, and account for both present and future climate conditions. Based on the review in Chapter 2, *SimStadt* was selected for its suitability for district-scale energy analysis. In this study, the *Heat Demand Analysis* workflow within *SimStadt* was used to estimate annual space heating and cooling demand.

The *Heat Demand Analysis* workflow consists of a series of interconnected modules that process geometric, physical, usage, climatic, and radiative data before calculating the building-level energy balance. The main modules include *ImportCityGML*, *Geometric Preprocessor*, *Geometric Estimator*, *Physics Preprocessor*, *Usage Preprocessor*, *WeatherProcessor*, *IrradianceProcessor*, and *Monthly Energy Balance*. An overview of these modules is shown in Figure 3.3.

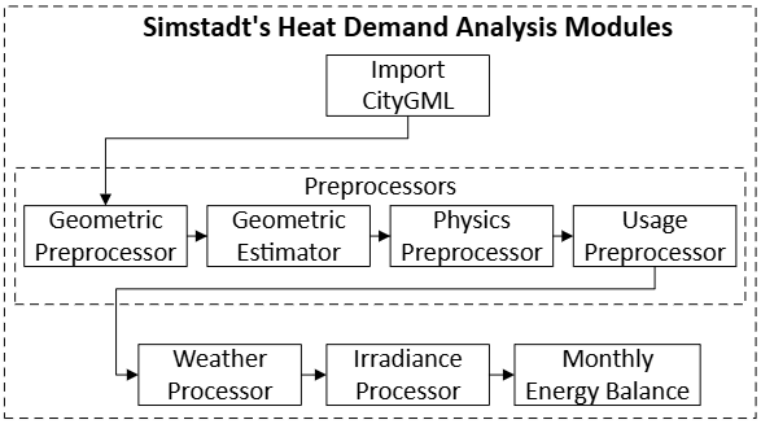


Figure 3.3.: Overview of the modules executed in the *SimStadt Heat Demand Analysis* workflow, including data import, preprocessing, climatic processing, and energy balance calculation.

To run the workflow, several input datasets must be prepared in formats compatible with *SimStadt*. These datasets describe the built environment, vegetation, weather, and the wider urban context. Because the geometric processors in *SimStadt* accept only CityGML-formatted building geometries, other spatial data such as vegetation layers were converted into equivalent CityGML geometries. This allowed vegetation objects to be included in the simulation alongside buildings, ensuring that shading and radiative effects were properly represented.

Weather data were processed through the *WeatherProcessor* module. The workflow requires monthly values of global horizontal irradiance (GHI) in W/m^2 and ambient air temperature in °C. These can be obtained from the INSEL offline database, the PVGIS online database, or local TMY3 files containing either hourly or monthly values. When only monthly data are available, *SimStadt* automatically generates synthetic hourly profiles for irradiance and temperature to support the energy balance calculation. In this study, monthly TMY3 data were used to enable consistency between present-day and future climate datasets.

The *IrradianceProcessor* module computes solar irradiance on building surfaces by considering direct, diffuse, and reflected radiation. Several radiation models are available in *SimStadt*. The `INSEL_Hay` and `INSEL_Perez` models provide quick estimates but do not account for shadowing, while the `SRA_Perez` variants incorporate shading effects through the Simplified Radiosity Algorithm (SRA). The `SRA_Perez_with_tiling` configuration was used in this study, as it includes shading from geometric inputs such as vegetation and improves computational efficiency by dividing the study area into smaller, overlapping tiles for parallel processing.

Overall, the datasets and preprocessing steps described above ensure that geometric, climatic, and contextual data are fully integrated within the *SimStadt Heat Demand Analysis* workflow, supporting consistent simulations for both present and future conditions. Table 3.1 summarises the datasets used, their main characteristics, and the preprocessing steps required to ensure compatibility.

Table 3.1.: Datasets required for the simulation workflow, including their purpose, format, and preprocessing considerations to ensure compatibility with *SimStadt*.

Dataset	Description	Preprocessing Considerations
Buildings	Geometric representations (LoD1 or LoD2) with construction year and usage type.	Data cleaning, error correction, and attribute enrichment.
Vegetation – Existing Trees	Locations and attributes of existing trees.	Conversion to CityGML geometries; seasonal variation considered.
Vegetation – Proposed Trees	Planting sites derived from land-use layers for future scenarios.	Scenario-specific selection; same representation as existing trees.
Weather Data	Monthly values of global horizontal irradiance and ambient temperature (TMY3).	Formatting and source selection.
Urban Context	District boundaries and land-use layers.	Coordinate system harmonisation and format conversion.

3.4. Modelling simplifications and assumptions

Building on the dataset requirements outlined in the previous section, additional simplifications and assumptions were needed to represent vegetation, seasonal dynamics, and future climate conditions within the simulation framework. These were necessary to ensure consistent modelling across all scenarios despite the geometric and functional limitations of *SimStadt*. The main assumptions are summarised as follows:

- **Tree Representation:** All trees were represented as simplified cylindrical geometries for processing within *SimStadt*. This decision was mainly driven by the computational and algorithmic constraints of the Simplified Radiosity Algorithm (SRA) used in the *IrradianceProcessor*. According to the *SimStadt* documentation [HFT Stuttgart, 2024], the SRA can become slow or unstable when applied to large and complex geometric scenes. Simplifying the vegetation geometry was therefore necessary to maintain numerical stability and manageable computation times.

  Alternative representations, such as detailed tree models available in the original CityGML dataset from the Rotterdam Municipality, were considered but not adopted. While this form could, in theory, provide a more realistic depiction of canopy volume and shading distribution, its higher polygon counts and irregular surface geometries would substantially increase the computational burden on the SRA, with limited improvement in radiative accuracy at the neighbourhood scale. Cylindrical geometries were therefore selected as a compromise: they more plausibly capture the vertical structure of trees than cubes while remaining computationally efficient for geometric and radiative processing.

  Furthermore, to ensure that vegetation objects were retained throughout the workflow, each tree was assigned a generic construction year and the `residential building`

category (code 1010). This step prevented the *PhysicsPreprocessor* from discarding non-building geometries, allowing all trees to be included in the radiative calculations across all scenarios.

- **Foliage Density:** For deciduous trees, seasonal variation in leaf coverage was represented by assigning full foliage in summer ($1 \times D_c$) and reduced foliage in winter ($0.64 \times D_c$), where D_c is the cylindrical diameter of each tree. The 0.64 factor was chosen as a simplified approximation based on studies reporting that the Leaf Area Index (LAI) of temperate deciduous trees typically decreases by 40–60% from summer (e.g., 3–5 m^2/m^2) to winter (e.g., 1–3 m^2/m^2). This approach allowed the model to capture the main seasonal effects on shading while avoiding the need for detailed phenological data, which were not available for the study area. However, it only differentiates between deciduous and evergreen trees and does not account for species-specific canopy characteristics, gradual seasonal transitions, or interannual variability.
- **Proposed Trees:** All proposed trees in current and future scenarios were assumed to be deciduous and were assigned uniform height and cylindrical diameter across all locations. This assumption ensured comparability across the study area and reduced uncertainties related to species-specific growth data, which were unavailable for all proposed planting sites. Potential planting sites were identified within available open spaces according to land-use suitability, while areas overlapping with infrastructure, water bodies, buildings, or roads were excluded using predefined distance rules. The remaining suitable areas were then populated with evenly spaced planting points to represent possible future tree locations.
- **Future Tree Growth:** For trees with known planting years, growth until 2050 was estimated using a simple linear growth rate. To maintain realistic tree dimensions within dense urban environments, maximum values of +2 m for cylindrical diameter (D_c) and +2.5 m for height (H) were imposed, reflecting typical pruning and maintenance practices that limit tree size near infrastructure and utilities.
- **Future Climate Conditions:** Monthly changes in average temperature and global radiation were incorporated for the 2050 climate scenarios. This temporal resolution was chosen to ensure consistency with the datasets used in weather processor modelling.

3.5. Model configuration

The model configuration stage prepared all spatial datasets for the simulation workflow in *SimStadt*. It consisted of three main steps: (i) preparing the building model, (ii) preparing the vegetation models for existing and proposed trees, and (iii) combining all datasets into a single, simulation-ready model.

3.5.1. Building model preparation

The building model was prepared using CityGML LoD2 geometries, with attributes including construction year, usage type, and heated floor area. Data cleaning steps involved correcting geometry errors, harmonising coordinate systems, and enriching building attributes with additional parameters required by *SimStadt* (e.g., construction year, building usage). The cleaned and formatted building model served as the base layer for all scenarios.

3.5.2. Vegetation model preparation

Two vegetation models were developed to represent existing and proposed trees. Both models were prepared in the CityGML format so they could be processed together with the building dataset in SimStadt. Data for existing trees were obtained from the municipal vegetation database. The raw dataset was cleaned by separating tree crowns, removing duplicates, and trimming the extent to match the study area. Tree crowns were then converted from three-dimensional geometries to two-dimensional footprints. Each footprint was classified as either deciduous or evergreen. Seasonal conditions were modelled for both current and future scenarios. For the summer model, only trees located within the study boundary were retained, and any overlap with building footprints was eliminated. The processed dataset was saved as the final summer model. For the winter model, crown diameters were reduced to represent seasonal shrinkage, and the resulting dataset was saved as the winter model. All two-dimensional crowns were extruded into three-dimensional Level of Detail 1 (LOD1) tree models.

For the proposed vegetation, potential planting areas were identified using land-use and open-space layers. The study area was divided into suitable (A1) and unsuitable (A2) zones. Buffer constraints were applied to A2, and unsuitable regions were excluded to produce the refined A1–A2 area. A tile grid was then generated to structure the remaining space. Each cell within the grid was evaluated, and only those with a minimum area of 19 m^2 were retained. From these filtered cells, points were generated and assigned elevation values to create an intermediate dataset of proposed tree locations. Using this dataset, tree polygon boundaries were produced for both summer and winter conditions under current and future scenarios. These two-dimensional polygons were then extruded into three-dimensional LOD1 tree models with uniform dimensions and growth parameters.

3.5.3. Model integration

For each scenario and season, the final input model was generated by integrating the processed building and vegetation datasets. The resulting datasets formed the basis for all simulations carried out in this study. Table 3.2 provides an overview of the scenario contents for both summer and winter runs.

Table 3.2.: Scenario datasets prepared for summer and winter simulations. Summer runs use full tree canopy dimensions, while winter runs use reduced dimensions.

Scenario (Summer/Winter)	Buildings	Existing trees	Proposed trees
S0 (Current Climate)	✓	–	–
S1 (Current Climate)	✓	✓	–
S2 (Current Climate)	✓	✓	✓
S3 (Future Climate)	✓	–	–
S4 (Future Climate)	✓	✓	–
S5 (Future Climate)	✓	✓	✓

3.6. Simulation, post-processing, analysis, and visualisation

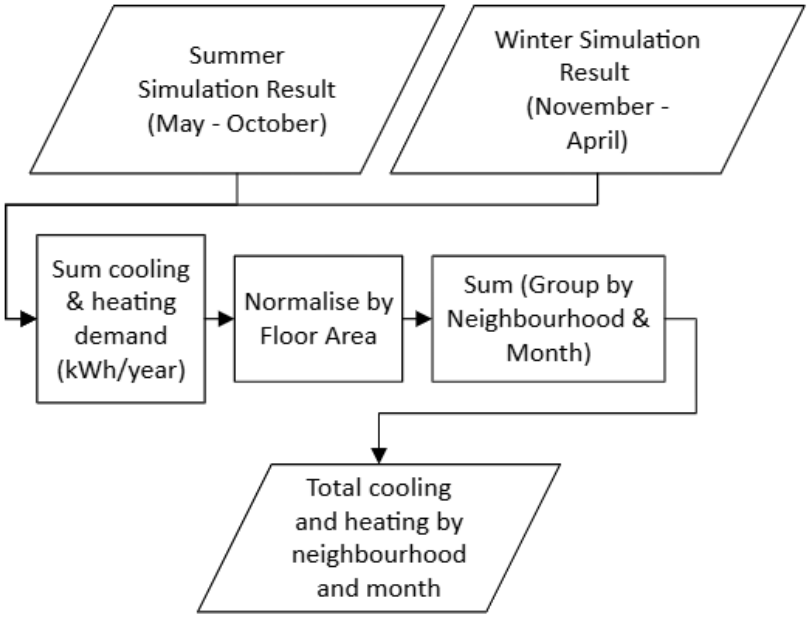


Figure 3.4.: Flowchart for post-processing workflow.

After preparing the input datasets for each scenario and season, simulations were carried out to estimate building-level heating and cooling demand under both present and future climate conditions. The post-processing workflow, illustrated in Figure 3.4, began by loading the summer and winter simulation results separately. For the summer dataset, only rows corresponding to May–October were retained, while November–April rows were used for the winter dataset. These seasonal datasets were then combined to produce full-year values by summing the monthly results, yielding the total annual heating and cooling demand (kWh/year) for each building. To enable comparisons across buildings of different sizes, the annual demand was normalised by dividing by each building's floor area, resulting in heating and cooling demand per unit area (kWh/m²/year). The processed results were then linked to the building polygon dataset, and further aggregation was performed by neighbourhood and month. This neighbourhood-level aggregation was used to assess how climate change alone is expected to influence energy demand.

Figure 3.5 illustrates the next steps taken for analysing the impact of additional tree planting on building heating and cooling demand under both current and future climate conditions. Scenarios with existing trees only were compared to those including both existing and proposed trees to isolate vegetation effects. For each climate condition, absolute and relative differences in energy demand per unit floor area were calculated, and spatial patterns were visualised using colour-coded maps. The contribution of each proposed tree was evaluated by comparing energy demand in scenarios with and without that tree. Trees that reduced heating or cooling demand were classified as having a positive impact, while those with no change or higher demand were classified as having no or a negative impact. The final output

was a tree impact map, showing the spatial distribution of trees with positive, neutral, and negative effects on building heating and cooling demand.

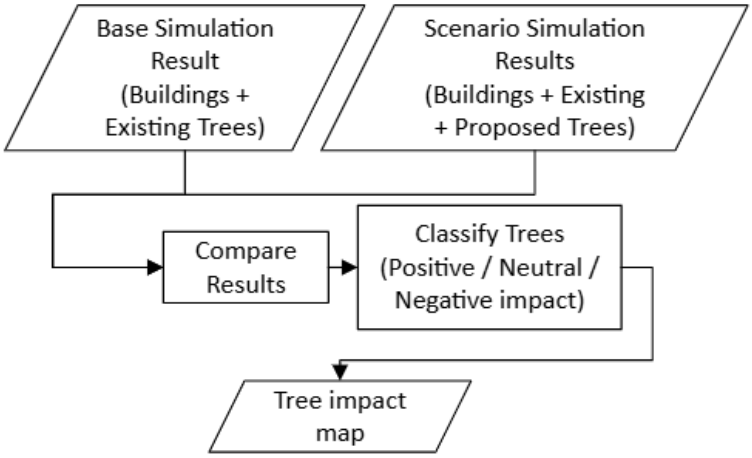


Figure 3.5.: Flowchart for analysis and visualisation.

4. Experiments

This chapter presents the experiments conducted to evaluate the proposed methodology. It describes the datasets used, the experimental setup, and the implementation details necessary to reproduce the results.

4.1. Study area

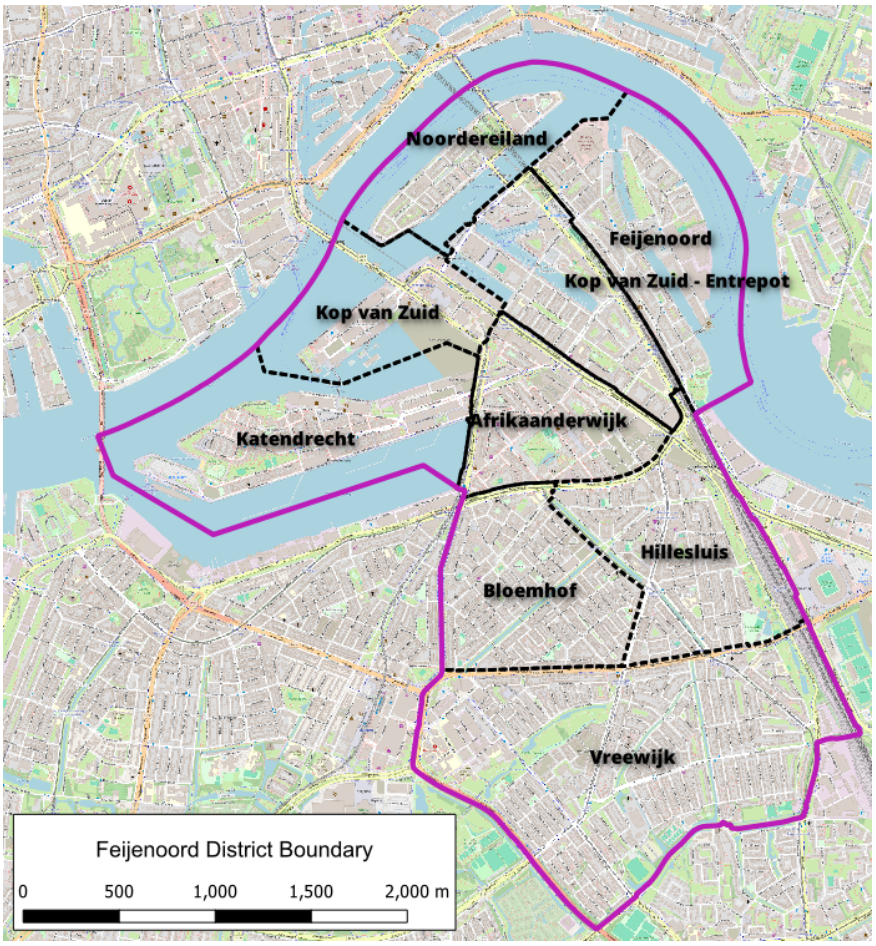


Figure 4.1.: Feijenoord District

The Feijenoord district is a densely populated area with characteristics that make it an ideal location for this study. Feijenoord is a predominantly urban area with one of the most 'stony' neighbourhoods in Rotterdam, where the limited presence of green spaces is impacting residents' health and liveability, particularly during summer heat events [URBACT, 2020]. Furthermore, its location below sea level and exposure to climate vulnerabilities have identified it as a priority area within Rotterdam's long-term urban resilience planning [URBACT, 2020]. The Feijenoord district in Rotterdam has nine neighbourhoods, which are Afrikaanderwijk, Bloemhof, Hillesluis, Feijenoord, Vreewijk, Kop van Zuid, Noordereiland, Katendrecht, and Entrepot. An overview of the district's boundaries is shown in Figure 4.1.

4.2. Data required

4.2.1. Building model in CityGML LoD2

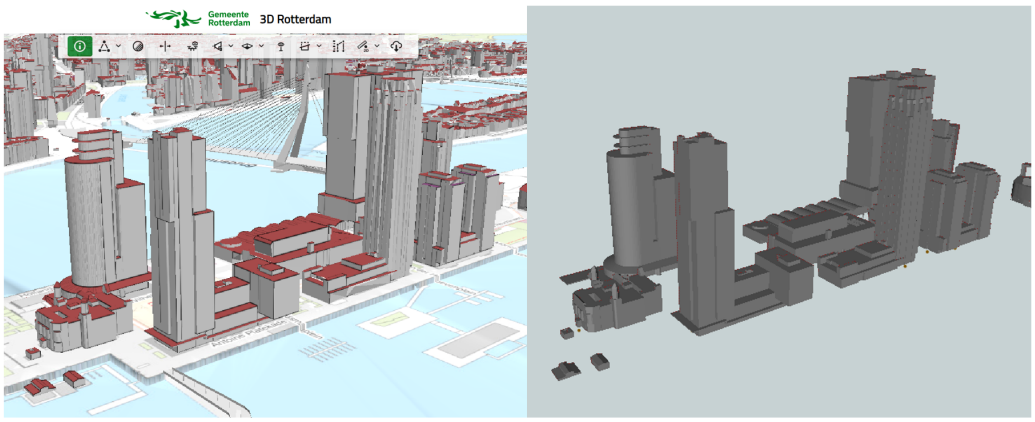


Figure 4.2.: Building dataset viewed on the 3D Rotterdam web viewer (left) and in FME Data Inspector (right). The dataset represents the CityGML LoD2 building model of the Rotterdam area.

Figure 4.2 shows the LoD2 building dataset as viewed on the 3D Rotterdam platform and in FME Data Inspector for inspection and processing. The Rotterdam 3D city model provides geometric and semantic data for buildings [Gemeente Rotterdam, nd]. The building data is available as open data in the CityGML format and can be accessed through the municipality's official data portal. Corrections to the dataset supplied by the municipality were carried out in an earlier project supervised by the supervisors of this study. This previous work [Gao et al., 2025] involved verifying geometric correctness using the CityDoctor tool and generating additional outputs. One of its outcomes was the development of a pipeline for cleaning, correcting, and enriching the CityGML building data after reprojection to EPSG:28992.

4.2.2. Current and 2050 projection climate inputs

The current climate data, provided in TMY3 format from *previous work* [Gao et al., 2025], represent monthly values for Rotterdam and serve as the baseline for energy demand sim-

ulations. Table 4.1 presents the monthly radiation values and temperature for the current climate, while Table 4.2 summarises air pressure, wind speed, and cloud cover, which are assumed to remain unchanged in the 2050 scenario.

Month	G_{Gh}	G_{Bn}	G_{Dh}	Temp (°C)
Jan	29	9	19	4.1
Feb	56	23	33	4.5
Mar	104	48	56	6.7
Apr	167	85	83	9.6
May	210	109	100	13.3
Jun	225	114	110	16.2
Jul	214	107	107	18.2
Aug	181	89	92	18.1
Sep	125	58	68	15.3
Oct	71	28	42	11.6
Nov	33	10	23	7.6
Dec	21	6	15	4.8

Table 4.1.: Monthly global (G_{Gh}), beam (G_{Bn}), diffuse (G_{Dh}) radiation in kWh/m^2 and average air temperature (°C) for current climate (1991–2019).

Month	p (hPa)	FF (m/s)	N (1–8)
Jan	1017	5.4	6
Feb	1016	5.2	6
Mar	1016	4.8	5
Apr	1015	4.2	5
May	1016	4.0	5
Jun	1007	3.9	5
Jul	1016	3.8	5
Aug	1016	3.6	5
Sep	1016	3.7	5
Oct	1015	4.4	6
Nov	1013	4.6	6
Dec	1015	5.1	6

Table 4.2.: Monthly mean air pressure (p), wind speed (FF), and cloud cover (N) for the projected 2050 climate scenario.

For the 2050 scenario, global radiation and temperature data were obtained from [KNMI, 2025], which contains historical meteorological observations transformed using the KNMI'23 climate projections. The data correspond to station 461 (Barendrecht) with auxiliary input from station 344 (Rotterdam) in Zuid-Holland (longitude 4.535°E, latitude 51.838°N). Among the four KNMI'23 scenarios (Wd, Wm, Md, Mm), the *Md* pathway was selected as it represents a mid-range emission trajectory, avoiding both high- and low-emission extremes while remaining relevant for policy and research applications [van Dorland et al., 2023].

4.2.3. Vegetation data

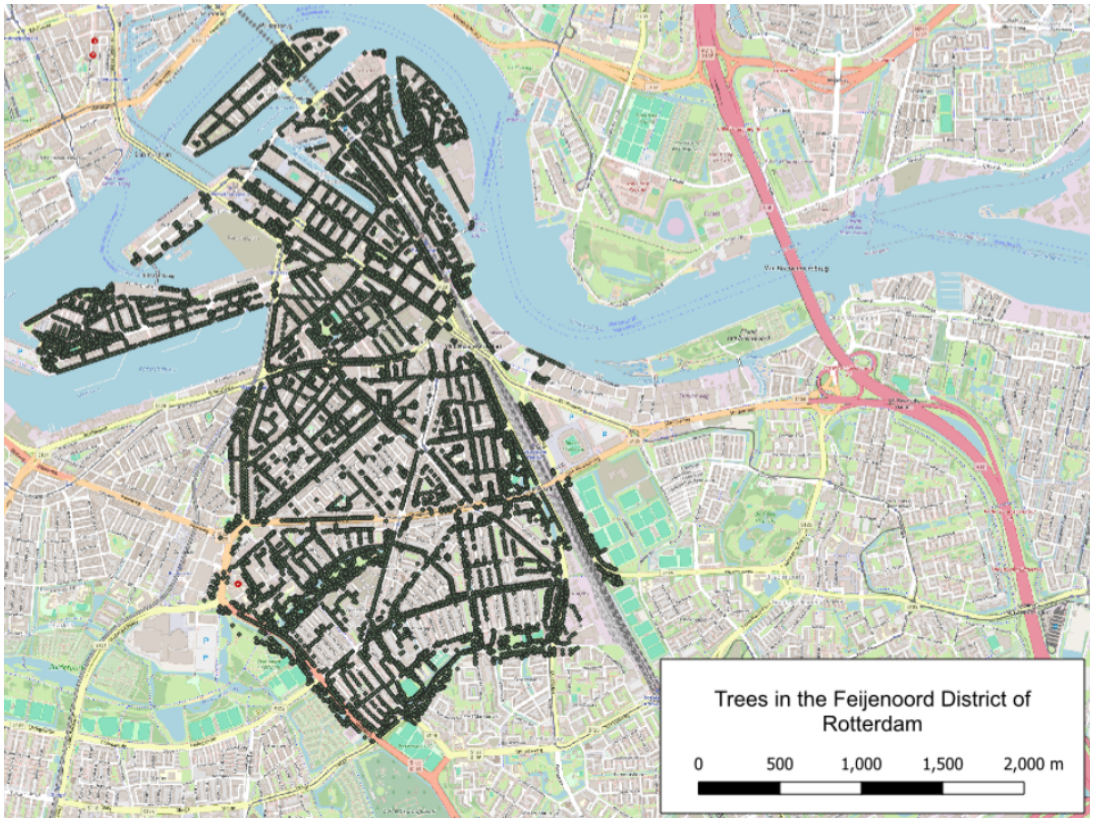


Figure 4.3.: Trees in the Feijenoord District of Rotterdam

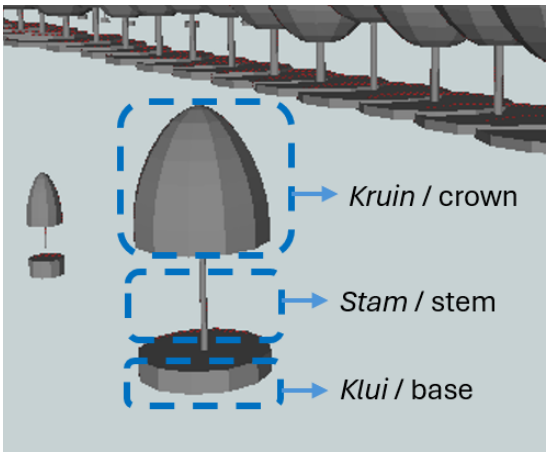


Figure 4.4.: Tree Implicit Geometry

Tree data were extracted from the vegetation features of the Rotterdam 3D city model. The spatial distribution of the extracted tree points for the Feijenoord district is illustrated in Figure 4.3. The data are available per neighbourhood. In CityGML, trees are represented as *SolitaryVegetationObject*, which inherits from the *_VegetationObject* and *_CityObject* classes. The dataset therefore contains a combination of core GML identifiers, standard CityGML attributes, vegetation-specific attributes, and locally defined Application Domain Extension (ADE) attributes originating from the municipal tree registry. A summary of these attributes is provided in Table A.1. As shown in Figure 4.4, in the dataset, the tree representation is decomposed into three components: *kruin* (crown), *stam* (trunk), and *kluit* (root base). These components are parametrised by the corresponding attributes in the dataset, which are tree height, crown diameter, and trunk diameter.

4.2.4. Land use layers

The land-use layers, including vegetated terrain, non-vegetated terrain, functional areas, roads, and water bodies, were obtained from the *Basisregistratie Grootschalige Topografie* (BGT) dataset via PDOK [PDOK, 2025]. Building data was extracted from the 3D CityGML building footprint dataset. Additional information on underground cables and pipelines was provided by the Municipality of Rotterdam (private dataset, not publicly available). The extracted layers and their corresponding geometry types are summarised in Table 4.3.

Table 4.3.: Extracted layers and their geometry types

Layer	**Geometry Type**
Vegetated terrain (*begroeidterreindeel*)	Polygon
Non-vegetated terrain (*onbegroeidterreindeel*)	Polygon
Functional areas (*functioneelgebied*)	Polygon
Buildings (*pand*)	Polygon
Roads (*wegdeel*)	Polygon
Water bodies (*waterdeel*)	Polygon
Cables and Pipes	Line
Utility boxes (*kast*)	Point
Wells (*put*)	Point
Masts (*mast*)	Point
Poles (*paal*)	Point

4.2.5. Data summary

Table 4.4 provides an overview of the main datasets, their temporal coverage, and the corresponding sources.

Data Category	Dataset	Data Period	Source
Buildings	Rotterdam 3D City Model (Bullding LoD2)	–	[Gemeente Rotterdam, nd]
Climate (Current)	TMY3 data for Rotterdam	1991–2019	*Previous work: a DigiTwins4PEDs project supervised by the supervisors* [Gao et al., 2025]
Climate (Projection)	KNMI'23 Scenario Md	2050	[KNMI, 2025]
Vegetation	Rotterdam 3D City Model (SolitaryVegetationObject)	–	[Gemeente Rotterdam, nd]
Land Use	Basisregistratie Grootschalige Topografie (BGT)	–	[PDOK, 2025]
Underground Utilities	Municipality of Rotterdam (private dataset)	–	Municipality of Rotterdam

Table 4.4.: Summary of datasets used in this study.

4.3. Tools and software

SimStadt was chosen as the UBEM platform to perform energy demand and solar potential simulations. It provided the computational framework for analysing building energy performance at the district scale. For data processing, integration, and enriching the CityGML model with energy-related information, the Feature Manipulation Engine (FME) served as the primary tool. Its capabilities enabled efficient data conversion and preprocessing to prepare inputs for the simulations. Finally, QGIS was used for spatial analysis and visualisation. It facilitated the interpretation of simulation results and supported the creation of maps and other spatial outputs.

4.4. Implementation details

As described in the methodology chapter, the research framework follows a five-stage process. This section focuses on the stages that follow scenario development, where the modelling simplifications and assumptions introduced earlier are implicitly applied. Using the datasets and tools presented in the previous sections, the implementation includes data preparation, simulation setup, and the steps for execution, post-processing, analysis, and visualisation.

4.4.1. Preparing building data

As described in the methodology, the raw CityGML files were processed following the workflow outlined in [Gao et al., 2025]. Geometry correction and validation were performed in that earlier work and are not explained in this thesis. Data cleaning and formatting in this study followed the same procedure established by [Gao et al., 2025] and are described in Section 4.4.5, as the building data preparation was integrated with the simulation model configuration.

4.4.2. Preparing existing tree data

Figure 4.5 shows the complete processing workflow for deriving both the summer and winter of existing tree boundaries. As described in Section 4.2, vegetation representation in this study is structured into three components. The processing begins by filtering the CityGML dataset to extract only tree crowns, identified by `gml_id` values ending with _k, using the *TestFilter* transformer. To ensure unique records, a *DuplicateFilter* transformer is applied. This step is necessary because the original CityGML data were downloaded using bounding boxes instead of the precise extents of each neighbourhood, which can lead to overlapping or duplicated features along boundary areas.

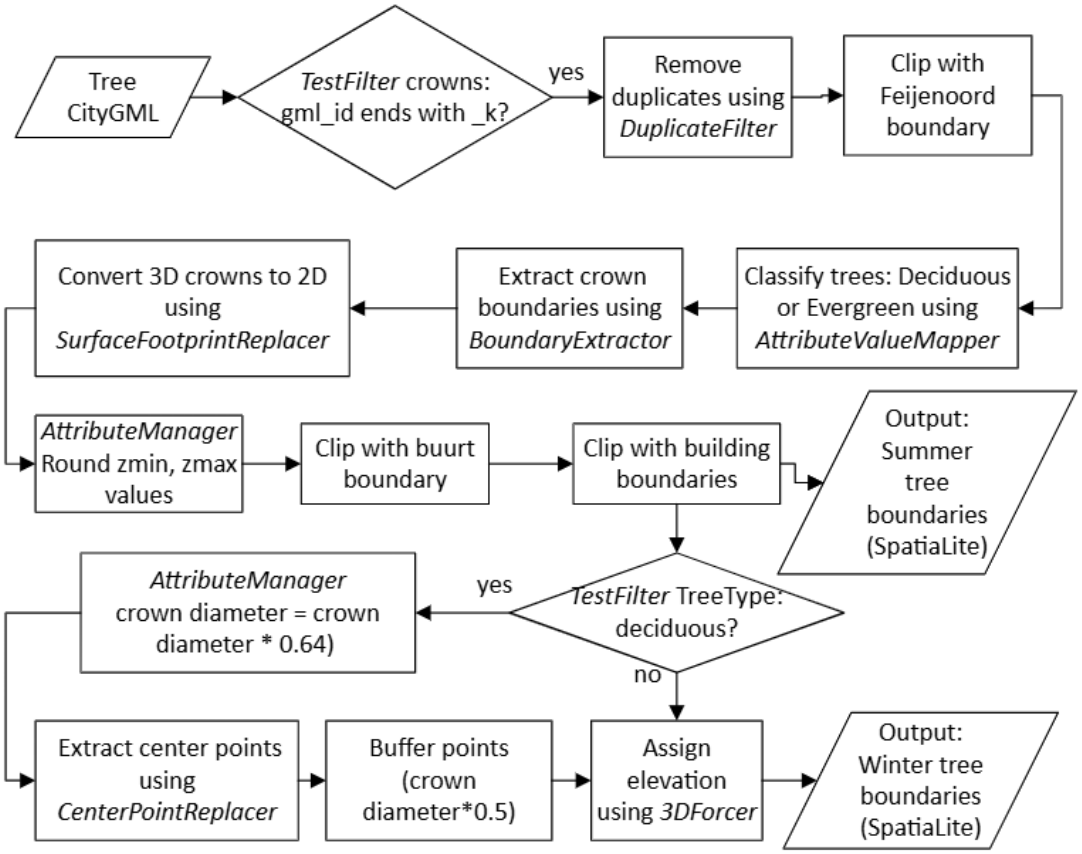


Figure 4.5.: Flowchart illustrating the complete processing workflow for deriving both summer and winter tree boundaries from CityGML data.

Following this filtering, the dataset is clipped to the Feijenoord boundary to retain only trees located within the study area. After this spatial filtering, new attributes are generated to classify trees as either deciduous or evergreen, based on their genus. The classification of tree genera (Table A.2) follows Givnish [2002] and Mueller et al. [2012]. Genera explicitly identified as evergreen in these sources, including needle-leaved conifers (*Pinus, Picea, Abies, Cedrus, Taxus, Thuja, Chamaecyparis, Cupressocyparis*) and certain evergreen broadleaves (*Ilex, Arbutus*), were classified as evergreen. Deciduous conifers, such as *Larix*, *Taxodium*, and

Metasequoia, were noted as exceptions that shed their foliage seasonally [Givnish, 2002]. All remaining genera in the Rotterdam dataset were classified as deciduous, reflecting their dominant leaf habit in temperate climatic conditions. This reclassification was implemented using the *AttributeValueMapper* transformer.

The crown boundaries are next extracted using the *BoundaryExtractor* transformer to derive the top and bottom crown heights (`_zmax` and `_zmin`). The 3D crown geometry is then converted into a 2D representation (circle polygons) using the *SurfaceFootprintReplacer* transformer, after which additional attribute operations such as rounding `_zmin` and `_zmax` values are applied to simplify the dataset. To further refine the data, it is first clipped using the neighbourhood boundary to optimise data management and visual inspection, and then clipped again with the building boundaries to prevent any overlap with buildings. Together, these steps produce the summer current tree boundaries, which are finally exported in the SpatiaLite data format. The SpatiaLite format is used because it stores both spatial and attribute data within a single SQLite database, allowing large datasets, spatial indexes, and multiple geometry types to be managed efficiently in a single file. This structure supports faster querying and simplifies data handling during analysis. It is also widely supported by GIS software such as QGIS and FME, which facilitates further analysis and integration.

To derive the winter tree boundaries, the processing is divided based on tree type using the *TestFilter* transformer. For deciduous trees, the `citygml_crown_diameter` attribute is modified using the expression `@mult(@Value(citygml_crown_diameter), 0.64)`, after which the centre points are extracted with the *CenterPointReplacer* transformer. These points are then buffered using the formula `@mult(@Value(citygml_crown_diameter), 0.5)` to create the reduced crown areas. For evergreen trees, the original crown boundaries are retained without modification. The final winter boundaries are then assigned elevation values using the *3DForcer* transformer with the previously derived `_zmin` values. The resulting dataset is subsequently exported in the SpatiaLite format as the winter tree boundaries.

4.4.3. Preparing proposed tree data

Proposed planting locations were identified to illustrate potential future greening scenarios. Figure 4.6 illustrates the complete workflow, highlighting the processing steps that result in the generation of planting points. To identify areas suitable for new planting, relevant land-use categories were first selected from the BGT layers. These categories, illustrated in Figure 4.7, include vegetated and unvegetated terrain parts, recreation areas such as parks, playgrounds, sports fields, and allotment gardens, as well as low-intensity circulation zones including driveways, parking areas, pedestrian zones, and footpaths.

Areas unsuitable for planting were then identified based on BGT land-use features and underground infrastructure, as shown in Figure 4.8. Feature-specific buffer distances were applied to define planting exclusion zones: 7 m for regional road carriageways; 10 m for level crossings and railway tracks; 3 m for local road carriageways, public transport lanes, bicycle paths, footpaths on stairs, buildings, water surfaces, and existing trees; 1 m for utility points such as pits, service boxes, masts, and poles; and 1.5 m for underground elements including pipes and cable corridors. The complete list of spatial layers used in this classification is provided in Table 4.5.

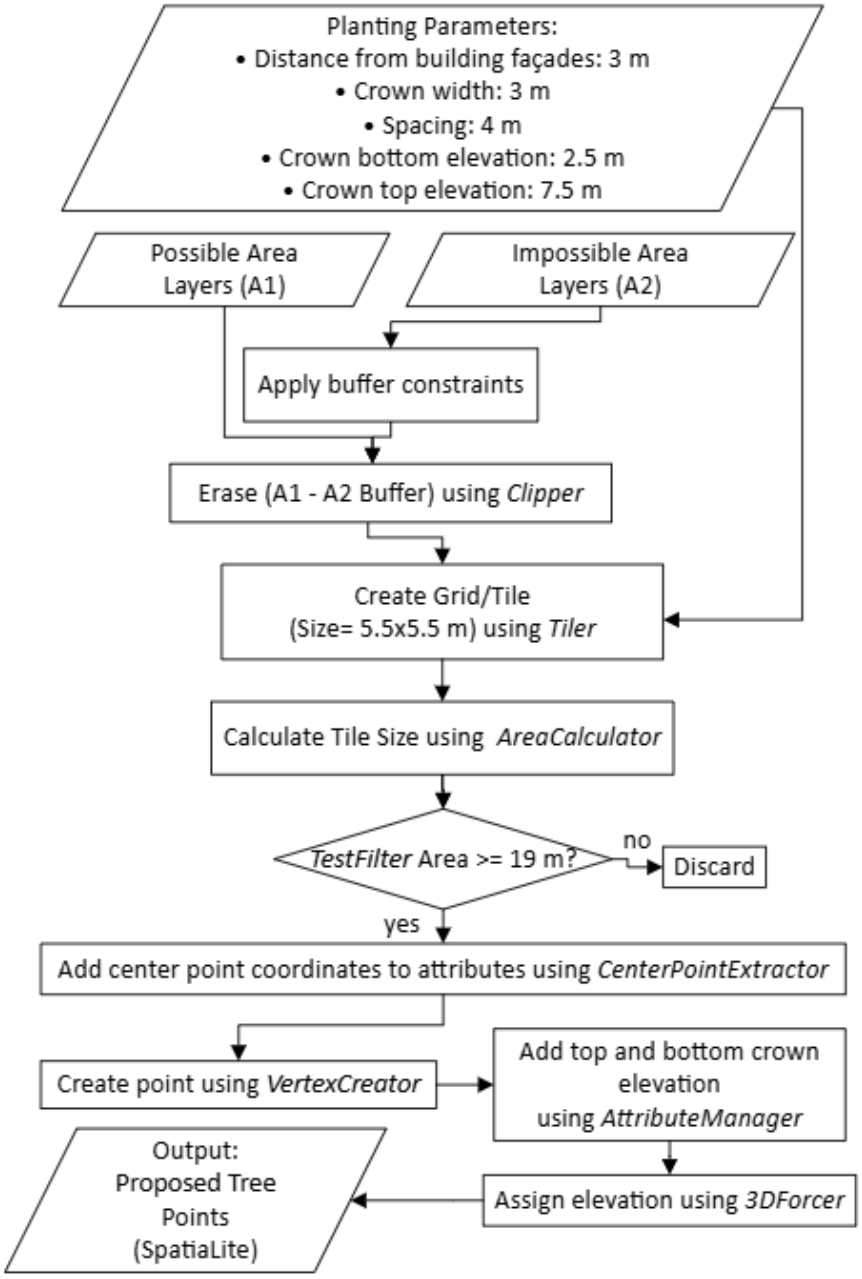


Figure 4.6.: Workflow for tree planting point generation



Figure 4.7.: BGT land-use layers defining areas suitable for planting

The buffer distances in Table 4.5 were determined to minimise potential conflicts between new planting areas and existing land uses, infrastructure, and operational needs. The chosen distances reflect three main considerations. First is safety and operational clearance, which informed the largest buffer distances. For instance, a 10 m buffer was applied around railways and level crossings to ensure that vegetation does not interfere with visibility, signalling systems, or access for maintenance vehicles. Moderate buffers of 3 m were used for roads, footpaths, and water bodies to maintain safe separation from traffic flow, pedestrian movement, and hydrological structures. Second is infrastructure protection, which guides the smaller buffer distances. Features such as pits, service boxes, masts, and poles were assigned 1.5 m buffers to prevent root intrusion into underground utilities or obstruction of overhead structures while preserving maintenance access. And third is spatial coherence and visual impact, which influenced the consistent use of 3 m buffers for similar land uses such as local roads, bicycle paths, and water surfaces. Applying uniform setbacks simplifies the planting design and supports a coherent landscape structure.

Table 4.5.: Possible and impossible planting areas with buffer constraints.

Layer	Feature / Subcategory	Buffer Distance
Possible Areas		
begroeidterreindeel	*begroeidterreindeel* — Vegetated terrain part	–
onbegroeidterreindeel	*onbegroeidterreindeel* — Unvegetated terrain part	–
functioneelgebeid	*hondenuitlaatplaats* = Dog walking area	–
	recreatie_park = Recreation: park	–
	recreatie_speeltuin = Recreation: playground	–
	recreatie_sportterrein = Recreation: sports field	–
	recreatie_volkstuin = Recreation: allotment garden	–
wegdeel_traffic_area	*inrit* = Driveway / entrance ramp	–
	parkeervlak = Parking area	–
	voetgangersgebied = Pedestrian zone	–
	voetpad = Footpath / sidewalk	–
Impossible Areas		
wegdeel_traffic_area	*rijbaan_regionale_weg* = Regional road carriageway	7 m
	overweg = Level crossing	10 m
	spoorbaan = Railway track	10 m
	OV_baan = Public transport lane	3 m
	voetpad_op_trap = Footpath on stairs	3 m
	fietspad = Bicycle path	3 m
	rijbaan_lokale_weg = Local road carriageway	3 m
pand	*pand* = Building/structure	3 m
waterdeel	*waterdeel* = Water surface	3 m
put_kast_mast_paal	*put* = Pit, well, manhole	1 m
	kast = Utility enclosure / service box	1 m
	mast = Mast / tower	1 m
	paal = Pole	1 m
Existing trees	–	3 m
Cables and pipes	*Buis* = Pipe	1.5 m
	Kabelbedzijde = Cable side strip	1.5 m
	Kabelgeul = Cable trench	1.5 m
	Lijnverbindingssymbool = Line connection symbol	1.5 m



Figure 4.8.: BGT land-use layers defining areas unsuitable for planting

Overlaying the spatial layers with these buffer constraints produced polygons representing areas suitable for planting. These polygons provide the spatial framework for locating potential planting points; however, the next step is to define planting parameters that balance energy performance goals with regulatory requirements.

Establishing these parameters requires understanding how tree placement affects both building energy use and legal constraints. [Rouhollahi et al., 2022] demonstrated through simulation that deciduous trees planted 3 m from east and west façades can significantly reduce summer cooling demand, while a 5 m distance on north façades benefits winter heating. Although based on Australian climates, these geometric principles can be adapted for temperate regions, such as the Netherlands, by selecting suitable species and planting configurations. In Rotterdam, however, minimum distances from property boundaries are set by law: 2 m nationally [Netherlands Government, 2022] and as little as 0.5 m locally in dense urban areas [Gemeente Rotterdam, 2020]. These setbacks restrict available space and determine feasible planting layouts.

Considering these constraints and focusing on summer cooling, this study models a single scenario: deciduous trees positioned 3 m from building façades, with 3 m crown width, 4 m spacing, and crown heights from 2.5 m to 7.5 m. This height range reflects the growth form of small urban tree species suited to dense areas, where space limitations restrict both total height and crown spread. A 2.5 m clear stem allows pedestrian and vehicle passage beneath the canopy, while a total height of 7.5 m provides adequate shading without conflicting with nearby buildings or infrastructure.

With suitable areas defined and scenario parameters specified, planting points are generated within these polygons using a grid-based method. The area is divided into 5.5 × 5.5 unit tiles with the Tiler transformer, after which the AreaCalculator computes the area of each tile. The TestFilter retains only tiles with an area of 19 or greater, and the CenterPointExtractor determines the centre coordinates of these tiles. Finally, the VertexCreator converts these coordinates into point geometries with a specified Z-value and coordinate system (EPSG:28992).

4.4.4. Configuring the Tree Model

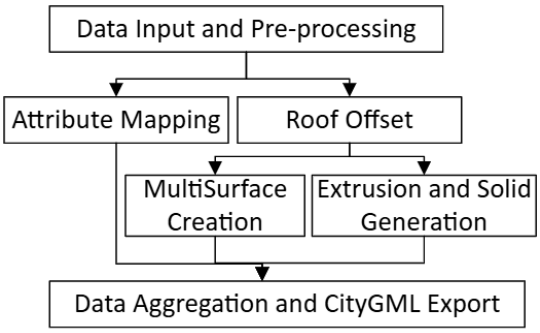


Figure 4.9.: General workflow for generating LoD1 tree models in FME Workbench.

As described in Sections 4.4.2 and 4.4.3, the tree datasets consisted of polygon layers delineating canopy boundaries under summer and winter conditions. While these layers provided

two-dimensional representations of tree extents, they were not directly compatible with the SimStadt environment, which requires three-dimensional (3D) geometries in CityGML Level of Detail (LoD) 1 or LoD2 formats. To generate LoD1-compliant tree models, the canopy polygons were transformed into 3D geometries using a workflow developed in FME Workbench. The process involved spatial and attribute preparation, height and offset definition, geometry creation, and final aggregation and export to CityGML (Figure 4.9).

Table 4.6.: Attributes assigned to tree polygons prior to geometry generation

Attribute	Value / Description
`name`	*Trees_Building*
`class`	*Building*
`function`	*1010*
`usage`	*Residential*
`storeys_ab`	Calculated as `@round(@div(@Value(_offset_roof),3),0)` (assuming a floor height of 3 m per storey)
`storeys_be`	*0*
`constr_y`	*1930*
`ga_people`	*5*
`ground_z`	*zmin* (bottom crown height or lowest elevation point)
`roof_z`	*zmax* (top crown height or highest elevation point)
`is_part`	*0*

Data Input and Pre-processing

In the initial stage, two SpatiaLite databases containing building footprint boundaries and tree canopy polygons for the target neighbourhood were read into the workspace. Building polygons were buffered and subsequently used to erase intersecting portions of the tree canopy layer. This step ensured that no tree geometry overlapped with building boundaries before further attribute processing. Each canopy polygon was assigned semantic attributes that are needed to comply with the CityGML *Building* schema (Table 4.6). However, it should be noted that the attribute names presented here are not the standard; they are renamed during later processing to match with the CityGML *Building* schema.

Attribute Mapping

Once the attribute assignment was completed, the canopy polygons proceeded through a *Attribute mapping* step. This step comprised an `AttributeManager`, two `AttributeSplitter` transformers, and an `AttributeRemover`. The `AttributeManager` was used to rename existing attributes to match the CityGML *Building* schema conventions. For instance, attributes such as `class`, `storeys_ab`, and `constr_y` were renamed to `citygml_class`, `citygml_storeys_above_ground`, and `citygml_year_of_construction`, respectively, ensuring semantic alignment with the target data model. Subsequently, the two `AttributeSplitter` transformers were configured to handle the `function` and `usage` attributes. Each transformer separated semicolon-delimited values into list attributes named `citygml_function` and `citygml_usage`, enabling multi-valued information to be stored in compliance with CityGML list structures. Finally, an `AttributeRemover` was applied to delete the original `function` and `usage` attributes. This step prevented redundancy by retaining only the newly created list-based

attributes. The *Attribute mapping* sequence thus standardised attribute names and formats, preparing the dataset for the subsequent geometry generation stage. Following this, a `GeometryRemover` transformer was applied to eliminate the geometric components of the features.

Roof Offset

Once the attribute preparation was complete, the canopy polygons entered *Roof offset* process. This sequence included an `AttributeKeeper`, an `AttributeRenamer`, and an `Offsetter`. The `AttributeKeeper` ensured that only relevant parameters related to canopy height and roof elevation were retained, while the `AttributeRenamer` standardised attribute names such as `_offset_roof` and `roof_z`. An `Offsetter` transformer, configured in Cartesian coordinate mode with all offset values set to zero, was included as a preparatory step to confirm geometric consistency before the surface reconstruction stage. Although it did not apply any physical translation to the features, it provided flexibility for future vertical adjustments if required.

MultiSurface Creation

Following the offset stage, the features proceeded to the *Create MultiSurface* sub-workflow and *Extruder* sub-workflow. For the *Create MultiSurface* process, it consisted of an `Orientor`, a `FaceReplacer`, and an `Aggregator`. The `Orientor` was configured with the orientation type set to *Reverse* and appearance flipping enabled, ensuring that all polygon normals were correctly oriented outward from the tree crown volumes. Subsequently, the `FaceReplacer` operated in automatic mode for both thickness and angular tolerances, reconstructing misaligned, overlapping, or non-planar faces into valid surfaces with consistent topology. Finally, the `Aggregator` assembled all corrected faces belonging to the same tree crown into a unified geometry. Group processing was enabled using the attribute `gml_id_building`, and the aggregation mode was set to *Geometry – Assemble One Level* with a homogeneous collection type. This configuration ensured that each tree was represented as a single, coherent *MultiSurface* feature, preserving consistent metadata and creating a complete 3D envelope suitable for CityGML export.

Next process for *Create MultiSurface* sub-workflow is *Create CityGML ID and LoD0 footprint attributes*, consisting of an `AttributeCreator` followed by a `GeometryPropertySetter`. The `AttributeCreator` introduced two key attributes: `gml_id` and `citygml_lod_name`. The `gml_id` attribute was defined using the expression `MultiSurf_UUID_@UUID()`, which automatically generates a globally unique identifier for each feature. The attribute `citygml_lod_name` was assigned the value `lod0FootPrint`, defining the geometric level of detail associated with the MultiSurface representation. The subsequent `GeometryPropertySetter` transferred these attributes from the feature level to the geometry level by applying the *Traits From Attributes* property mode. The transformer was configured to overwrite existing geometry properties and remove the source attributes after assignment, using `citygml_lod_name` and `gml_id` as the source attributes. This ensured that each MultiSurface geometry carried the corresponding LoD and identifier traits required for correct encoding within the CityGML schema. The process concludes with the *LoD0 attributes rename and geometry removal* subworkflow, which standardises attribute names and removes unnecessary geometry to prepare the dataset for integration. This sub-workflow consists of an `AttributeKeeper` followed

by an AttributeRenamer. The AttributeKeeper retains only the attribute gml_id_building, discarding all other attributes and associated geometry to maintain a minimal and consistent data structure. The output is then processed by the AttributeRenamer, which renames gml_id_building to gml_id.

Extrusion and Solid Generation

Parallel to this, the *Extruder* sub-workflow was executed. This sub-workflow converted the canopy polygon features into volumetric geometries through a sequence of geometric coercion and attribute assignment processes. It began with an Extruder transformer configured with the *Direction* parameter set to *Auto* and the *Distance* parameter linked to the attribute _offset_roof. The output from the Extruder was processed by two consecutive GeometryCoercer transformers. The first GeometryCoercer converted the geometry type to fme_composite_surface, and the second GeometryCoercer further converted the resulting geometries to fme_brep_solid. Following the geometry coercion, an AttributeCreator was applied to define two new attributes: gml_id and citygml_lod_name. The gml_id attribute was generated using the expression Solid_UUID_@UUID(), while citygml_lod_name was assigned the value lod1Solid. These attributes were then transferred from the feature level to the geometry level using a GeometryPropertySetter. The transformer was set to the *Traits From Attributes* mode, with the parameters configured to overwrite existing properties and remove the source attributes after assignment. The source attributes were specified as citygml_lod_name and gml_id. The sub-workflow concluded with an AttributeKeeper and an AttributeRenamer. The AttributeKeeper retained only the attribute gml_id_building, ensuring that unnecessary attributes were excluded from the output. The AttributeRenamer subsequently renamed gml_id_building to gml_id.

Data Aggregation and CityGML Export

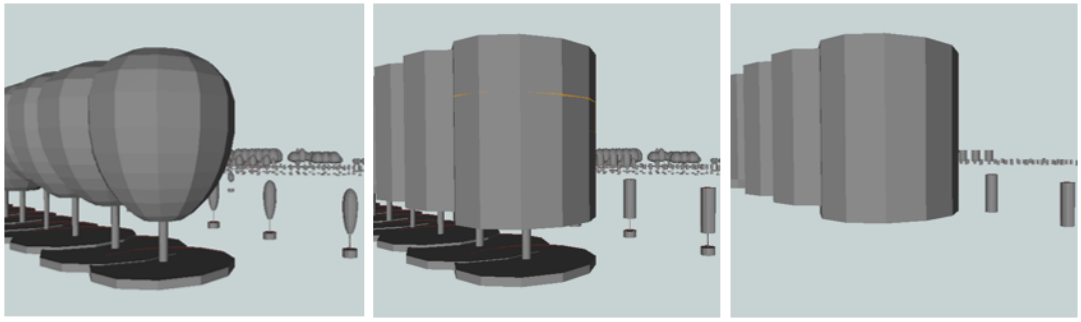


Figure 4.10.: Simplification of tree geometries. The original models (left) and their simplified cylindrical representations (right). The middle image shows the overlap, showing that only the crown region was represented as cylinders.

In the final stage, the outputs generated from the preceding subsubsections, namely *Attribute Mapping*, *Height and Offset Preparation*, *MultiSurface Creation*, and *Extrusion and Solid Generation*, were consolidated using an Aggregator transformer. The transformer was set to group

features by the attribute `gml_id`, with the aggregation mode defined as *Geometry – Assemble One Level* and the aggregate type specified as *Homogeneous Collection (If Possible)*. Attribute accumulation was executed in *Merge Incoming Attributes* mode. The aggregated results were then transferred to the *Building CityGML Writer*, which encoded the *MultiSurface* and *Solid* geometries according to the CityGML *Building* module specifications. The resulting dataset contained LoD0 and LoD1 representations of trees and buildings, each with valid identifiers and geometry properties suitable for use within the SimStadt simulation environment.

Figure 4.10 illustrates the result of simplifying the original tree geometries into cylindrical forms. The original tree models are shown on the left, while the simplified cylindrical models appear on the right. The middle image shows the cylinders overlaid on the original trees, indicating that only the crown part of each tree was generated in cylindrical form.

4.4.5. Configuring the simulation model

After the tree model was configured, the simulation model was prepared using an FME Workbench workflow adapted from the method described by [Gao et al., 2025]. In that approach, building data preparation was treated as a *data integration* step to ensure compatibility with the ALKIS code system, a standardised German cadastral classification used by the SimStadt simulation tool. Accordingly, Dutch building functions from the 2D BAG dataset were mapped to corresponding ALKIS codes using QGIS and FME, with the results stored in the `citygml_function` attribute for direct use in SimStadt. In this study, the workflow was extended by adding the outputs of the tree extrusion workflow as an additional input within the FME Workbench. This produced a CityGML dataset containing both vegetation and building elements, resulting in simulation-ready data for SimStadt. For each neighbourhood, twelve datasets were generated. Table 4.7 lists, for illustration purposes, the configurations created for the Afrikaanderwijk neighbourhood. The "future trees" represent the same tree geometries as in the current climate scenario but with applied growth parameters; this also applies to the proposed tree configurations.

Table 4.7.: Simulation-ready CityGML files prepared for the Afrikaanderwijk neighbourhood. Each scenario was simulated separately for summer and winter, resulting in twelve independent datasets.

ID	File Name	Description
S0	Model_NT_Afr.gml	No trees (current climate)
S1A	Model_CT_Afr_Summer.gml	Existing trees (current climate)
S1B	Model_CT_Afr_Winter.gml	Existing trees (current climate)
S2A	Model_PT_Afr_Summer.gml	Existing + proposed trees (current climate)
S2B	Model_PT_Afr_Winter.gml	Existing + proposed trees (current climate)
S3	Model_FNT_Afr.gml	No trees (future climate)
S4A	Model_FT_Afr_Summer.gml	Future existing trees (future climate)
S4B	Model_FT_Afr_Winter.gml	Future existing trees (future climate)
S5A	Model_FPT_Afr_Summer.gml	Future existing + proposed trees (future climate)
S5B	Model_FPT_Afr_Winter.gml	Future existing + proposed trees (future climate)

Although the content of the S0 and S3 datasets is identical, as both represent models without trees, their filenames differ to prevent overwriting of simulation results after running the simulations. These twelve datasets represent six scenario types, each simulated independently for summer and winter conditions. Figure 4.11 presents examples of the simulation-ready 3D city models for the Afrikaanderwijk neighbourhood.

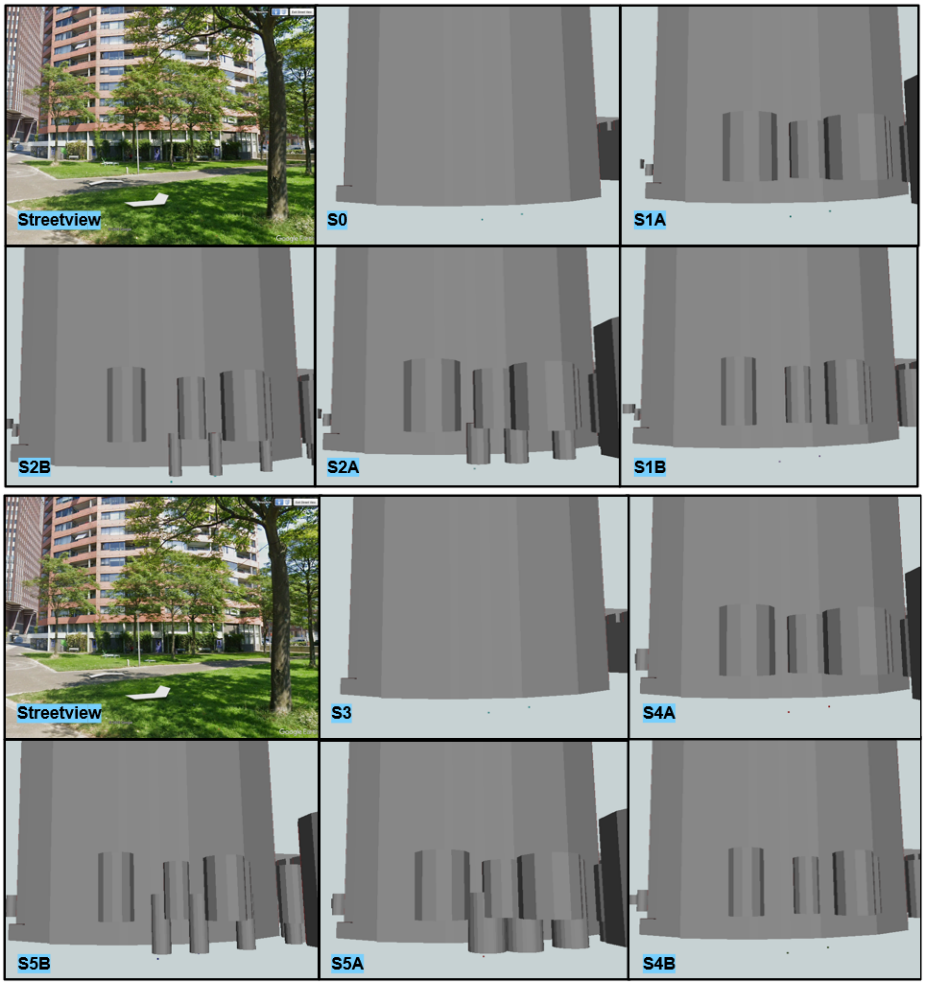


Figure 4.11.: Examples of simulation-ready 3D models for Afrikaanderwijk. Source: Google Street View imagery (captured July 2024; approximate camera location: X = 93746.1464, Y = 435553.1237; CRS: EPSG:28992).

4.4.6. Processing climate data

From *previous work* [Gao et al., 2025], current climate data were provided in monthly form and stored in the TMY3 (Typical Meteorological Year) format. The exact formatting was applied to the projected climate. For average temperature and global horizontal irradiance (G_{gh}), daily values were averaged by month across all years to obtain long-term monthly means for the 2050 scenario. Direct normal irradiance (G_{bn}) was estimated using the ratio of

direct to global irradiance from current climate data, and diffuse horizontal irradiance (G_{dh}) was calculated as $G_{dh} = G_{gh} - G_{bn}$. Table 4.8 summarises the resulting monthly values for the projected 2050 climate scenario.

Month	G_{gh}	G_{bn}	G_{dh}	Temp (°C)
Jan	28.62	8.88	19.74	5.0
Feb	56.87	23.36	33.51	4.9
Mar	102.47	47.29	55.18	7.3
Apr	171.22	87.15	84.07	10.6
May	215.12	111.66	103.46	14.3
Jun	231.81	117.45	114.36	17.1
Jul	228.91	114.46	114.46	19.7
Aug	190.55	93.70	96.85	19.9
Sep	127.36	59.10	68.26	16.6
Oct	72.44	28.57	43.87	12.8
Nov	34.68	10.51	24.17	8.8
Dec	21.53	6.15	15.38	5.7

Table 4.8.: Monthly global (G_{gh}), beam (G_{bn}), and diffuse (G_{dh}) radiation in kWh/m^2 and average air temperature (°C) for the projected 2050 climate scenario.

4.4.7. Scope adjustment due to computational constraints

The initial plan was to simulate all neighbourhoods in the Feijenoord district to achieve a complete district-scale analysis. During preliminary tests, differences in simulation time and the success rate of individual runs were observed across neighbourhoods, particularly when tree data were included. To document these differences, the input data size, simulation time, and success status for each neighbourhood and scenario were recorded. Table 4.9 shows that simulation times ranged from under two hours for smaller neighbourhoods such as Noordereiland to nearly eight hours for Vreewijk, with longer runtimes when proposed tree scenarios were included.

Table 4.9.: File size and simulation time per neighbourhood including tree data (preliminary tests).

Neighbourhood	**File Size (MB)**	**Simulation Time (h)**
Afrikaanderwijk	31.93	1:45
Bloemhof	79.04	3:48
Feijenoord	34.32	2:00
Hillesluis	53.67	2:47
Katendrecht	28.23	2:00
Kop van Zuid Entrepot	34.24	3:00
Kop van Zuid	11.42	2:00
Noordereiland	14.54	2:00
Vreewijk	152.08	7:44

To assess computational feasibility, the success or failure of each run was also recorded

for current and proposed tree scenarios under summer and winter conditions. As shown in Table 4.10, most baseline simulations with today's trees completed successfully, while several runs with proposed trees or winter conditions did not, especially for larger neighbourhoods such as Bloemhof, Feijenoord, and Vreewijk.

Table 4.10.: Simulation success for each neighbourhoods across scenarios. A tick (V) indicates successful completion; cells marked 'X' indicate failed runs.

Neighbourhoods	Today Trees (Summer)	Today Trees (Winter)	Proposed Trees (Summer)	Proposed Trees (Winter)
Afrikaanderwijk	**V**	**V**	**V**	**V**
Bloemhof	V	V	X	X
Feijenoord	V	X	X	X
Hillesluis	**V**	**V**	**V**	**V**
Katendrecht	**V**	**V**	**V**	**V**
Kop van Zuid Entrepot	V	V	X	V
Kop van Zuid	**V**	**V**	**V**	**V**
Noordereiland	**V**	**V**	**V**	**V**
Vreewijk	V	X	X	V

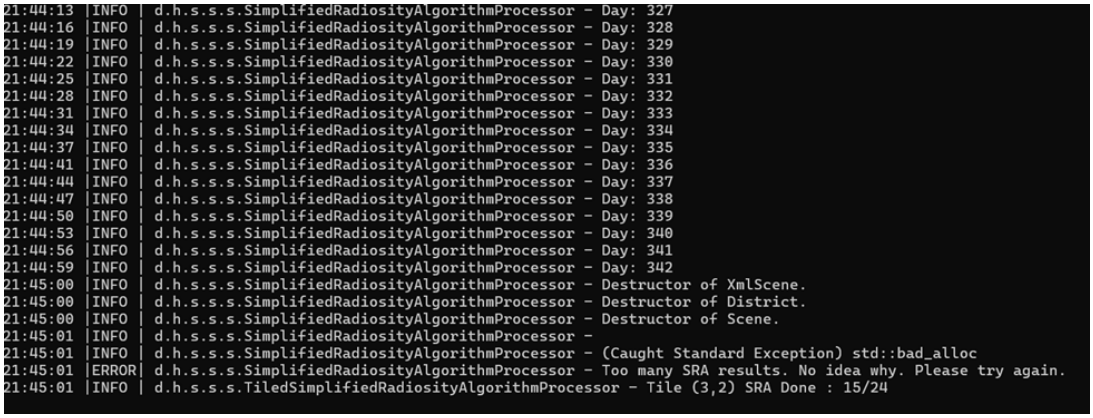


Figure 4.12.: Example of a memory allocation error (std::bad_alloc) encountered during the simulation.

The error message that occurred in the failed runs is shown in Figure 4.12. It indicates a memory allocation failure during the radiosity computation stage. The simulation terminated with a `std::bad_alloc` exception, which occurs when the program requests more memory than the system can provide. The accompanying log entry, stating that there were too many Simplified Radiosity Algorithm (SRA) results, suggests that the simplified radiosity algorithm generated an unexpectedly large number of intermediate results, exceeding the available memory resources.

According to the SRA SimStadt documentation [HFT Stuttgart, 2024], the SRA can become slow or unstable when applied to scenes containing a large number of buildings. The documentation notes that simulations involving more than approximately 500 buildings may exceed the capacity of some systems and therefore recommends subdividing the CityGML model into smaller spatial tiles using the `SRA_Perez_with_tiling` option in the `IrradianceProcessor`. In this study, this configuration was used with a tile side length of 50 m and a 10% overlap between tiles. Despite this setting, several simulations exhibited instability and memory allocation errors. This outcome may be related to the inclusion of vegetation objects represented as building geometries, which increased the total number of surfaces and geometric complexity within each tile. The issue, therefore, appears to be influenced not only by the number of buildings per tile but also by the cumulative data load associated with vegetation representation and overall scene complexity during the radiosity computation. This behaviour indicates a scalability limitation in the current implementation, where complex geometries and the inclusion of vegetation as building objects can lead to excessive memory demand.

Based on these results, two neighbourhoods were selected for detailed analysis: **Kop van Zuid** and **Afrikaanderwijk**. These neighbourhoods were selected because simulations ran successfully across all scenarios and provided more than one case to confirm reproducibility. They also represent different spatial contexts: Kop van Zuid is situated along the riverfront, where urban heat island effects may be higher, while Afrikaanderwijk forms part of the continuous urban fabric. Only two neighbourhoods were included due to time constraints for the thesis.

4.5. Simulation setup in SimStadt

After all the data were ready for the selected neighbourhoods, the simulation was executed. Before executing the simulation, a project environment and a dedicated project directory must be defined in SimStadt. Because the analysis considered both present-day and future climate scenarios, two separate projects were created. The only difference between these projects was the weather data provided to the `Weather Processor`, which was based on current climate conditions for one project and on projected climate scenarios for the other. All other input parameters remained identical.

To perform the heating and cooling demand simulation, SimStadt executed a sequence of modules. Parameters for these modules were either taken from the default SimStadt configuration or specified as custom inputs where necessary. The processing steps and their input parameters chosen are summarised in Table 4.11. Explanation of each module, including its purpose and role within the simulation workflow, is provided below.

- **ImportCityGml:** This module imported the CityGML files containing the 3D building geometries into the project environment. Two parameters were specified: the Minimal LOD was set to `LOD_0`, and the Maximal LOD was set to `LOD_2`. These settings defined the minimum and maximum levels of detail for the imported geometries.

- **Geometric Preprocessor:** This module in Simstadt analysed the complete geometry of the building model to ensure data consistency. It calculated building coordinates, heights, and volumes, identified neighbouring buildings, and classified surfaces as

Table 4.11.: Simulation setup in SimStadt

Process Step	Parameter Input
ImportCityGml	**Minimal LOD**: LOD_0 **Maximal LOD**: LOD_2
Geometric Preprocessor	-
Geometric Estimator	-
Physics Preprocessor	**Type assignment**: `GERMAN_BUILDING_TYPES_ASSIGNMENT` **Building physics library**: Dutch building physics library (XML, based on the NTA8800 standard)
Usage Preprocessor	**Building usage library**: `GERMANY`
Weather Processor	**Weather data source:** `TMY3_MONTHLY_FILE` **TMY3 Filename**: S0-S2=`Rotterdam-mon.tmy3` S3-S5=`Rotterdam-mon-proj.tmy3`
Irradiance Processor	**Radiation Model**: `SRA_Perez_with_tiling` **Tile Overlap**: 10 **Tile Side Length**: 50
Monthly Energy Balance	**Calculation mode**: `HEATING_AND_COOLING` **Consumer behaviour**: `IWU_NUTZUNG`

roofs, walls, or ground elements. In addition, it determined whether walls were exterior or shared between buildings and checked the plausibility of the calculated building volumes.

- **Geometric Estimator:** This module estimated missing geometric attributes in the building dataset. Parameters derived included roof type, average storey height, attic and basement heating types, number of storeys above ground, basement ceiling height above ground, heated volume, heated area, and thermal boundary areas. These estimates ensured that all buildings had a complete geometric description for the subsequent simulation steps.

- **Physics Preprocessor:** In this module, thermal and physical building properties were assigned using the `GERMAN_BUILDING_TYPES_ASSIGNMENT` option. The Dutch building physics library, provided in XML format and based on the NTA8800 standard, was used for construction parameters. Buildings without a defined construction year were excluded from the analysis. For the remaining buildings, the preprocessor determined the building type (e.g., single-family house, high-rise) and assigned properties such as storey height, thermal bridge U-value, and infiltration rate. These assignments were based on the building type, construction year, and refurbishment standard (e.g., standard or EnEV2016). Construction types, U-values, and window-to-wall ratios were assigned to all surfaces. Where necessary, outdated building data could be statistically updated using an assessment scenario, for example, by assuming that a certain percentage of buildings had been retrofitted to a higher standard.

- **Usage Preprocessor:** This module defines building usage zones (e.g., residential, office) based on the building function. The default `GERMANY` building usage library was applied. Parameters such as occupancy density, internal heat gains, set-point temperatures, domestic hot water consumption, and ventilation rates were assigned based on the usage type. Buildings with unknown functions were either assumed to be residential or excluded from the analysis. For German residential buildings, the number of households and occupants was estimated where necessary.

- **Weather Processor:** This module retrieved weather data for the project locations using the `TMY3_MONTHLY_FILE` data source. The file TMY3 provides monthly averages for temperature, solar radiation, and wind speed. In this module, these monthly values were converted into synthetic hourly data to provide the temporal resolution required for the simulation.

- **Irradiance Processor:** This module calculated solar radiation on building surfaces using the `SRA_Perez_with_tiling` model. Parameters specified included the **Tile Side Length** (50), **Tile Overlap** (10), as well as the azimuth and tilt resolution. The tiling settings controlled the spatial discretisation of the building surfaces, while the SRA model accounted for direct, diffuse, and reflected radiation, as well as shadowing effects from neighbouring buildings and terrain.

- **Monthly Energy Balance:** In the final module, a monthly energy balance was applied to each building to calculate heating and cooling demands at a monthly resolution. The implementation followed the German norm `DIN V 18599-2`, using a static thermal model to account for all heat sources (e.g., internal gains, solar gains) and sinks (e.g., transmission and ventilation losses) within each building zone. The Calculation Mode was set to `HEATING_AND_COOLING`, and the Consumer Behaviour model `IWU_NUTZUNG` was applied. The output provided monthly energy demand profiles for the entire building stock.

4.5.1. Post-processing, analysis, and visualisation

The overall workflow for this process is illustrated in Figure 4.13. After running the simulation, *Simstadt* produces tabular data in `.csv` format. Although the output files contain monthly data for the entire year, only specific months are used for aggregation: May to October for the summer period and November to April for the winter period. After filtering the data accordingly, the results are aggregated to obtain annual values, including *Yearly Cooling Demand (kWh/year)* and *Yearly Heating Demand (kWh/year)*, as well as normalized values such as *N_YCD (kWh/m^2/year)* and *N_YHD (kWh/m^2/year)*. For visualisation and comparison, the aggregated data is merged with the building polygons to enable spatial representation. In addition, a separate `.csv` file is exported containing the total monthly heating and cooling demand per district, which is later used to analyse demand statistics for each district under different scenarios.

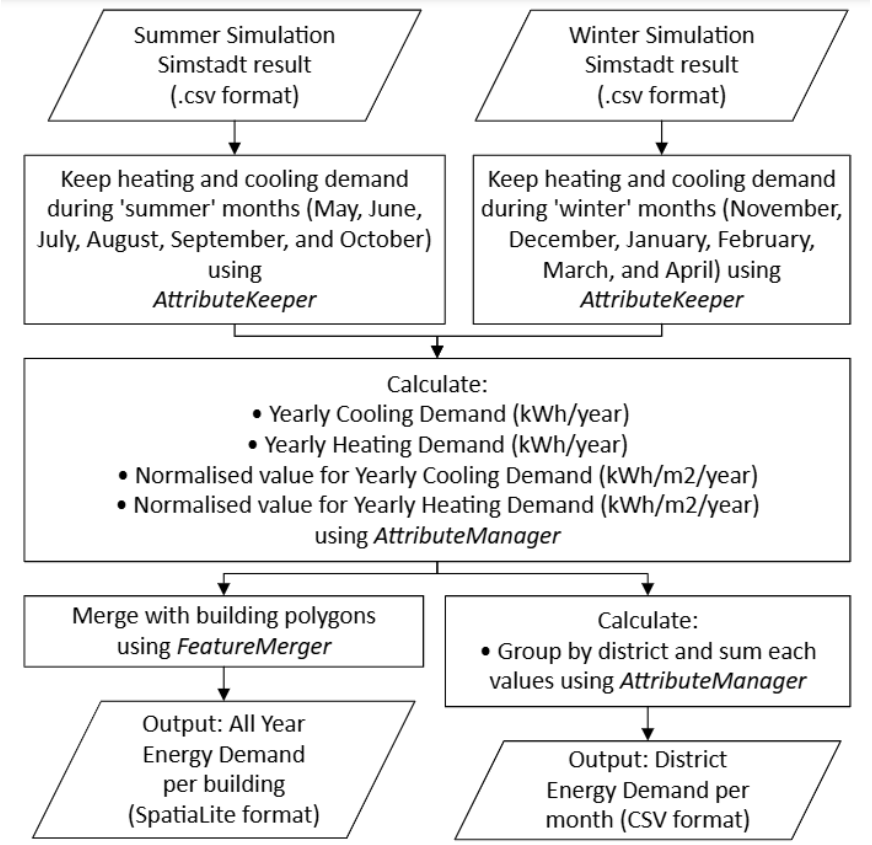


Figure 4.13.: Workflow for post-processing

5. Results and analysis

This chapter presents the findings in relation to the main research question: how the spatial representation of tree planting can be integrated into neighbourhood-scale UBEM to assess its effectiveness in reducing heating and cooling demand under projected 2050 climate conditions.

The results are presented in four stages. First, energy demand under current and projected 2050 climate conditions is analysed for the baseline scenario without additional vegetation. This provides a reference for understanding the influence of climate change on heating and cooling demands. Second, the proposed tree planting scenario is described, including its design approach, spatial extent, and modelling assumptions, to clarify the basis for subsequent analysis. Third, the effects of the proposed planting on heating and cooling demand are examined under both current and future climate conditions to assess its role in reducing cooling demand and any associated changes in energy demands. Finally, the spatial distribution of existing and potential vegetation is reviewed in relation to the 30–30–300 guideline to evaluate how the proposed planting aligns with broader urban greening objectives.

5.1. Energy demand results

Energy demand results are presented using cooling and heating demand maps. The classification ranges for cooling demand were chosen to reflect meaningful differences in building energy performance. The ranges are $0-50$, $50-100$, $100-200$, $200-300$, $300-500$, $>$ 500 kWh/m^2/year. Buildings with less than 50 kWh/m^2/year are typically considered very low demand or nearly zero-energy buildings. Values between 100–200 kWh/m^2/year often represent standard or average buildings in many climates, while demands above 500 kWh/m^2/year are indicative of extremely high energy use, which is often associated with poorly insulated or inefficient buildings. Some of the maps are shown in Appendix B

To evaluate the plausibility of these results, one simulation case was selected for statistical check: the Kop van Zuid simulation without trees under the current climate scenario.

Table 5.1.: Statistical for the Kop van Zuid simulation without trees under the current climate scenario

Simulation Result	0-50	50-100	100-200	200-300	300-500	>500	Max	Min
Cooling Demand	58	19	21	10	6	7	1475.363	0
Heating Demand	43	6	19	9	14	30	3895.175	0

The statistical results for the Kop van Zuid case show the distribution of energy demand across the building stock. Under current climate conditions, most buildings have low cooling demand, with 58 buildings in the 0–50 kWh/m²/year range and seven buildings above

500 kWh/m²/year. This suggests that cooling requirements are limited for most buildings, while a smaller number have higher demand. The maximum cooling demand of 1475.36 kWh/m²/year is above typical levels; in the Netherlands, annual cooling demand for buildings is usually below 50–100 kWh/m²/year even in warmer years, so such a high value is unlikely to be realistic.

For heating demand, the distribution is different. Forty-three buildings fall below 50 kWh/m²/year, while 30 buildings exceed 500 kWh/m²/year. The maximum heating demand of 3895.18 kWh/m²/year is also far above typical Dutch values; for older residential buildings, annual heating demand rarely exceeds 300–400 kWh/m²/year, indicating that extreme values in the simulation may stem from modelling assumptions rather than actual building performance.

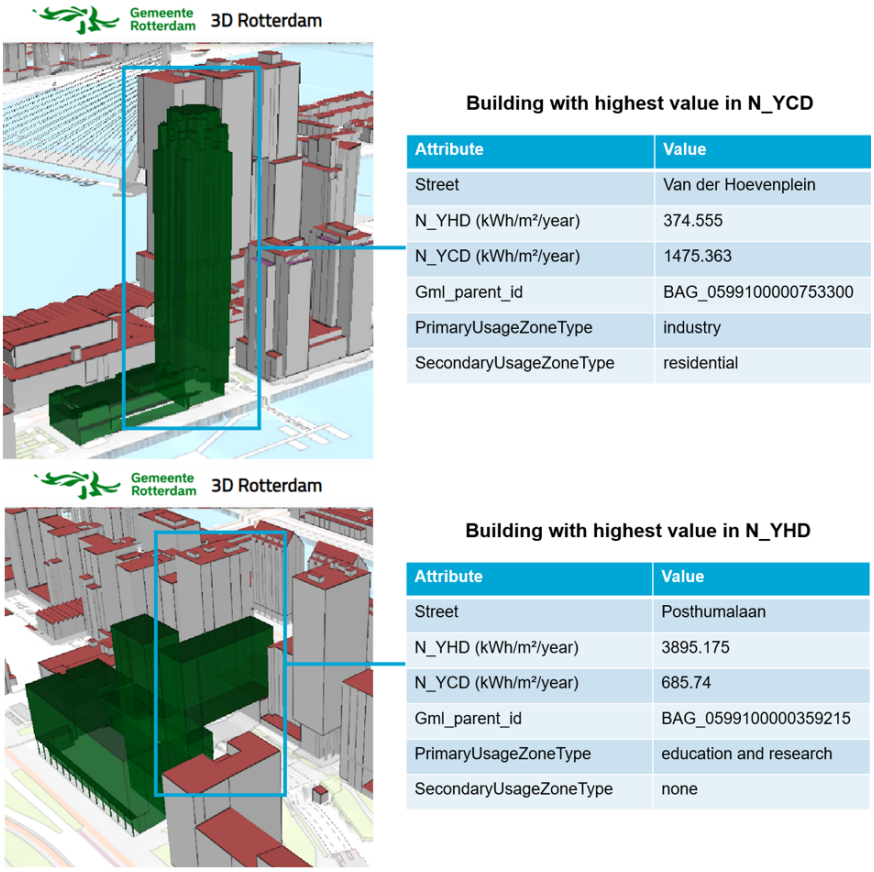


Figure 5.1.: Buildings with the highest simulated cooling (top) and heating (bottom) demand in Kop van Zuid.

To identify the sources of the extreme simulated energy values, Figure 5.1 presents the buildings with the highest cooling and heating demand in the Kop van Zuid area. The highest simulated cooling demand (1475.36 kWh/m²/year) occurs at Van der Hoevenplein, in a building with industrial primary and residential secondary use. The mixed-use character

may contribute to the elevated cooling load due to internal heat gains from industrial activities. However, these simulated values exceed realistic levels for Dutch conditions and are likely influenced by model assumptions. The building with the highest cooling demand is also relatively tall, which may help explain the extreme value. When the number of storeys is unknown, SimStadt estimates it by dividing the building height by 3 m and multiplying the result by the footprint area. In this case, the building has a large footprint, but only part of it extends to its full height. Consequently, SimStadt may overestimate the total floor area, leading to unrealistically high specific cooling demand values.

The highest simulated heating demand (3895.18 kWh/m²/year) is found at Posthumalaan, in a building classified as having educational, research, and unknown uses. Unlike the previous case, this building is not particularly tall, so the overestimation mechanism related to floor area does not apply here. SimStadt uses the DIN V 18599 standard for energy balance calculations, which relies on a monthly balance method and predefined building archetypes. As this standard and its typologies were developed for German conditions, certain default parameters such as insulation levels, internal gains, and system efficiencies may not fully reflect the Dutch building stock. For example, buildings used for education and research typically require higher ventilation rates and longer occupancy hours. When such a building is represented by a generic German archetype in SimStadt, these characteristics may not be accurately captured, potentially leading to an overestimation of heating demand.

Previous work [Gao et al., 2025] using SimStadt for Rotterdam reported similarly high simulated energy demand values, even after repairing building geometries and attributes. The authors noted that these results can be caused by remaining geometric inaccuracies, estimated or missing attribute values, and simplifications in the DIN V 18599 monthly balance approach, which does not fully include effects such as shading, infiltration, or local microclimate. The same factors are likely responsible for the very high values found in the Kop van Zuid case. These results should therefore be viewed as modelling artefacts rather than realistic representations of building performance. Because such limitations are part of the SimStadt framework, they are also expected to influence other neighbourhoods and scenarios, including those with tree planting and future climate conditions. While it is important to acknowledge their presence, these artefacts do not affect the main conclusions of this thesis. This is because the analysis is based on relative differences between scenarios rather than absolute energy demand values.

5.2. Comparative analysis

5.2.1. Current vs. future climate scenarios

This section compares heating and cooling energy demand between 2023 and 2050 to evaluate the influence of projected climate change on building energy requirements. The comparison uses the baseline scenario without additional vegetation to isolate the effects of changing climate conditions.

Cooling demand

Figures 5.2 show that most buildings are projected to require more cooling energy in 2050 compared to 2023. This is a logical outcome because rising average temperatures and more

frequent extreme heat events increase the number of hours when indoor spaces exceed comfort thresholds.

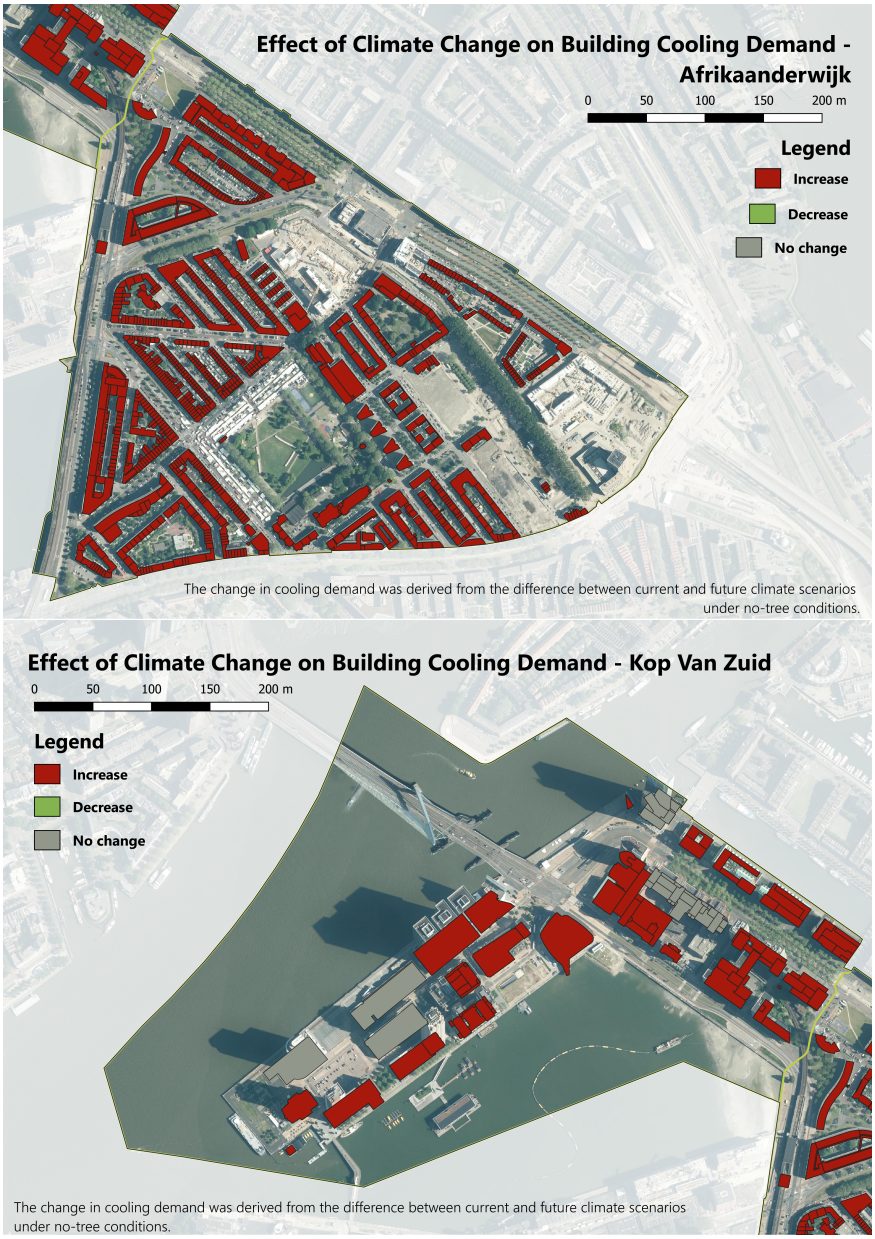


Figure 5.2.: Change in cooling demand resulting from climate change in Afrikaanderwijk and Kop van Zuid under no tree condition.

For further analysis, Table 5.2 and Table 5.3 summarise the total monthly cooling demand for the Afrikaanderwijk and Kop van Zuid neighbourhoods, respectively, for the years 2023 and 2050, along with the percentage increase.

Month	2023 (kWh)	2050 (kWh)	Increase (%)
January	12308	15344	24.67
February	16108	17945	11.40
March	47880	54459	13.74
April	172428	233558	35.45
May	625445	823641	31.69
June	1327695	1631190	22.86
July	1986226	2789310	40.43
August	1675741	2548531	52.08
September	556068	821030	47.65
October	115723	168101	45.26
November	28090	37761	34.43
December	13422	16788	25.08

Table 5.2.: Comparison of total monthly cooling demand for the entire Afrikaanderwijk neighbourhood in 2023 and 2050, with percentage change

Month	2023 (kWh)	2050 (kWh)	Increase (%)
January	16326	20644	26.45
February	24278	27622	13.77
March	83660	98322	17.53
April	305316	414975	35.92
May	1040387	1340997	28.89
June	2058473	2460357	19.52
July	2983802	3911168	31.08
August	2665634	3712255	39.26
September	1106996	1547943	39.83
October	268683	402707	49.88
November	46222	69931	51.29
December	16951	22153	30.69

Table 5.3.: Comparison of total monthly cooling demand for the entire Kop van Zuid neighbourhood in 2023 and 2050, with percentage change

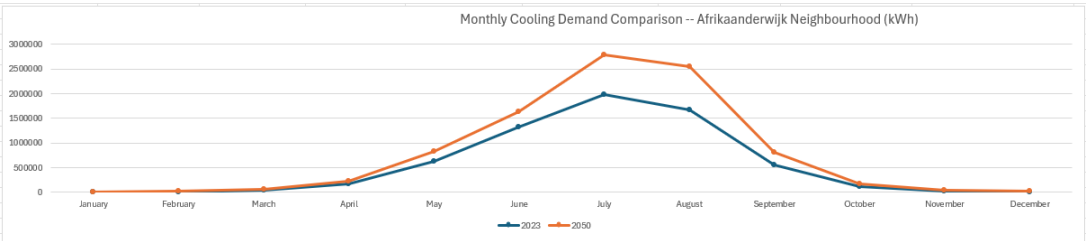


Figure 5.3.: Cooling Demand Comparison Graph (2023 vs. 2050) – Afrikaanderwijk

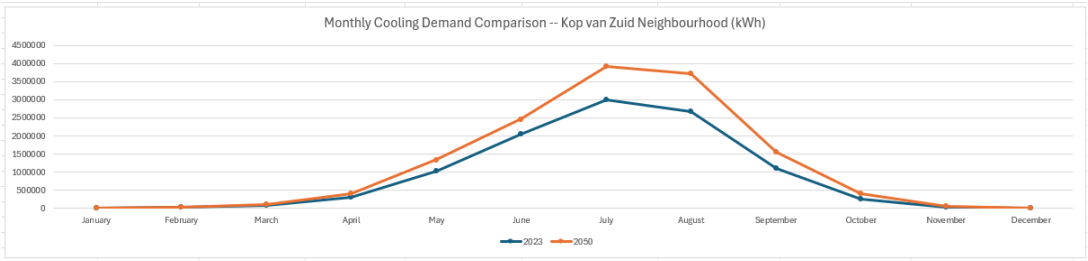


Figure 5.4.: Cooling Demand Comparison Graph (2023 vs. 2050) – Kop van Zuid

Tables 5.2 and 5.3, along with Figures 5.3 and 5.4, provide monthly details, showing that cooling demand in 2050 is consistently higher than in 2023. Peak demand occurs in July and August for both neighbourhoods, with Afrikaanderwijk seeing the most significant summer increases, while Kop van Zuid shows bigger relative rises in autumn, especially in October and November. The results also show some cooling demand in the colder months (September–April), which is higher than what would usually be expected in the Netherlands. This may be due to how SimStadt models buildings, for example, by including internal heat gains from occupants and appliances, solar gains on sunny days, and fixed temperature set-points that trigger cooling whenever limits are exceeded. Some buildings, such as offices or shops, may also require cooling throughout the year. These factors likely explain why the model predicts more cooling outside the summer months than would normally occur in reality.

Heating demand

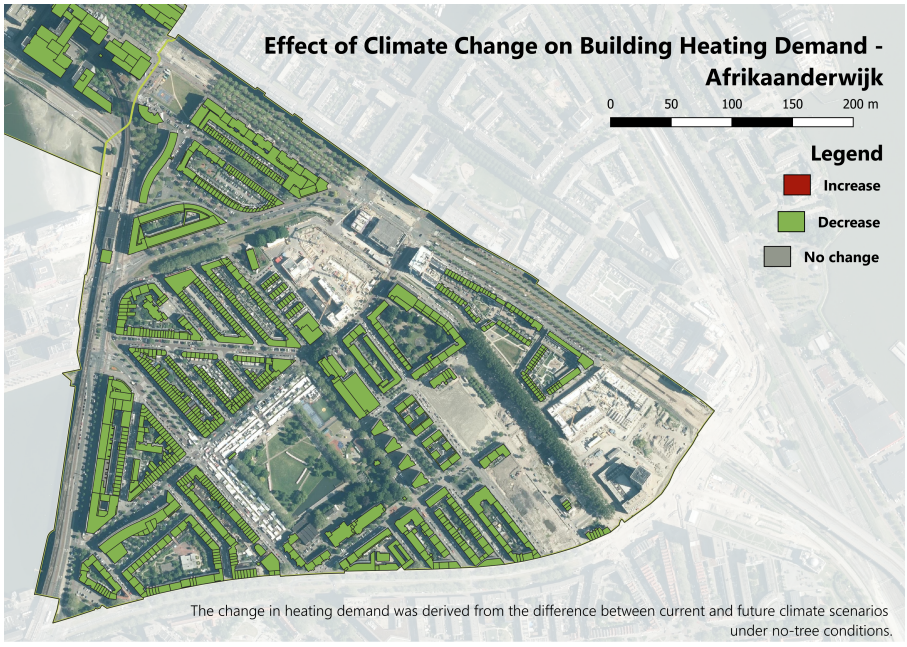


Figure 5.5.: Change in heating demand resulting from climate change in Afrikaanderwijk under no tree condition.

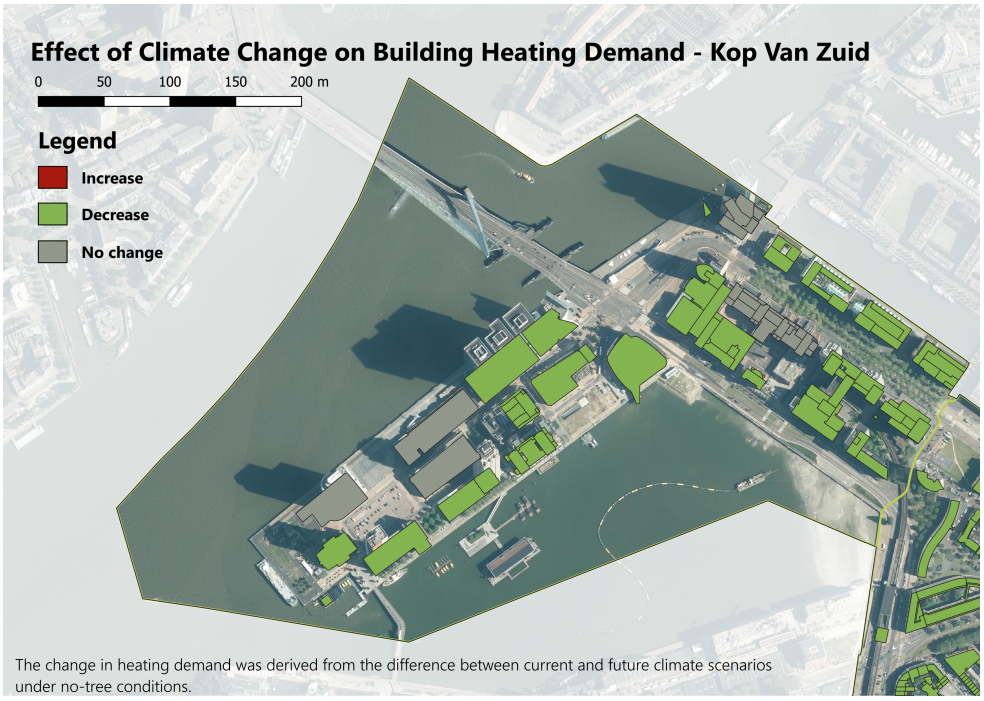


Figure 5.6.: Change in heating demand resulting from climate change in Kop van Zuid under no tree condition

Figures 5.5 and 5.6 indicate that most buildings will require less heating energy in 2050 compared to 2023. This reduction is logically consistent with projected climate warming, which leads to higher average outdoor temperatures and consequently less energy required to maintain indoor thermal comfort.

Month	2023 (kWh)	2050 (kWh)	Decrease (%)
January	6147102	5675308	-7.68
February	5030375	4815952	-4.26
March	3885532	3575124	-7.99
April	1909883	1459788	-23.57
May	483301	276262	-42.84
June	47408	15964	-66.33
July	2262	40	-98.23
August	3850	33	-99.14
September	239878	70475	-70.62
October	1759268	1211623	-31.13
November	4082124	3428498	-16.01
December	5933970	5433342	-8.44

Table 5.4.: Comparison of total monthly heating demand for the entire Afrikaanderwijk neighbourhood in 2023 and 2050, with percentage change

Month	2023 (kWh)	2050 (kWh)	Decrease (%)
January	4348356	3941143	-9.36
February	3522337	3344641	-5.04
March	2634571	2407540	-8.62
April	1342564	1053841	-21.51
May	412947	260444	-36.93
June	63268	28000	-55.74
July	7315	377	-94.85
August	11527	366	-96.82
September	232607	93109	-59.97
October	1182099	850671	-28.04
November	2685353	2211211	-17.66
December	4150518	3726722	-10.21

Table 5.5.: Comparison of total monthly heating demand for the entire Kop van Zuid neighbourhood in 2023 and 2050, with percentage change

Table 5.4 and Table 5.5, together with Figures 5.7 and 5.8, also show lower heating demand across all months in 2050. The most significant reductions occur in June, July, and August, when heating demand is very small, while spring and autumn months, such as April, May, September, and October, also show clear decreases. Winter months like January, February, and December continue to have the highest heating demand, but with smaller reductions compared to other periods. Overall, the results reflect how warmer future conditions shorten the duration and lessen the intensity of the heating season. Transitional periods are most affected because milder temperatures quickly eliminate the need for heating, whereas persistent cold spells in winter maintain a baseline demand even under future climate scenarios.

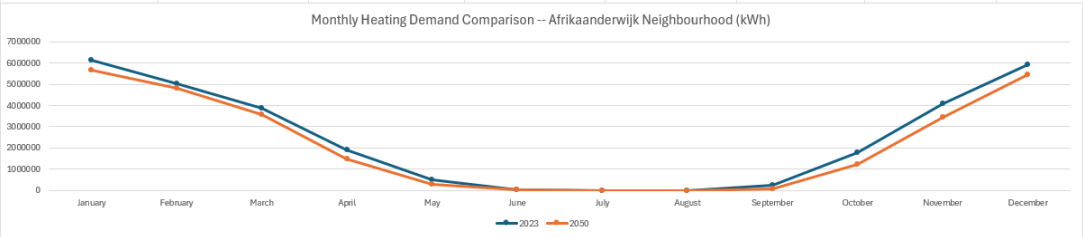


Figure 5.7.: Heating Demand Comparison Graph (2023 vs. 2050) – Afrikaanderwijk

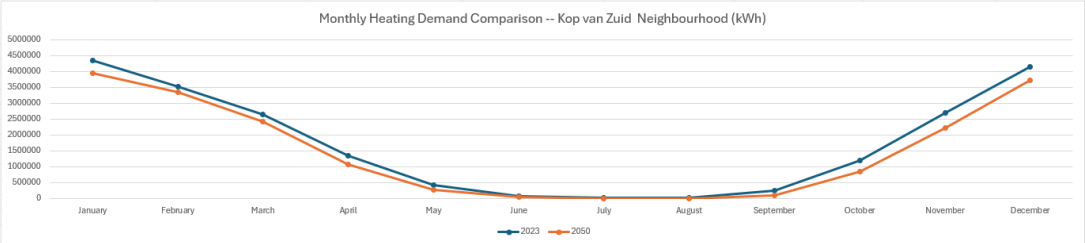
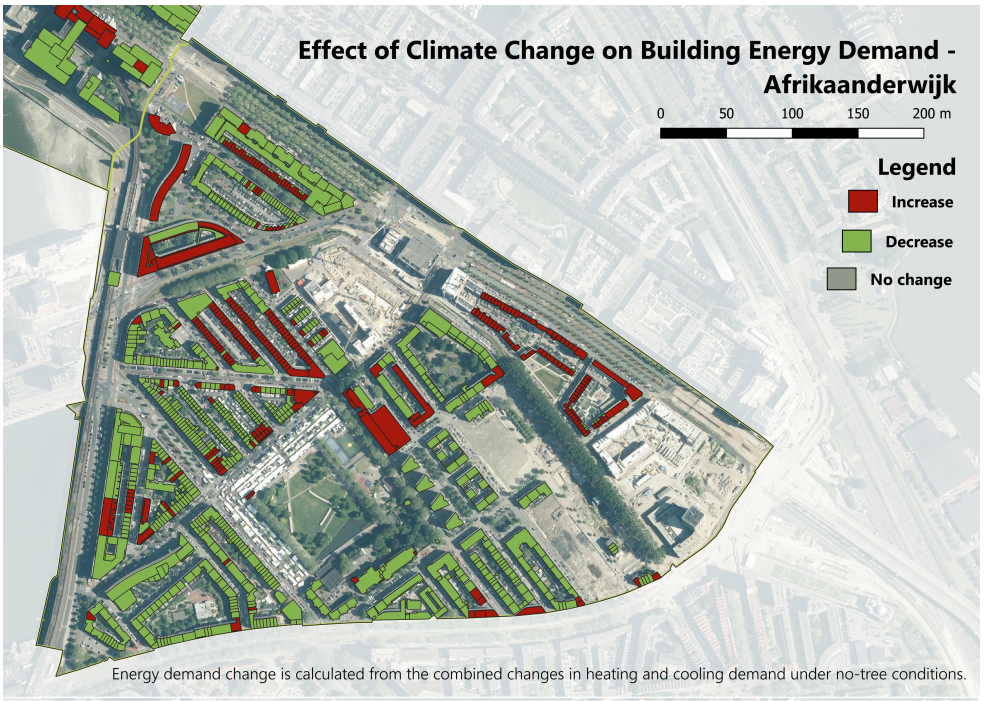


Figure 5.8.: Heating Demand Comparison Graph (2023 vs. 2050) – Kop van Zuid

Cooling + heating demand



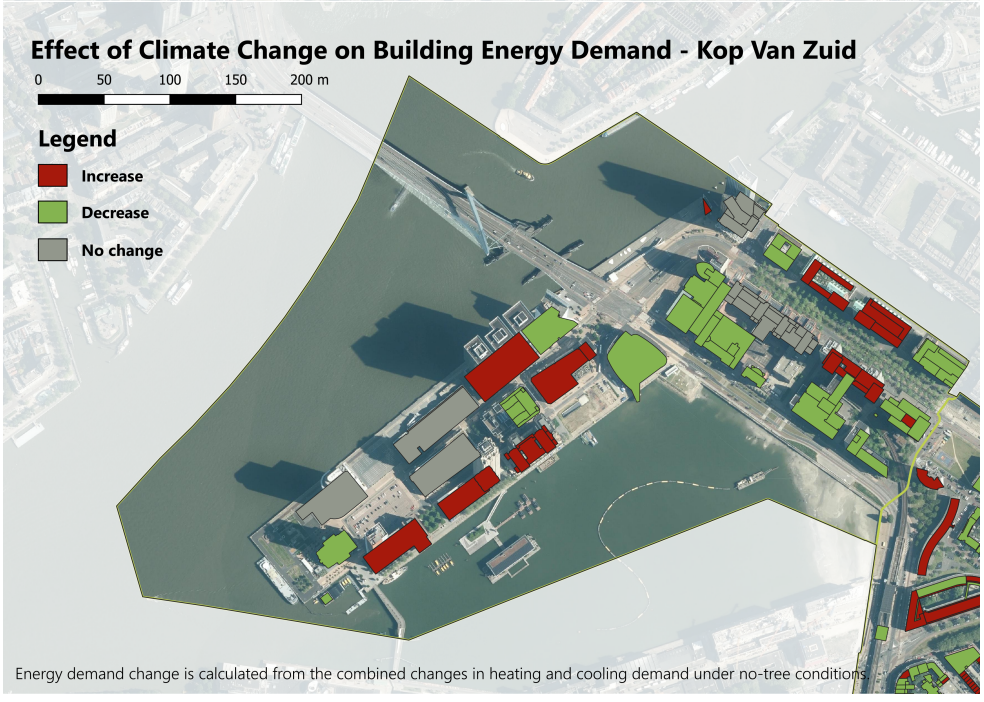
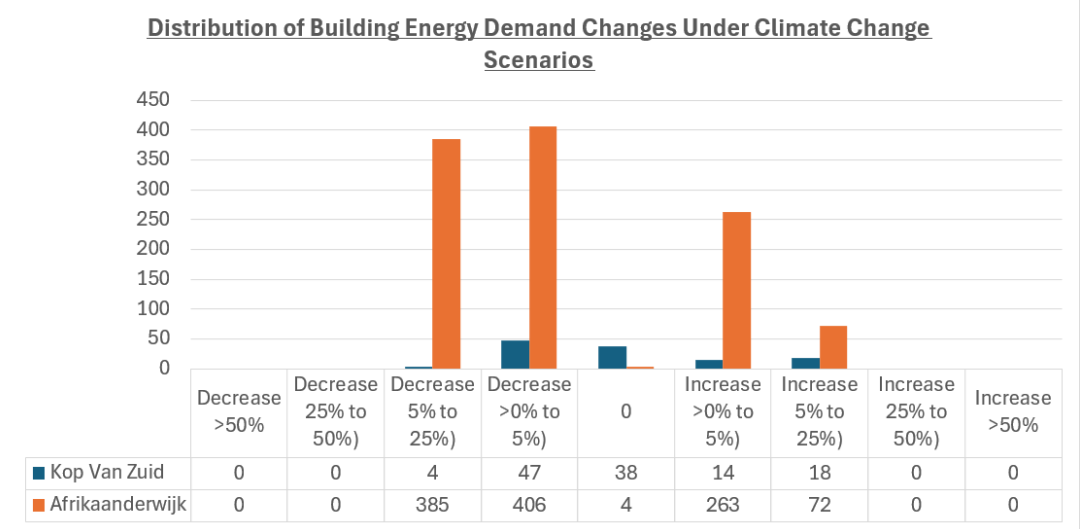


Figure 5.9.: Change in Energy demand resulting from climate change in Afrikaanderwijk and Kop Van Zuid under no tree condition.

The combined impact of rising cooling requirements and declining heating needs determines the net change in building energy demand between 2023 and 2050. Figures 5.9 illustrate these overall changes for Afrikaanderwijk and Kop van Zuid, respectively. From the maps, it is clear that most buildings in both neighbourhoods show reduced annual energy use.



	Decrease >50%	Decrease 25% to 50%)	Decrease 5% to 25%)	Decrease >0% to 5%)	0	Increase >0% to 5%)	Increase 5% to 25%)	Increase 25% to 50%)	Increase >50%
Kop Van Zuid	0	0	4	47	38	14	18	0	0
Afrikaanderwijk	0	0	385	406	4	263	72	0	0

Figure 5.10.: Distribution of changes in building energy demand under climate change scenarios for Afrikaanderwijk and Kop Van Zuid

The distribution of building-level energy demand changes in Figure 5.10 provides additional insight into the maps. In Afrikaanderwijk, most buildings show decreases of up to 25%, indicating that reductions in heating demand generally outweigh the increase in cooling demand across the majority of the building stock. Only a small share of buildings experience increases above 25%, suggesting that large net rises in energy use are relatively limited under the no-tree scenario. In Kop van Zuid, the pattern is more mixed. While some buildings still show moderate decreases, a greater proportion exhibits small to moderate increases (up to 25%). This likely reflects the more decisive influence of growing cooling needs in this neighbourhood, possibly linked to factors such as building design, internal heat gains, or lower shading levels.

Taken together, the results show that while neighbourhood-level changes in total annual energy demand due to climate change appear modest, building-level impacts vary. Some buildings are likely to experience more significant increases in cooling demand even as heating needs decline, highlighting the importance of targeted rather than uniform adaptation measures.

While the distribution analysis shows the variability in energy demand changes at the building level, it does not show how these shifts translate into overall energy use for each neighbourhood. To address this, Table 5.6 summarises the total annual cooling, heating, and combined energy demand for 2023 and 2050. This helps to connect the spatial and building-level patterns with the aggregate energy implications of climate change.

Table 5.6.: Annual energy demand for cooling, heating, and total energy in 2023 and 2050 for Kop van Zuid and Afrikaanderwijk (no tree cover scenario). Change denotes the absolute difference (2050–2023), while % Change denotes the relative change.

Neighborhood	Cooling	Heating	Total Energy Demand
Kop van Zuid			
2023	10,616,728	20,593,462	31,210,190
2050	14,029,074	17,918,065	31,947,139
Change	3,412,346	-2,675,397	736,949
% Change	32.14%	-12.99%	2.36%
Afrikaanderwijk			
2023	6,577,134	29,524,953	36,102,087
2050	9,157,658	25,962,409	35,120,067
Change	2,580,524	-3,562,544	-982,020
% Change	39.23%	-12.07%	-2.72%

The results in Table 5.6 show clear seasonal shifts in energy demand between 2023 and 2050 for both neighbourhoods. Cooling demand is increasing by 39.23% in Afrikaanderwijk and 32.14% in Kop van Zuid. This pattern is consistent with projections for warmer climate conditions, where higher outdoor temperatures drive greater cooling requirements during the summer months. The larger increase in Afrikaanderwijk suggests that local factors such as building density, construction materials, or urban layout may amplify the sensitivity of energy demand to rising temperatures. Meanwhile, heating demand declines in both neighbourhoods, falling by 12.99% in Kop van Zuid and 12.07% in Afrikaanderwijk. These reductions reflect milder winter conditions expected under climate change scenarios, particularly during transitional seasons like spring and autumn when heating needs are already relatively low.

From an annual perspective, the opposing trends in cooling and heating partially offset one another. Kop van Zuid experiences a slight net increase in total annual energy demand of 2.36%, while Afrikaanderwijk shows a small overall decrease of 2.72%. Although the total annual changes appear modest, they mask a growing seasonal imbalance: cooling is becoming increasingly dominant during the summer, while heating requirements in winter continue to decline.

This seasonal imbalance has implications for future energy planning. Rising summer cooling loads are likely to increase peak electricity demand, potentially placing additional stress on distribution networks and energy supply systems, even if total annual consumption remains relatively stable. At the same time, the gradual reduction in heating demand provides a limited compensating benefit, as it does not align with periods of peak system use. Together, these findings indicate the need for adaptation measures that can help moderate cooling requirements, particularly during the summer, to limit peak energy demand under future climate conditions.

Urban greening, such as through additional tree planting, has been widely proposed as a strategy to moderate rising cooling demand. In the context of building energy use, trees can reduce solar gains on façades and roofs through shading, thereby lowering indoor cooling requirements during summer periods. However, this same shading can also limit beneficial solar gains in winter, potentially reducing passive heating and creating trade-offs between

seasons. These interactions highlight the need to assess both the benefits and potential drawbacks of tree planting. The following section, therefore, introduces the proposed planting scenario, which forms the basis for evaluating its effects on building energy demand under both current and future climate conditions.

5.2.2. Identification of potential planting areas

Following the procedure outlined in Section 4.4.3, a total of 11.8 hectares in Kop van Zuid and 21.8 hectares in Afrikaanderwijk were identified as plantable areas for additional tree planting. These correspond to approximately 45% of the total land area in Kop van Zuid (26.1 ha) and 35.5% of the total land area in Afrikaanderwijk (61.6 ha). Figure 5.11 and figure 5.12 illustrate the spatial distribution of these potential planting areas across both neighbourhoods. From the maps, it can be observed that some areas identified as plantable are, in fact, logically unsuitable for tree planting. However, this does not affect the generation of plantation points, as only areas within 5 meters of building boundaries are considered for this purpose. This approach ensures that only trees likely to influence the energy demand analysis are included. Additionally, limiting the selection to these areas helps reduce computational load, since no trees are added in locations far from buildings. For Kop van Zuid, a total of 374 proposed trees were generated, while Afrikaanderwijk has 1405 proposed trees. Figures 5.14 present the spatial distribution of these proposed plantation points for each neighbourhood.

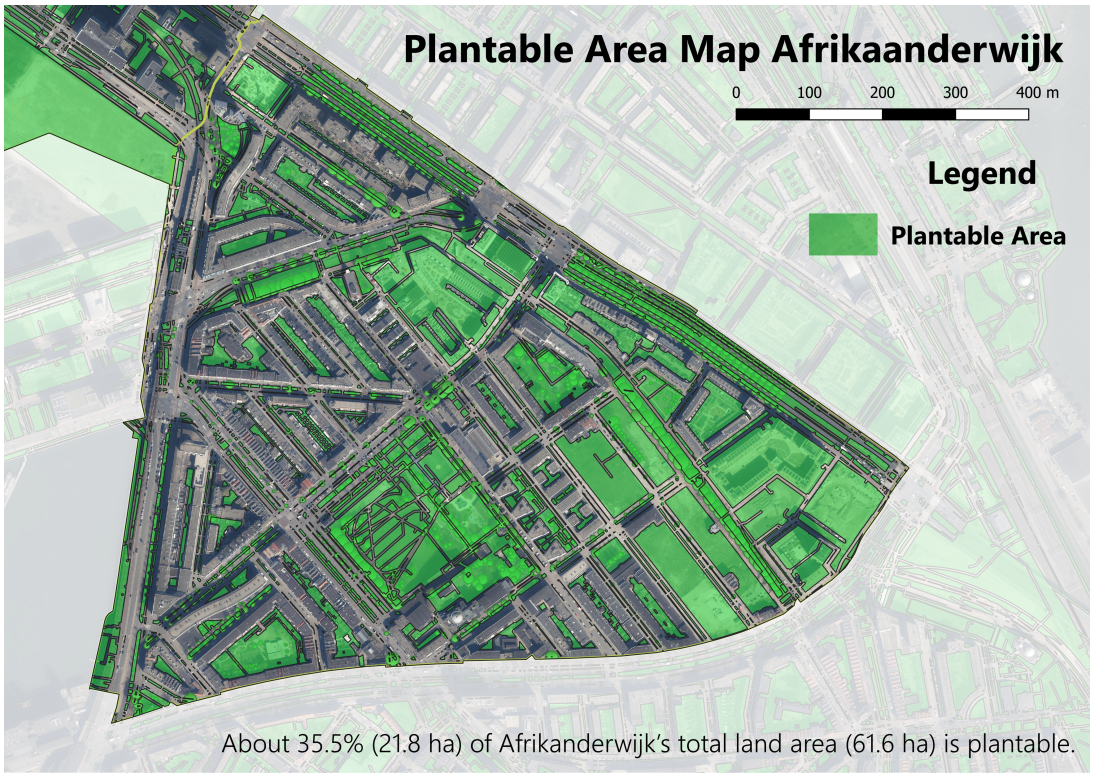


Figure 5.11.: Plantable areas identified in Afrikaanderwijk



Figure 5.12.: Plantable areas identified in Kop van Zuid

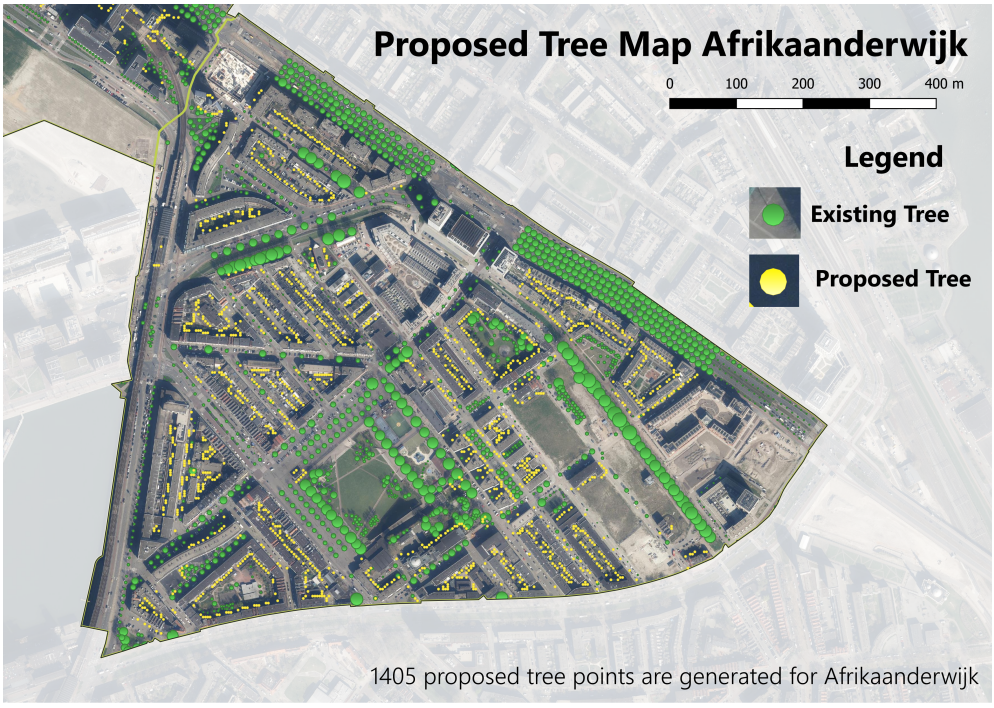


Figure 5.13.: Proposed tree points generated for Afrikaanderwijk (1405 points)



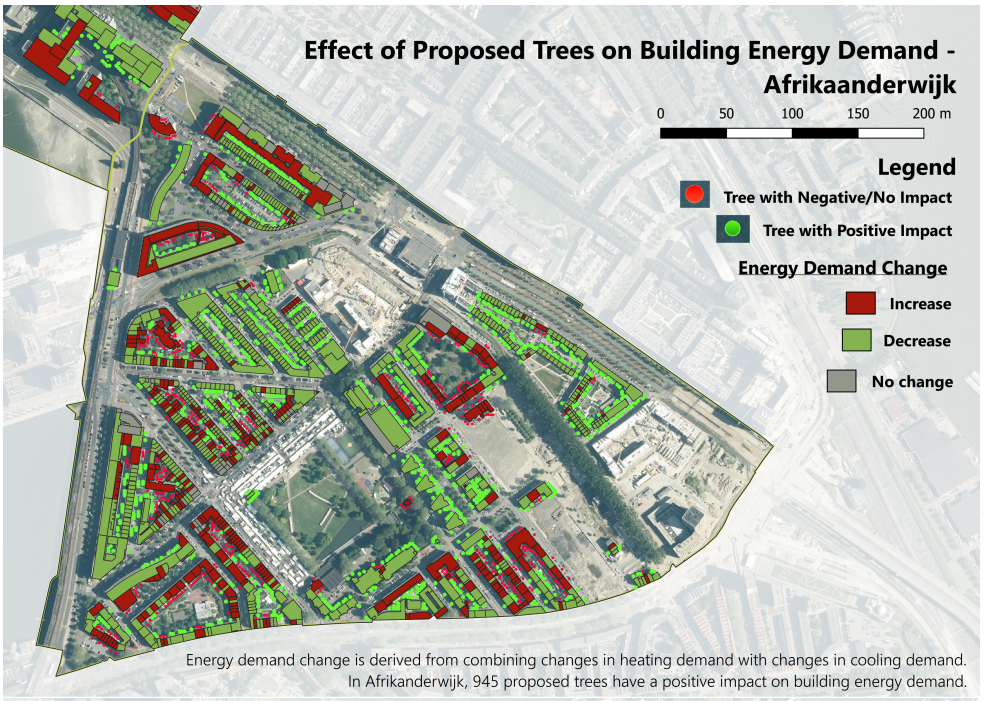
Figure 5.14.: Proposed tree points generated for Kop van Zuid (374 points)

5.2.3. Effectiveness of proposed tree planting strategies

The identification of plantable areas and the generation of proposed tree locations provide the spatial basis for assessing how additional shading may influence building energy demand. With the proposed planting scenario established, its effects are analysed by comparing energy demand in scenarios with and without the proposed trees under both current (2023) and projected (2050) climate conditions. The analysis proceeds in two steps: first, the impact of the proposed planting is evaluated for present-day conditions; second, its potential to mitigate the increased cooling requirements expected under future climate scenarios is assessed. Results are presented separately for cooling, heating, and total energy demand, followed by spatial maps indicating where the proposed trees offer the greatest benefits and where they may have neutral or adverse effects on building energy performance.

Some maps related to energy demand changes due to proposed tree planting are presented in Appendix C. The maps illustrate the spatial variation in building energy demand resulting from the introduction of trees. Buildings with green colour correspond to a decrease in energy demand, while those in red indicate an increase. Grey areas show no notable change. Tree symbols represent the projected effect of each tree: a positive impact refers to trees that contribute to reducing overall energy demand in nearby buildings, whereas a negative/no impact refers to trees that either increase energy demand or have no significant influence.

Under current climate



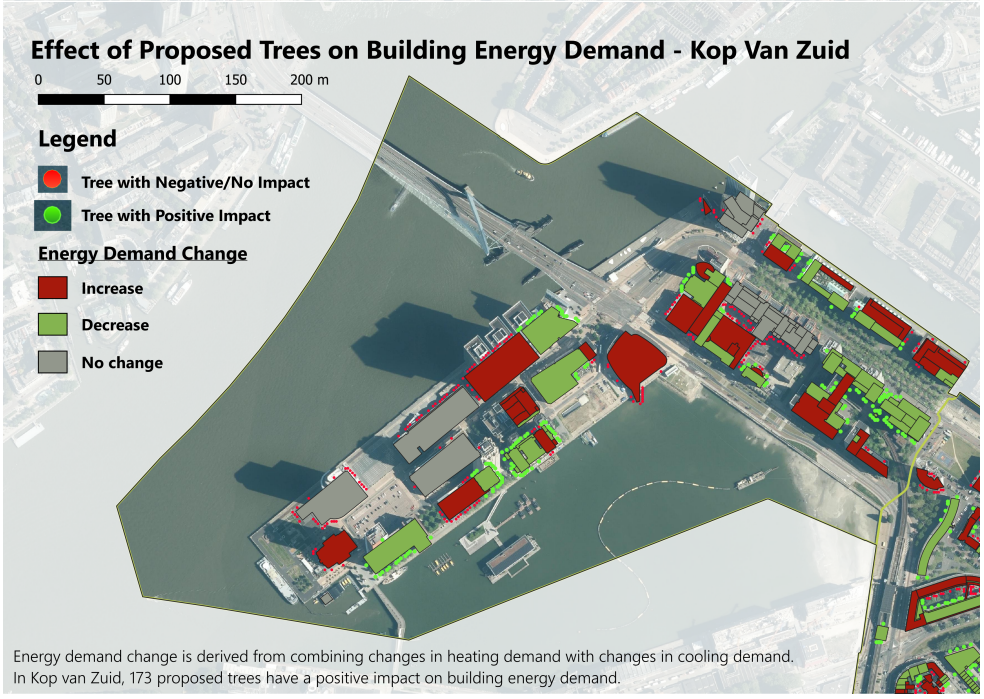


Figure 5.15.: Change in total energy demand resulting from proposed tree planting under the current climate in Afrikaanderwijk and Kop van Zuid.

Figures C.1 and C.2 show that the proposed tree planting reduces cooling demand for most buildings in Afrikaanderwijk and Kop van Zuid. This reduction results from increased shading and lower surface temperatures, which limit heat gains through building envelopes and reduce the need for mechanical cooling during warmer periods. At the same time, Figures C.3 and C.4 show that heating demand increases for many buildings because additional shading lowers winter solar gains. To assess the overall impact on energy demand, cooling and heating changes were combined in Figures 5.15. These maps show where trees lead to net energy savings. Under current conditions, 173 proposed trees in Kop van Zuid and 945 in Afrikaanderwijk reduce total annual energy demand.

Spatial patterns differ between the two neighbourhoods. In Afrikaanderwijk, most buildings show net reductions in energy demand, indicating that cooling savings usually exceed additional heating needs. In Kop van Zuid, results are more mixed, with some areas showing net increases in energy use. These differences are linked to variations in urban form, building orientation, and solar exposure, which affect the balance between cooling gains and heating penalties. Overall, trees lower total energy demand where shading reduces cooling needs without large heating penalties. Where heating penalties dominate, uniform planting is less effective, and placement that accounts for building façades and orientations is needed to achieve better results.

Representative Buildings

To show the range of outcomes, one building per neighbourhood in each category was selected under the current climate scenario. Based on absolute and percentage changes in cooling and total energy demand, the buildings were grouped into three categories: 1) building with the highest net benefit, 2) building with strong cooling reductions but notable heating penalties, and 3) building with the least overall benefit. These examples show where tree planting reduces energy use the most and where additional factors such as building orientation, insulation, or other cooling measures may be needed if heating penalties outweigh the benefits.



Figure 5.16.: Highest net benefits building in Afrikaanderwijk

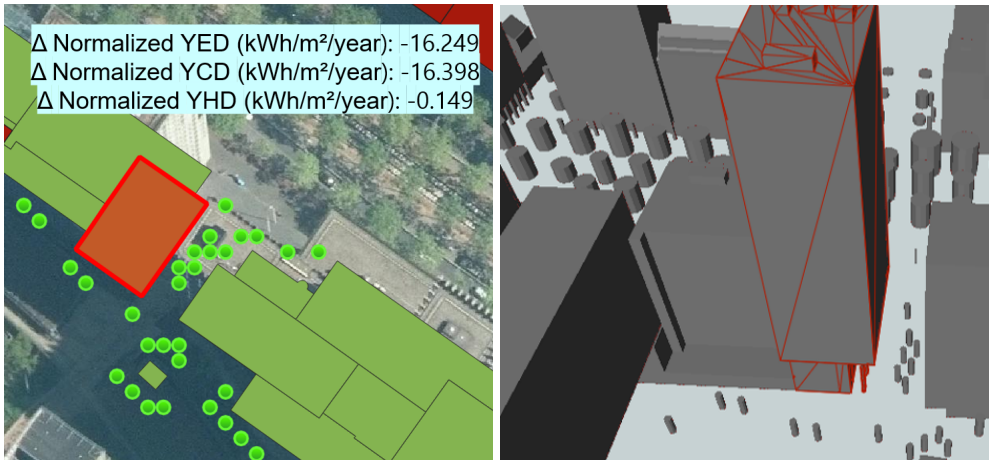


Figure 5.17.: Highest net benefits building in Afrikaanderwijk

For the highest net benefits category, in Afrikaanderwijk (Figure 5.16), cooling demand reductions reach about $-78\,\mathrm{kWh/m^2/year}$, with heating penalties around $-46\,\mathrm{kWh/m^2/year}$. Meanwhile, in Kop van Zuid (Figure 5.17), cooling reductions are smaller at around $-16\,\mathrm{k-Wh/m^2/year}$, while heating penalties remain minimal. The stronger effects in Afrikaanderwijk likely result from its more uniform low-rise building stock, while the mixed high-rise forms in Kop van Zuid reduce shading efficiency.

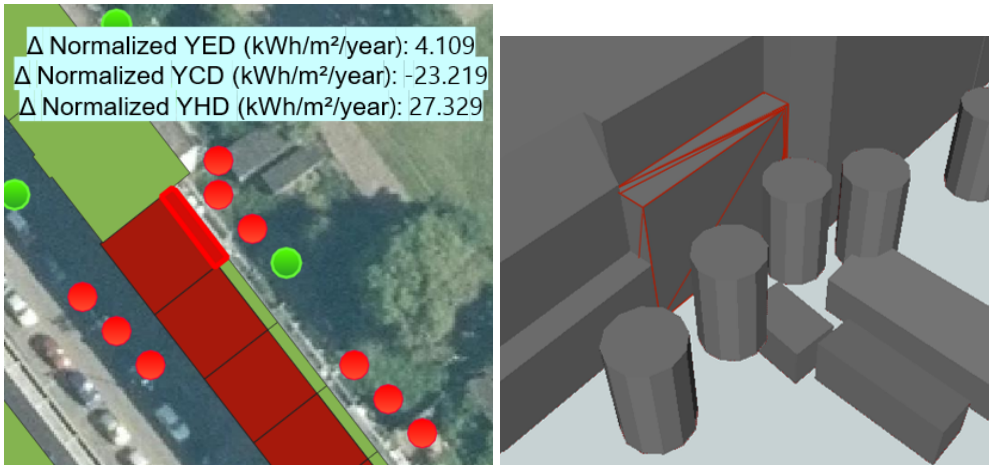


Figure 5.18.: Building with high cooling benefits but substantial heating penalties in Afrikaanderwijk



Figure 5.19.: Building with high cooling benefits but substantial heating penalties in Kop van Zuid.

For the strong cooling reductions but notable heating penalties category, in Afrikaanderwijk (Figure 5.18), cooling savings of about $-23\,\mathrm{kWh/m^2/year}$ are partly offset by heating increases of $+27\,\mathrm{kWh/m^2/year}$. And in Kop van Zuid (Figure 5.19), heating penalties exceed $+118\,\mathrm{kWh/m^2/year}$ despite cooling reductions of $-113\,\mathrm{kWh/m^2/year}$. These cases show how winter shading can reduce or even cancel out large summer energy savings when façades have high heating demand.



Figure 5.20.: Building heating penalties outweigh cooling benefits in Afrikaanderwijk.

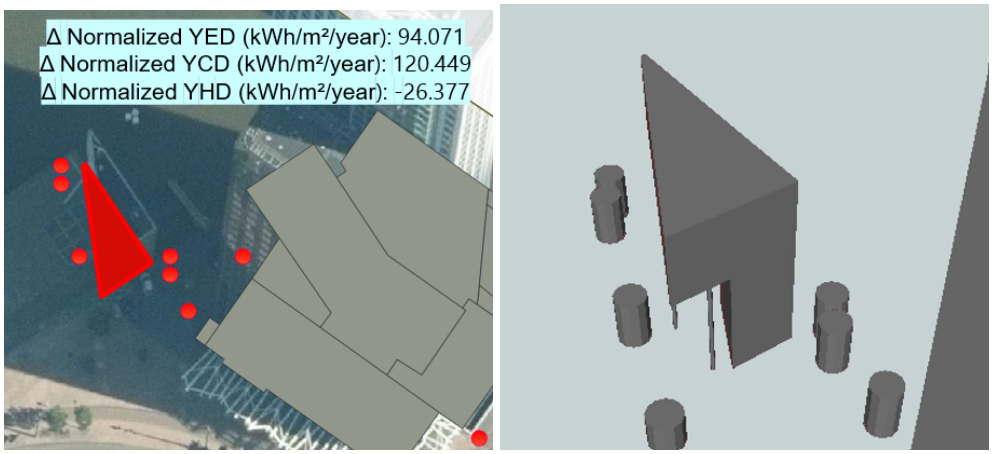


Figure 5.21.: Building heating penalties outweigh cooling benefits in Kop van Zuid.

Lastly, for the least overall benefit category, in Afrikaanderwijk (Figure 5.20), heating penalties reach $+43\,\mathrm{kWh/m^2/year}$, exceeding cooling reductions of only $-11\,\mathrm{kWh/m^2/year}$. Meanwhile, in Kop van Zuid (Figure 5.21), heating penalties reach $+120\,\mathrm{kWh/m^2/year}$ while cooling reductions are $-26\,\mathrm{kWh/m^2/year}$. These buildings are usually located where orientation and building height limit summer shading while increasing winter solar losses.

Across all cases, the results show that uniform tree planting may be unsuitable in areas with diverse urban forms. Planting strategies that consider building orientation, height, façade exposure, and seasonal solar access are needed to achieve net energy savings while avoiding large heating penalties.

Under 2050 climate

The same comparison was applied to the 2050 climate projections to examine how rising temperatures affect the energy impacts of tree planting. Figures C.5, C.6, C.7, and C.8 show that cooling demand continues to decline for most buildings under future conditions, while heating demand increases for many buildings.

Figures 5.22 show the net energy difference. Tree counts reveal shifts in net energy benefits. In Kop van Zuid, the number of proposed trees reducing total energy demand rises from 173 under current conditions to 235 under the 2050 scenario, increasing their share from 46% to 63%. Future warming raises cooling demand, allowing shading to offset additional winter heating requirements for a larger proportion of locations. Meanwhile, Afrikaanderwijk shows the opposite trend: beneficial trees decrease from 945 under current conditions to 742 under the 2050 scenario, thus lowering their share from 67% to 53%. Despite higher cooling demand in a warmer climate, factors such as urban morphology, building orientation, and seasonal solar exposure continue to constrain the extent to which additional shading reduces total annual energy demand.

Taken together, these results show that climate change does not uniformly improve the energy-saving potential of urban tree planting. While some locations, such as Kop van Zuid, benefit from a greater share of energy-reducing trees under future conditions, others, such as Afrikaanderwijk, show a more constrained response. Site-specific planning that accounts

for both urban form and long-term climate projections is therefore essential for maximising the net benefits of urban greening strategies.

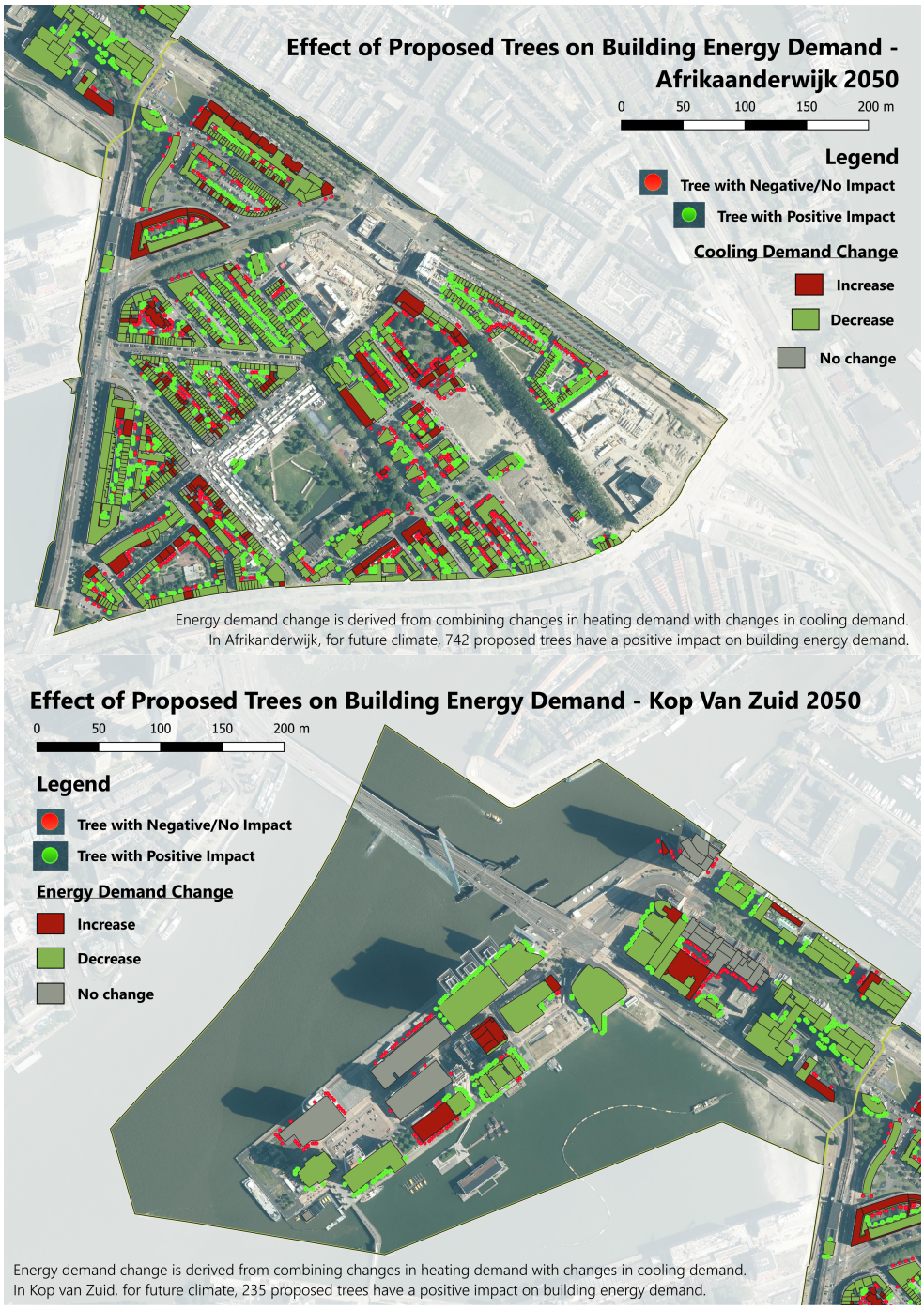


Figure 5.22.: Change in total energy demand resulting from proposed tree planting under the 2050 climate in Afrikaanderwijk and Kop van Zuid.

To evaluate the overall impact of the proposed trees under both current and future climate conditions, the annual energy demand for cooling, heating, and total energy consumption across the entire neighbourhood is summarised in Tables 5.7 and 5.8. Table 5.7 presents the results for the current climate, while Table 5.8 shows the projections under the future climate scenario. In each case, energy demands are compared between the existing tree coverage and the combined scenario of existing plus proposed trees for Afrikaanderwijk and Kop van Zuid.

Table 5.7.: Annual energy demand for cooling, heating, and total energy under the current climate for Afrikaanderwijk and Kop van Zuid, comparing existing trees and existing + proposed trees scenarios.

Neighborhood / Scenario	Cooling	Heating	Total Energy Demand
Afrikaanderwijk			
Existing Trees	6,207,070	29,857,855	36,064,925
Existing + Proposed Trees	6,019,078	30,053,765	36,072,843
Change	-187,992	195,910	7,918
% Change	-3.03%	0.66%	0.02%
Kop van Zuid			
Existing Trees	10,561,203	20,613,527	31,174,730
Existing + Proposed Trees	10,429,203	20,728,684	31,157,887
Change	-132,000	115,157	-16,843
% Change	-1.25%	0.56%	-0.05%

Table 5.8.: Annual energy demand for cooling, heating, and total energy under the future climate for Afrikaanderwijk and Kop van Zuid, comparing existing trees and existing + proposed trees scenarios.

Neighborhood / Scenario	Cooling	Heating	Total Energy Demand
Afrikaanderwijk			
Existing Trees	8,574,256	26,339,661	34,913,917
Existing + Proposed Trees	7,717,935	26,869,988	34,587,923
Change	-856,321	530,327	-325,994
% Change	-9.99%	2.01%	-0.93%
Kop van Zuid			
Existing Trees	13,943,506	17,942,320	31,885,826
Existing + Proposed Trees	13,711,659	18,060,193	31,771,852
Change	-231,847	117,873	-113,974
% Change	-1.66%	0.66%	-0.36%

Tables 5.7 and 5.8 confirm these patterns numerically. Under current conditions, cooling demand falls in both neighbourhoods by 3.03 % in Afrikaanderwijk and 1.25 % in Kop van Zuid, while heating demand increases slightly by 0.66 % and 0.56 %, respectively. Total annual energy demand shows almost no change in Afrikaanderwijk at 0.02 % and a small reduction in Kop van Zuid at 0.05 %.

Under 2050 conditions, cooling demand reductions become larger, particularly in Afrikaanderwijk at 9.99%, while heating demand rises by 2.01% in Afrikaanderwijk and 0.66% in

Kop van Zuid. The combined effect is a total energy reduction in both neighbourhoods, with 0.93% in Afrikaanderwijk and 0.36% in Kop van Zuid, showing that future warming increases cooling savings relative to heating penalties.

Overall, the results suggest that while future warming amplifies the cooling benefits of trees, heating penalties remain in some areas, making site-specific placement important for maximising net energy savings. The maps already indicate which trees have positive, neutral, or negative effects on building energy demand. Policymakers can therefore use this information to guide planting decisions, prioritising locations where shading delivers a net energy benefit while avoiding areas where additional heating penalties outweigh cooling gains. This targeted approach ensures that limited urban greening budgets achieve the greatest energy efficiency benefits.

However, it should be noted that the building models and simulations do not account for future renovation or refurbishment scenarios, such as improved insulation or passive heating strategies, which could reduce winter heating demand. In such cases, the negative or neutral impacts identified here might be mitigated in the future as buildings become more energy efficient. Moreover, planting trees at locations with neutral or negative energy impacts does not necessarily imply a negative environmental outcome; trees provide co-benefits such as improved air quality, stormwater regulation, and enhanced urban biodiversity, which are not captured by energy demand metrics alone. Therefore, the energy implications highlighted here should be considered alongside broader environmental, social, and climatic objectives before final planting decisions are made.

5.3. Urban vegetation and greening benchmark assessment

In this section, the current canopy coverage in both neighbourhoods is discussed in relation to the 30% target. This will provide planners with a clear picture of how existing conditions compare to the benchmark.



Figure 5.23.: Existing tree canopy coverage in Kop Van Zuid. Background Map Source: Luchtfoto 2025 Quick Ortho 8cm RGB

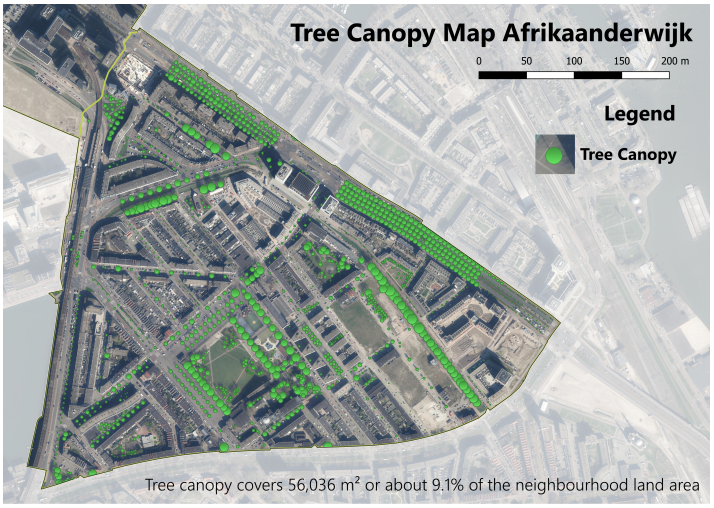


Figure 5.24.: Existing tree canopy coverage in Afrikaanderwijk. Background Map Source: Luchtfoto 2025 Quick Ortho 8cm RGB

The analysis quantified the extent of existing tree canopy within each neighbourhood, expressed as the proportion of land area covered by tree crowns. Water surfaces were excluded to ensure that only terrestrial land cover was considered. In Kop van Zuid, approximately 11,218 m^2 of tree canopy was identified, accounting for about 4.3% of the neighbourhood's land area. In Afrikaanderwijk, the canopy area covered roughly 56,036 m^2, representing approximately 9.1% of the land area. The spatial distribution of the canopy is shown in Figures 5.23 and 5.24. Both figures are well below the 30% target, indicating that neither neighbourhood currently complies with the benchmark.

It should be noted, however, that the 3D City Model of Rotterdam includes only public trees; private trees are excluded due to data protection regulations (GDPR). Consequently, some building areas with private gardens and courtyards are under-represented in terms of tree cover, as illustrated in Figure 5.25. Furthermore, Section 5.2.2 shows that substantial areas remain available for potential tree planting. These areas could, in principle, be used to approach the 30–30–300 guideline related to achieving 30% canopy cover. However, the results of this thesis indicate that meeting this benchmark alone is not sufficient for achieving positive energy districts. The energy demand analysis demonstrated that while additional trees often reduce cooling demand, especially under the 2050 climate scenario, they can also increase heating demand in winter, resulting in neutral or negative effects in some areas. Simply maximising canopy cover to meet the 30–30–300 target would therefore risk overlooking these trade-offs. The results also showed that the share of trees delivering net energy savings decreases in some locations under future conditions, indicating that a higher canopy cover does not necessarily lead to proportional energy efficiency improvements. Moreover, total annual energy changes were often small because cooling reductions and heating penalties partly offset each other. A planting strategy that combines canopy coverage targets with these spatial energy performance results would allow new trees to be placed where they deliver the most significant energy benefits while avoiding locations where shading leads to limited or negative outcomes. This approach would ensure that meeting the 30–30–300 guideline contributes not only to urban greening goals but also to long-term energy efficiency and climate adaptation objectives.



Figure 5.25.: Aerial view of Christiaan de Wetstraat and De la Reystraat in Afrikaanderwijk. Background Map Source: PDOK Luchtfoto 2023 Ortho 25cm RGB.

6. Conclusion

This chapter revisits the research questions, summarises the main findings in light of the methods adopted, and sets out the contributions, limitations, and directions for future work. The study developed a neighbourhood-scale simulation framework that integrates tree-planting scenarios into UBEM to quantify their effects on heating and cooling demand under present and projected 2050 climate conditions.

6.1. Research overview

RQ1. *How can tree planting scenarios, as nature-based strategies, be integrated into neighbourhood-scale simulation-based UBEM to evaluate their effectiveness in reducing heating and cooling demand under projected 2050 climate conditions?*

Answer. The thesis implemented a scenario-based workflow (Figure 3.1) that couples *SimStadt* with simplified vegetation representations and TMY3-format climate inputs (Section 3). Six scenarios (S0–S5; Figure 3.2) were run across current and 2050 climates. The framework produced building- and neighbourhood-level cooling/heating demand and enabled side-by-side attribution of climate vs. vegetation effects (Section 5).

RQ2. *How can a tree-planting strategy be incorporated within simulation-based UBEM to capture its impact on building energy demand at the neighbourhood scale?*

Answer. Trees were parameterised as cylindrical LoD1 volumes with seasonal canopies, imported as *Building*-typed CityGML features to pass geometric/physics preprocessors (Section 3.4). Planting points were generated within 3 m of façades using land-use and infrastructure buffers (Section 4.4.3).

RQ3. *What assumptions and simplifications are required for modelling the shading effects of trees on buildings under different climate conditions?*

Answer. Key simplifications were: (i) cylindrical tree volumes with seasonal diameter scaling for deciduous species (summer: $1.0D_c$; winter: $0.64D_c$) as a proxy for Leaf Area Index (LAI) changes; (ii) uniform dimensions for proposed deciduous trees; (iii) linear growth with capped diameter/height to reflect urban maintenance; and (iv) monthly climate inputs with synthetic hourly disaggregation in *SimStadt* (Section 3.4). These choices reduced data needs and computation while preserving the energy impacts of shading.

RQ4. *How can the simulated impacts of the tree planting strategy be interpreted to support urban planning and climate adaptation strategies at the neighbourhood scale?*

Answer. The analysis distinguishes locations where trees yield net energy savings from those where winter penalties dominate (Section 5). Under the current climate, Afrikaanderwijk exhibited more widespread net benefits than Kop van Zuid; under the 2050 climate, cooling benefits increased overall but remained spatially heterogeneous. The outputs (maps/tables) identify specific planting points that reduce total demand.

6.2. Synthesis of findings

Between 2023 and 2050, neighbourhood-level cooling demand rises notably (Afrikaanderwijk: +39.23%; Kop van Zuid: +32.14%), while heating demand falls by approximately 12% in both areas (Table 5.6). Net annual energy change remains small (Afrikaanderwijk: -2.72%; Kop van Zuid: $+2.36\%$), although the seasonal balance shifts as summer electricity for cooling becomes more prominent, with possible implications for peak demand (Figures 5.3 and 5.8). These results are consistent with rising average temperatures, longer and warmer summers, and more frequent extreme heat events in 2050 climate projections. At the same time, higher winter temperatures reduce the need for heating energy, particularly during the months of spring and autumn. Differences between the two neighbourhoods likely reflect variations in urban morphology and building stock, as dense, low-rise areas and mixed-use districts respond differently to warming trends compared to areas with larger, more exposed building volumes.

Adding the proposed deciduous trees leads to moderate cooling demand reductions at the neighbourhood scale (Afrikaanderwijk: -3.03%; Kop van Zuid: -1.25%) and slight heating increases (Afrikaanderwijk: $+0.66\%$; Kop van Zuid: $+0.56\%$). The overall impact on total annual demand remains close to zero (Afrikaanderwijk: $+0.02\%$; Kop van Zuid: -0.05%; Table 5.7), with some variation at the building level (Figures 5.16 to 5.21). This pattern occurs because shading from trees effectively reduces summer solar gains on façades and roofs, but in winter, it can also block low-angle sunlight that would otherwise contribute to passive heating. Buildings with large south-facing windows or limited insulation are therefore more sensitive to winter shading penalties, while compact forms with limited solar access benefit less from additional tree cover in any season.

Under the 2050 climate scenario, cooling demand reductions become larger (Afrikaanderwijk: -9.99%; Kop van Zuid: -1.66%), while heating demand rises slightly (Afrikaanderwijk: $+2.01\%$; Kop van Zuid: $+0.66\%$), resulting in small net annual decreases (Afrikaanderwijk: -0.93%; Kop van Zuid: -0.36%; Table 5.8). The share of beneficial trees increases in Kop van Zuid (46% to 63%) but declines in Afrikaanderwijk (67% to 53%), showing that urban form, building orientation, and baseline shading levels influence the balance between cooling savings and heating penalties. In compact districts, additional trees sometimes reduce already limited winter solar access, while in areas with higher cooling exposure, more trees provide net summer benefits even when heating penalties persist.

Overall, trees reduce cooling needs consistently, especially as summers become warmer, but winter heating increases remain in some locations because shading affects solar gains when they are most valuable. Uniform canopy targets alone may not achieve net energy savings because they do not account for façade exposure and differences in building geometry. Planting strategies that consider these factors are likely to provide greater energy benefits while limiting unwanted winter effects.

6.3. Contributions

This study developed and tested a neighbourhood-scale workflow for integrating vegetation into urban building energy modelling using standard tools and data models such as CityGML. The workflow enables consistent comparison across multiple scenarios and remains compatible with existing UBEM tools. All scripts used for data preprocessing, scenario generation, simulation control, and post-processing of results are available in a public repository (https://github.com/adhisyetud/CoolTreesRotterdam). This repository is provided to support the transparency and reproducibility of the methods used in this thesis.

Vegetation was represented using a simplified CityGML *Building* parametrisation that can pass through SimStadt's preprocessors, allowing basic seasonal shading effects to be captured without additional modelling software. Spatial analysis was applied to identify feasible planting locations by incorporating legal and operational constraints and selecting areas near building façades where shading was expected to influence energy demand the most.

The results quantify climate-driven changes in energy demand, with clear increases in summer cooling needs and moderate decreases in winter heating demand. While the annual net changes at the neighbourhood level are small, the seasonal effects are more noticeable. Additional tree planting leads to modest energy savings at the neighbourhood scale under both current and future climate conditions, although building-level effects vary depending on location, orientation, and urban form.

The findings provide a map-based decision aid for planners to identify where trees are likely to reduce cooling demand without causing significant heating penalties. The results also highlight the need to balance tree canopy targets with energy outcomes. Rather than applying uniform planting strategies to meet coverage benchmarks, orientation-aware and façade-focused planting can better align urban greening objectives with long-term energy efficiency and climate adaptation goals.

6.4. Limitations and challenges

This study is subject to several limitations that influence the accuracy, interpretability, and generalisability of the results. First, the temporal resolution of the climate data was limited. Monthly climate inputs were converted into synthetic hourly profiles to meet the modelling software requirements. While this approach enabled consistent scenario comparisons, it inevitably reduced the accuracy of diurnal and peak load simulations.

Second, the building energy model relied on the DIN V 18599 standard, which applies monthly energy balances and predefined building archetypes. In this study, German usage libraries were combined with a Dutch construction library to approximate the characteristics of the Dutch building stock. This approach introduced uncertainty because the resulting archetypes may not fully reflect local construction practices, occupancy schedules, or heating and cooling system efficiencies in the Netherlands. The observation that some buildings exhibited unusually high heating or cooling demand values indicates that the results were sensitive to assumptions regarding internal loads, geometry simplifications, and system parameters, which were not calibrated against real-world data.

A third limitation concerns the representation of vegetation. Trees were modelled as simple cylindrical volumes with fixed seasonal factors and generic species assumptions. This static

representation neglects spatial and temporal heterogeneity in canopy density and species-specific leaf area dynamics. Consequently, the shading and cooling effects of trees were simplified compared to real-world conditions, where differences in growth rates, crown shapes, and seasonal phenology could influence their energy-saving potential.

A fourth constraint arose from computational limitations, which restricted the analysis to two neighbourhoods. In addition to long simulation times, several runs failed due to software-related issues, including memory allocation errors and instability in the radiosity algorithm when handling large or geometrically complex datasets. These issues were partly linked to the representation of vegetation as building geometries, which increased the number of surfaces and computational load. As a result, the analysis could not be extended to neighbourhoods with higher building densities or larger extents, limiting the generalisability of the findings to other urban forms, building heights, or spatial configurations.

Finally, the modelling framework assumed a static building stock over time, without accounting for future retrofitting, insulation upgrades, or replacement of heating and cooling systems. In reality, such interventions are likely to occur before 2050 and would reduce heating demand while potentially altering the balance between cooling benefits and winter shading penalties introduced by additional vegetation.

6.5. Recommendations for future work

Building on these limitations, future research could improve both the accuracy and applicability of the findings in several ways. First, the use of hourly climate data rather than synthetic profiles would allow for a more realistic representation of short-term variability and peak energy demands. Directly integrating high-resolution regional climate model outputs could enhance the simulation of diurnal temperature swings and extreme weather events, thereby producing more robust estimates of heating and cooling needs.

Second, uncertainty in building energy modelling could be reduced by calibrating archetypes against locally measured energy consumption and construction data. Incorporating sensitivity analyses on occupancy schedules, internal heat gains, and system efficiencies would help identify the parameters with the most considerable impact on energy demand predictions. This would enable model refinements where they matter most and improve confidence in scenario outcomes.

Third, future studies should employ more sophisticated vegetation models that can capture species-specific characteristics, growth patterns, and seasonal changes in leaf area index.

Fourth, future work should aim to expand the computational capacity and improve the stability of the modelling framework to enable analyses at larger spatial scales and across a broader range of neighbourhood typologies. Enhancements to the radiosity algorithm and memory management could help the model handle complex geometries and vegetation representations more efficiently, increasing its scalability and robustness. Scenario design could also be broadened to evaluate combined adaptation strategies, such as integrating urban greening with façade retrofits, reflective materials, natural ventilation, or external shading systems. Studying the interactions between these measures would clarify trade-offs between winter heating penalties and summer cooling benefits under future climate conditions.

Finally, integrating future retrofitting scenarios into the modelling framework would allow the analysis to account for expected improvements in insulation, heating systems, and cooling technologies. This would reveal how urban greening strategies interact with ongoing efforts to decarbonise and modernise the building stock, providing a more realistic picture of future energy demand patterns.

6.6. Conclusion

The study shows that integrating tree planting strategies into the neighbourhood scale UBEM is both feasible and informative. Warming climates increase cooling needs and reduce heating demand; trees can moderate the former but introduce winter trade-offs that vary by orientation and urban form. Neighbourhood-level annual changes are small on average, yet peak and building-level effects are not trivial. Consequently, energy-aware planting, targeted by façade orientation and local climate, offers a practical pathway to align urban greening with climate adaptation and building energy goals. The proposed workflow provides a transferable basis for such analyses, while the noted limitations point to concrete opportunities for refinement.

A. Tables

CityGML Component	Attribute	Description
GML Core	gml_id	Unique identifier of the object within the GML dataset.
	gml_parent_id	Identifier of the parent object.
CityObject Metadata	citygml_target_uri	URI reference to a related CityGML feature.
	citygml_feature_role	Role or relationship of the feature within the dataset.
	citygml_creationDate	Creation date of the CityGML feature entry.
Geometric Properties	citygml_height	Height of the tree.
	citygml_trunk_diameter	Diameter of the tree trunk.
	citygml_crown_diameter	Diameter of the tree crown.
Units	citygml_height_units	Measurement units for tree height.
	citygml_trunk_diameter_units	Measurement units for trunk diameter.
	citygml_crown_diameter_units	Measurement units for crown diameter.
VegetationObject Properties	tree_part	Part of the tree
Generic Attributes	Aanlegjaar	Planting year
	Beheerobjectomschrijving	Management description.
	Boom_id	Unique identifier
	Boomsortiment	Species (scientific)
	Boomsortiment_nederlands	Species (Dutch common name)
	Boomstatus	Status of the tree
	Brondatum	Date recorded or sourced.
	Buurt	Neighborhood
	Geslacht	Genus of the tree.
	Hoogte	tree height.
	Laatste_mutatie	Date of last update
	Ontwikkeling	Development stage of the tree
	Stamdiameter	Diameter of the trunk
	Stamlengte	Length of the trunk
	Straat	Street name where the tree is located.
	Thema	Thematic classification tag
	Wijk	District or ward in which the tree is located.

Table A.1.: Summary of attributes in the CityGML *SolitaryVegetationObject* dataset, grouped by CityGML schema components, with descriptions.

Table A.2.: Tree genus classification into deciduous and evergreen categories.

Deciduous		**Evergreen**	
• Ailanthus	• Cercis	• Pinus	• Cupressocyparis
• Robinia	• Cornus	• Ilex	• Picea
• Ulmus	• Nyssa	• Cedrus	• Chamaecyparis
• Platanus	• Catalpa	• Thuja	• Arbutus
• Tilia	• assortiment	• Taxus	• Sequoia
• Prunus	• Paulownia	• Abies	
• Gleditsia	• Larix		
• Fraxinus	• Castanea		
• Liriodendron	• Fagus		
• Liquidambar	• Davidia		
• Betula	• Metasequoia		
• Acer	• Juglans		
• Alnus	• Nothofagus		
• Crataegus	• Parrotia		
• Pyrus	• Ostrya		
• Malus	• Eucommia		
• Carpinus	• Stewartia		
• Sorbus	• Rhus		
• Pterocarya	• Ficus		
• Populus	• Morus		
• Salix	• Cladrastis		
• Tetradium	• Taxodium		
• Aesculus	• Gymnocladus		
• Quercus	• Hamamelis		
• Koelreuteria	• Carya		
• Corylus	• Laburnum		
• Ginkgo	• Toona		
• Magnolia	• Chitalpa		
• Styphnolobium	• Styrax		
• Syringa	• Celtis		
• Cercidiphyllum	• Zelkova		
• Amelanchier			

B. Energy Demand Results

B.1. Energy Demand under Current Climate

B.1.1. Without Trees

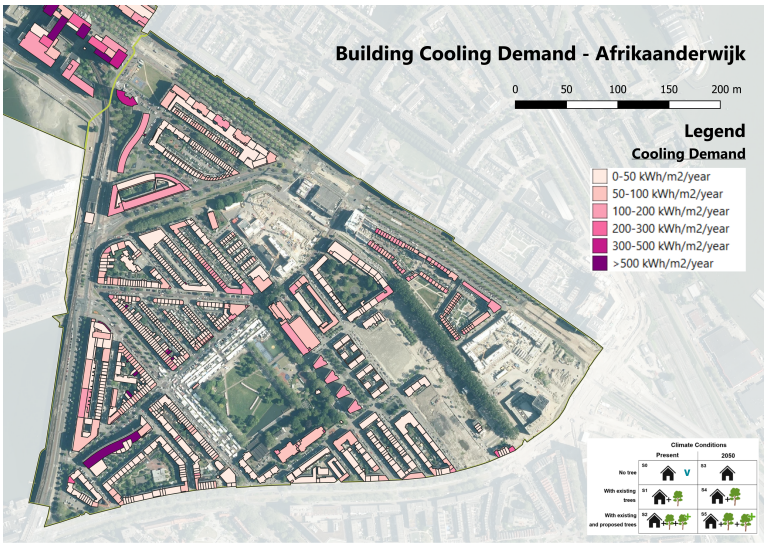


Figure B.1.: Cooling demand under current climate for the Afrikaanderwijk neighbourhood without trees.

B.1.2. With Existing Trees

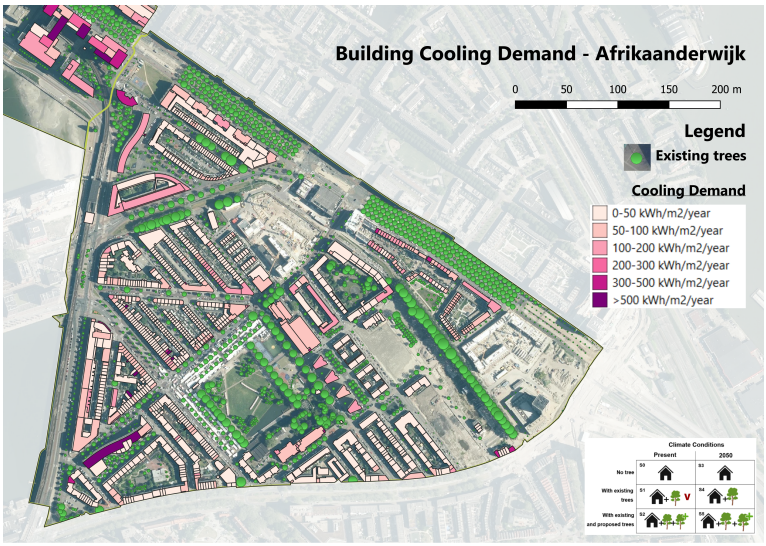


Figure B.2.: Cooling demand under current climate for the Afrikaanderwijk neighbourhood with existing trees.

B.1.3. With Existing and Proposed Trees

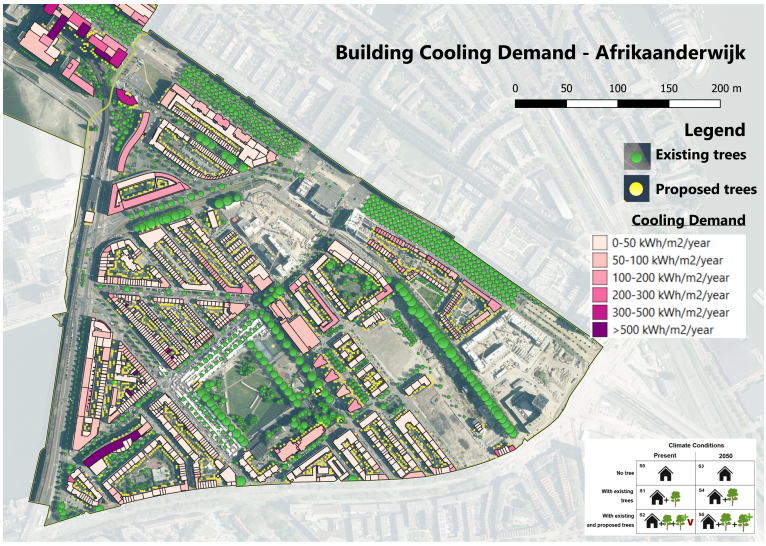


Figure B.3.: Cooling demand under current climate for the Afrikaanderwijk neighbourhood with existing and proposed trees.

C. Energy Demand Results Comparison (Proposed Trees Effect)

C.1. Under Current Climate

C.1.1. Cooling Demand Change

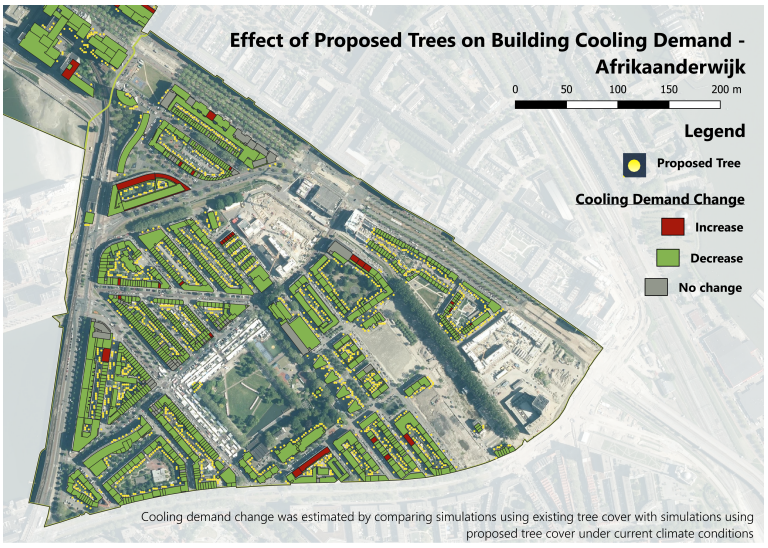


Figure C.1.: Change in cooling demand resulting from proposed tree planting under the current climate in Afrikaanderwijk.

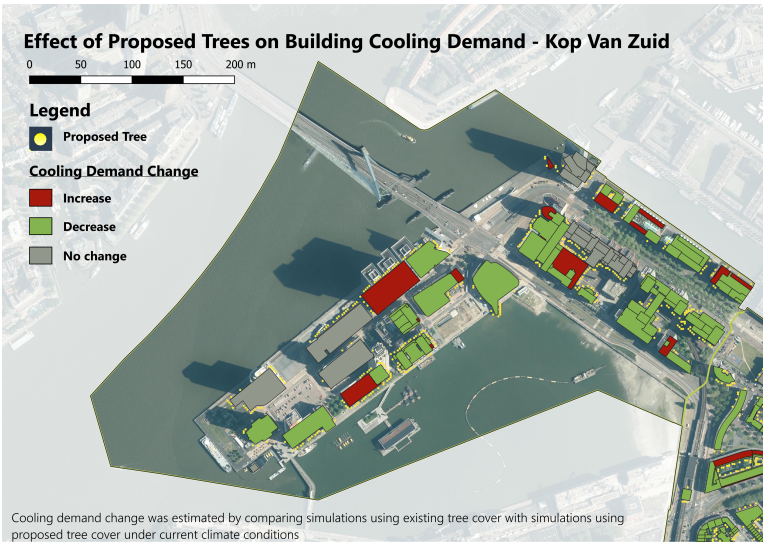


Figure C.2.: Change in cooling demand resulting from proposed tree planting under the current climate in Kop van Zuid.

C.1.2. Heating Demand Change

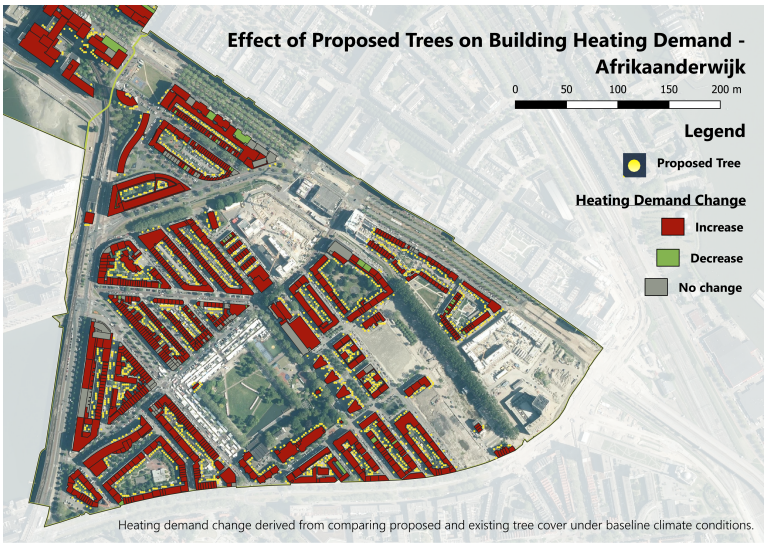


Figure C.3.: Change in heating demand resulting from proposed tree planting under the current climate in Afrikaanderwijk.

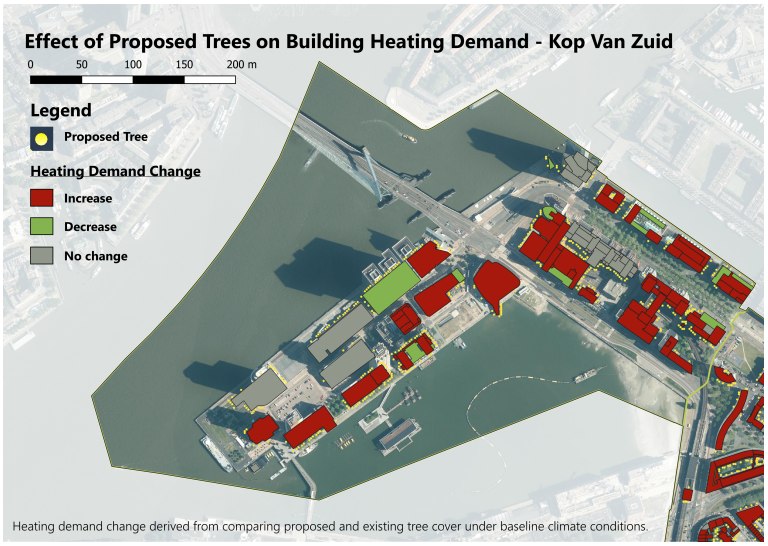


Figure C.4.: Change in heating demand resulting from proposed tree planting under the current climate in Kop van Zuid.

C.2. Under Future Climate

C.2.1. Cooling Demand Change

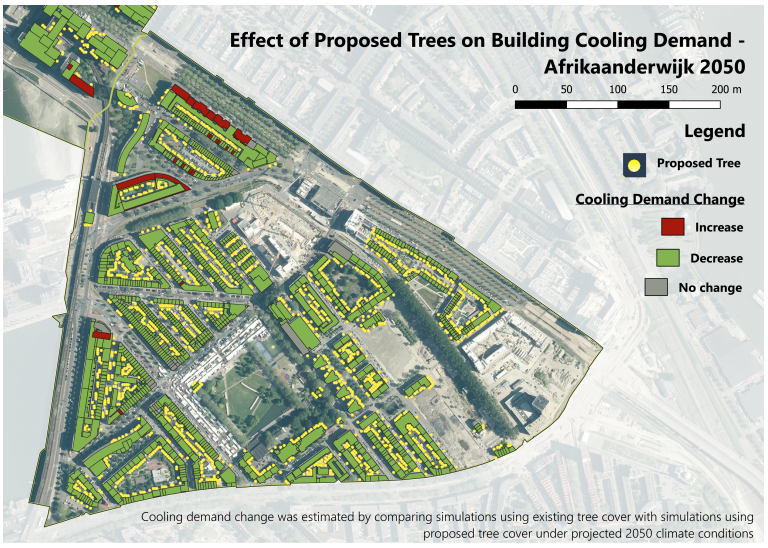


Figure C.5.: Change in cooling demand resulting from proposed tree planting under the 2050 climate in Afrikaanderwijk.

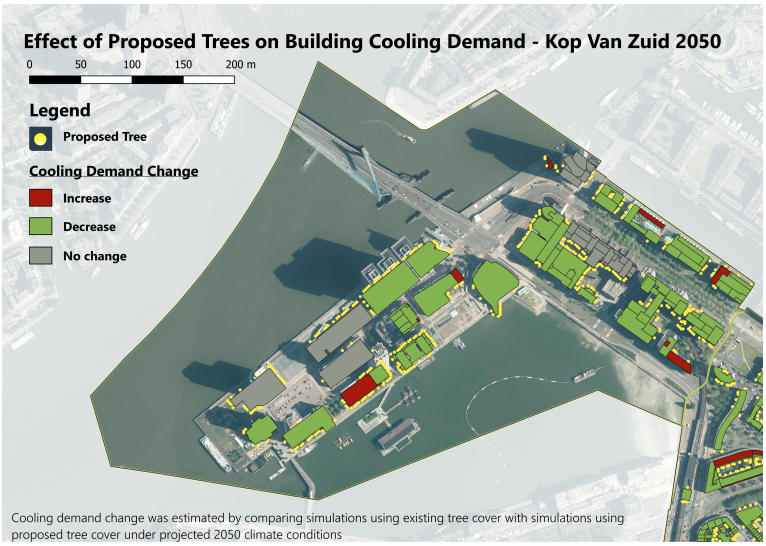


Figure C.6.: Change in cooling demand resulting from proposed tree planting under the 2050 climate in Kop van Zuid.

C.2.2. Heating Demand Change

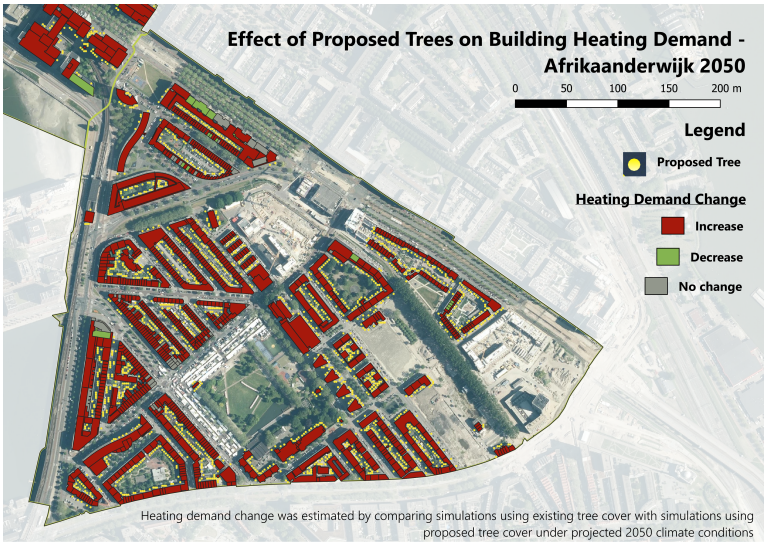


Figure C.7.: Change in heating demand resulting from proposed tree planting under the 2050 climate in Afrikaanderwijk.

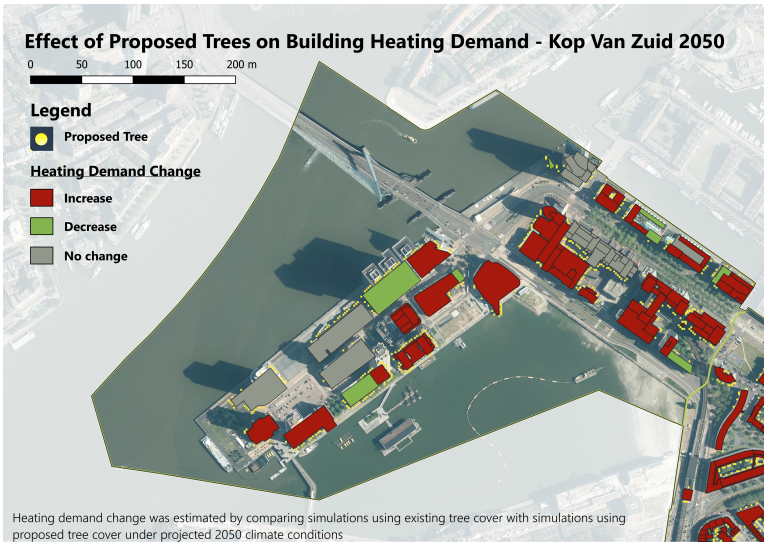


Figure C.8.: Change in heating demand resulting from proposed tree planting under the 2050 climate in Kop van Zuid.

Bibliography

(2016). Din v 18599-2: Energy efficiency of buildings—calculation of the net, final and primary energy demand for heating, cooling, ventilation, domestic hot water and lighting—part 2: Energy needs for heating and cooling of building zones. Pre-standard.

(2018). Din v 18599-1: Energy efficiency of buildings—calculation of the net, final and primary energy demand for heating, cooling, ventilation, domestic hot water and lighting—part 1: General balancing procedures, terms and definitions, zoning and evaluation of energy sources. Pre-standard.

(2020). Nta 8800:2020 energy performance of buildings – determination of the energy performance of residential and non-residential buildings – calculation method.

Abbasabadi, N. and Ashayeri, M. (2019). Urban energy use modeling methods and tools: A review and an outlook. *Building and Environment*, 161:106270.

Agugiaro, G., Benner, J., Cipriano, P., and Nouvel, R. (2018). The energy application domain extension for citygml: enhancing interoperability for urban energy simulations. *Open Geospatial Data, Software and Standards*, 3(2):1–30.

Ali, U., Shamsi, M. H., Hoare, C., Mangina, E., and O'Donnell, J. (2021). Review of urban building energy modeling (ubem) approaches, methods and tools using qualitative and quantitative analysis. *Energy and Buildings*, 246:111073.

ASHRAE (2014). *Load Calculation Applications Manual*. Atlanta, GA, 2nd edition.

Biljecki, F., Stoter, J., Ledoux, H., Zlatanova, S., and Çöltekin, A. (2015). Applications of 3d city models: State of the art review. *ISPRS International Journal of Geo-Information*, 4(4):2842–2889. https://www.mdpi.com/2220-9964/4/4/2842.

Brackney, L., Parker, A., Macumber, D., and Benne, K. (2018). *Building Energy Modeling with OpenStudio: A Practical Guide for Students and Professionals*. Springer.

Burdet, E., Colombert, M., Morand, D., and Diab, Y. (2014). Integrated canopy, building energy and radiosity model for 3d urban design. In *arXiv preprint arXiv:1411.4956*.

Czekajlo, A., Alva, J., Szeto, J., Girling, C. L., and Kellett, R. (2023). Impact of 2050 tree shading strategies on building cooling demands. *Buildings and Cities*, 4(1):817–837.

Elnagar, E., Gendebien, S., Georges, E., Berardi, U., Doutreloup, S., and Lemort, V. (2023). Framework to assess climate change impact on heating and cooling energy demands in building stock: A case study of belgium in 2050 and 2100. *Energy and Buildings*, 298:113547.

European Commission (2020). Positive energy districts and neighbourhoods for sustainable urban development. Retrieved January 15, 2024, from https://setis.ec.europa.eu/working-groups/positive-energy-districts_en.

Eurostat (2023). Energy consumption in households — heating, water heating and cooling shares (2023). Online statistics.

Ferrando, M. and Causone, F. (2019). An overview of urban building energy modelling (ubem) tools. In *Proceedings of the 16th IBPSA Conference*, Rome, Italy.

Ferrando, M., Causone, F., Hong, T., and Chen, Y. (2020). Urban building energy modeling (ubem) tools: A state-of-the-art review of bottom-up physics-based approaches. *Sustainable Cities and Society*, 62:102408.

Gao, W., Agugiaro, G., and León-Sánchez, C. (2025). Data-driven energy simulations to evaluate positive energy district potential in rotterdam. *ISPRS Annals of the Photogrammetry, Remote Sensing and Spatial Information Sciences*, X-4/W7-2025:25–32. 9th International Conference on Smart Data and Smart Cities (SDSC), 2–5 September 2025, Kashiwa, Japan.

García-López, J., Sendra, J. J., and Domínguez-Amarillo, S. (2024). Validating 'gis-ubem'—a residential open data-driven urban building energy model. *Sustainability*, 16(6):2599.

Gemeente Rotterdam (2020). Bomenverordening rotterdam. Municipal ordinance setting minimum tree planting distances at 0.5 m in dense urban areas.

Gemeente Rotterdam (n.d.). 3d rotterdam. Retrieved March 12, 2025, from https://www.3drotterdam.nl/.

Ghiassi, N. and Mahdavi, A. (2017). Re-diversification of predictions of a reductive urban energy modeling method. In *Proceedings of Building Simulation 2017*, pages 151–160, San Francisco, USA. IBPSA.

Ghiaus, C. (2022). Causality issue in the heat balance method for calculating the design heating and cooling load. *arXiv*.

Givnish, T. J. (2002). Adaptive significance of evergreen vs. deciduous leaves: Solving the triple paradox. *Silva Fennica*, 36(3):703–743.

GmbH, D. E.-A. (2023). *Guide to energy performance assessment according to DIN V 18599 (2nd ed.)*. Deutsche Energie-Agentur GmbH, Berlin, Germany. Published by the Buildings Forum for Climate Neutrality.

Gröger, G., Kolbe, T. H., Nagel, C., and Häfele, K.-H. (2012). Ogc city geography markup language (citygml) encoding standard. Technical Report OGC 12-019, Open Geospatial Consortium. Version 2.0.0, Approved 2012-04-04.

Hashemi, F., Marmur, B., Passe, U., and Thompson, J. R. (2018). Developing a workflow to integrate tree inventory data into urban energy models. In *Proceedings of the Symposium on Simulation for Architecture Urban Design (SimAUD)*, pages 331–336, Delft, Netherlands.

HFT Stuttgart (2024). Simplified radiosity algorithm (sra) documentation. https://simstadt.hft-stuttgart.de/related-softwares/simplified-radiosity-algorithm/. Accessed: 2025-09-15.

Hong, T., Chen, Y., et al. (2020). Urban building energy modeling (ubem) tools: A state-of-the-art review of bottom-up physics-based approaches. *Sustainable Cities and Society*, 62:102408.

Incropera, F. P., DeWitt, D. P., Bergman, T. L., and Lavine, A. S. (2011). *Fundamentals of Heat and Mass Transfer*. John Wiley & Sons, 7 edition.

International Energy Agency (2021). World energy outlook 2021. Retrieved January 15, 2024, from https://www.iea.org/reports/world-energy-outlook-2021.

International Organization for Standardization (2008). Energy performance of buildings – calculation of energy use for space heating and cooling (iso 13790:2008). Retrieved from url{https://www.iso.org/standard/41975.html.

International Organization for Standardization (2017). Energy performance of buildings – energy needs for heating and cooling, internal temperatures and sensible and latent heat loads – part 1: Calculation procedures.

JPI Urban Europe (2019). Positive energy districts: Framework definition. Retrieved January 15, 2024, from https://jpi-urbaneurope.eu/ped.

KNMI (2025). Knmi klimaatscenario's – tijdreeks. Online dataset. Accessed: 2025-09-15.

Konijnendijk, C. C. (2023). Evidence-based guidelines for greener, healthier, more resilient neighbourhoods: Introducing the 3–30–300 rule. *Journal of Forestry Research*, 34(3):821–830.

Liu, Y. (2008). Effects of shelterbelt trees on reducing heating-energy consumption in buildings. *Applied Energy*, 85(11):1185–1192.

Masson-Delmotte, V. et al., editors (2022). *Climate Change 2022: Mitigation of Climate Change*, chapter Chapter 6: Energy Systems. IPCC.

Middel, A., Chhetri, N., and Quay, R. (2015). Urban forestry and cool roofs: Assessment of heat mitigation strategies in phoenix residential neighborhoods. *Urban Forestry & Urban Greening*, 14(1):178–186.

Mosteiro-Romero, M., Maiullari, D., van Esch, M. P., and Schlüter, A. (2020). An integrated microclimate-energy demand simulation method for the assessment of urban districts. *Frontiers in Built Environment*, 6:553946.

Mueller, K. E., Hobbie, S. E., Oleksyn, J., Reich, P. B., and Eissenstat, D. M. (2012). Do evergreen and deciduous trees have different effects on net n mineralization in soil? *Ecology*, 93(6):1463–1472.

Netherlands Government (2022). Dutch civil code, book 5: Real property rights. Article 5:42 regulates minimum planting distances for trees and hedges.

Noardo, F., Arroyo Ohori, K., Biljecki, F., Ellul, C., Harrie, L., Krijnen, T., Eriksson, H., Van Liempt, J., Pla, M., Ruiz, A., Hintz, D., Krueger, N., Leoni, C., Leoz, L., Moraru, D., Vitalis, S., Willkomm, P., and Stoter, J. (2021). Reference study of citygml software support: the geobim benchmark 2019 – part ii. *Transactions in GIS*, 25(2):842–868.

Nouvel, R., Brassel, K.-H., Bruse, M., Duminil, E., Coors, V., Eicker, U., and Robinson, D. (2015). Simstadt, a new workflow-driven urban energy simulation platform for citygml city models. In *CISBAT 2015*. Swiss Federal Institute of Technology (EPFL).

Nouvel, R., Zirak, M., Coors, V., and Eicker, U. (2017). The influence of data quality on urban heating demand modeling using 3d city models. *Computers, Environment and Urban Systems*, 64:68–80. https://doi.org/10.1016/j.compenvurbsys.2016.12.005.

Nouvel, R., Zirak, M., Dastageeri, H., Coors, V., and Eicker, U. (2014). Urban energy analysis based on 3d city model for national scale applications. In *Proceedings of the Fifth German-Austrian IBPSA Conference (BauSIM 2014)*, pages 83–89, Aachen, Germany. IBPSA.

Ohori, K. A., Biljecki, F., Kumar, K., Ledoux, H., and Stoter, J. (2018). Modelling cities and landscapes in 3d with citygml. In *Building Information Modelling*, pages 199–215. Springer.

Owen, D., Fitch, A., Fletcher, D., Knopp, J., Levin, G., Farley, K., Banzhaf, E., Zandersen, M., Grandin, G., and Jones, L. (2024). Opportunities and constraints of implementing the 3–30–300 rule for urban greening. *Urban Forestry & Urban Greening*, 98:128393.

PDOK (2025). Basisregistratie grootschalige topografie (bgt) - feijenoord. Accessed: 2025-09-15.

Perez-Lombard, L., Ortiz, J., and Pout, C. (2008). A review on buildings energy consumption information. *Energy and Buildings*, 40(3):394–398.

Programme, U. N. E. (2019). 2019 global status report for buildings and construction: Towards a zero-emission, efficient and resilient buildings and construction sector.

Reinhart, C. F. and Davila, C. C. (2016). Urban building energy modeling – a review of a nascent field. *Building and Environment*, 97:196–202.

Reiser, C., David, R., Faigl, M., and Baumann, O. (2008). Din 18599 – accounting for primary energy: New code requires dynamic simulation. In *Proceedings of SimBuild 2008: Third National Conference of IBPSA-USA*, pages 170–173, Berkeley, CA, USA. IBPSA-USA.

Rouhollahi, M. et al. (2022). Potential residential tree arrangement to optimise dwelling energy demands under present and future climate conditions. *Energy and Buildings*, 263:112027.

Seto, K. C., Dhakal, S., Bigio, A., Blanco, H., Delgado, G. C., Dewar, D., Huang, L. O., Inaba, A., Kansal, A., Lwasa, S., McMahon, J. E., Müller, D. B., Murakami, S., Nagendra, H., and Ramaswami, A. (2014). Human settlements, infrastructure and spatial planning. *Climate Change 2014: Mitigation of Climate Change. Contribution of Working Group III to the Fifth Assessment Report of the Intergovernmental Panel on Climate Change*.

Shashua-Bar, L., Pearlmutter, D., and Erell, E. (2011). The influence of trees and grass on outdoor thermal comfort in a hot-arid environment. *International Journal of Climatology*, 31(10):1498–1506.

Smart Cities Marketplace (2021). Positive energy districts: Fact sheet.

Swan, L. G. and Ugursal, V. I. (2009). Modeling of end-use energy consumption in the residential sector: A review of modeling techniques. *Renewable and Sustainable Energy Reviews*, 13(8):1819–1835.

Tsoka, S. et al. (2021). Assessing the effects of urban street trees on building energy loads: A coupled envi-met / energyplus study. *Sustainable Cities and Society*, 65:102639.

United Nations (2019). World urbanization prospects: The 2019 revision. Retrieved January 15, 2024, from https://population.un.org/wup/.

URBACT (2020). Rotterdam integrated action plan for urban resilience. https://archive.urbact.eu/sites/default/files/resilient_europe_rotterdam_action_plan_final.pdf. Accessed: 2025-05-29.

U.S. Department of Energy (2017). Building energy modeling 101: what it is and the role of doe's. https://www.energy.gov/eere/buildings/articles/building-energy-modeling-101-what-it-and-what-does-role. Accessed: 2025-09-15.

U.S. Department of Energy (n.d.). Building energy modeling inputs and framework for simulations. https://www.energy.gov/eere/buildings/about-building-energy-modeling. Accessed: 2025-09-15.

van Dorland, R., van der Wiel, K., et al. (2023). Knmi'23 climate scenarios for the netherlands: Storyline scenarios of regional climate change. Accessed: 2025-09-15.

Yin, Y. (2024). Cooling benefits of canopy evapotranspiration at microclimate scale. *Sustainability*, 16(12):4955.

Ziter, C. D., Pedersen, E. J., Kucharik, C. J., and Turner, M. G. (2019). Scale-dependent interactions between tree canopy cover and impervious surfaces reduce daytime urban heat during summer. *Proceedings of the National Academy of Sciences*, 116(15):7575–7580.

Ürge Vorsatz, D., Cabeza, L. F., Serrano, S., Barreneche, C., and Petrichenko, K. (2015). Heating and cooling energy trends and drivers in buildings. *Renewable and Sustainable Energy Reviews*, 41:85–98.


TUDelft